

## ADVANCED SDD SYSTEM FOR SYNCHROTRON APPLICATIONS

S. Barkan<sup>1</sup>, V. D. Saveliev<sup>1</sup>, Y. Wang<sup>1</sup>, L. Feng<sup>1</sup>, M. Zhang<sup>1</sup>, E. V. Damron<sup>1</sup>, Y. Tomimatsu<sup>1</sup>, R. Goldsbrough<sup>2</sup>

<sup>1</sup>Hitachi High-Technologies Science America, Inc. 19865 Nordhoff St., Northridge, CA 91324, USA

<sup>2</sup>Quantum Detectors Ltd. Atlas Building, Fermi Avenue, Harwell Oxford, OX11 0QX, UK

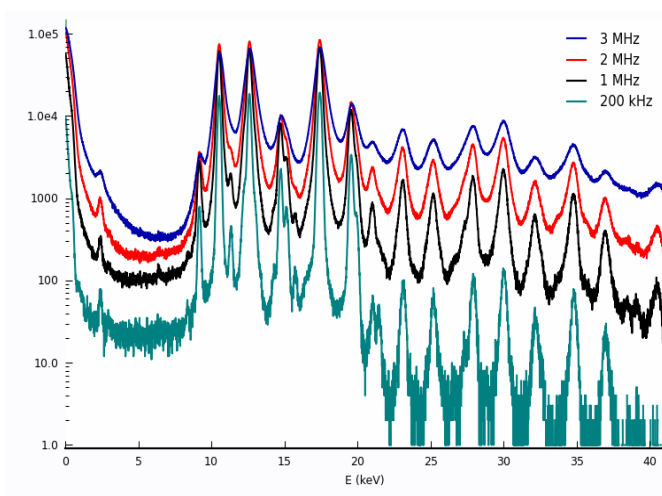
### Abstract

By combining a 4-element Silicon Drift Detector (SDD), the “Vortex ME-4”, with an advanced Digital Processor (DPP), the “Xspress3”, extremely high count-rate performance has been achieved. Preliminary results of the system were published earlier [1]. Using this advanced x-ray spectrometer, high quality images were generated with short acquisition times.

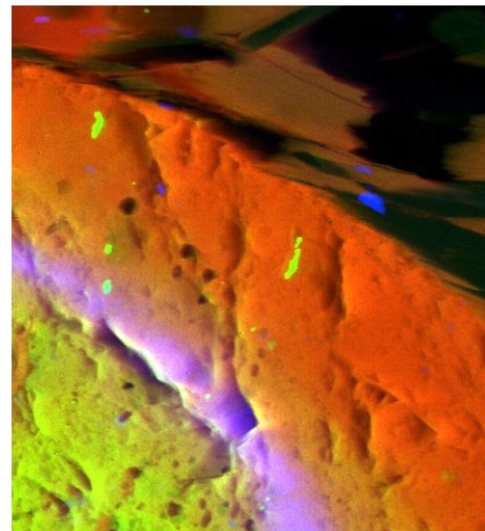
The Vortex ME-4 was equipped with 1 mm thick SDDs and ASIC electronics for enhanced performance at short peaking time. The 1 mm thick SDD produces higher quantum efficiency at high energy. Together with the Xspress3 DPP, the system was operated at the GSECARS, Advanced Photon Source (APS), Argonne National Laboratories (ANL). A 3 MHz output count rate (OCR) with a dead time of 20% was the experimental condition for collecting the data presented.

Figure 1 presents a spectrum collected with the new Vortex ME-4 and the Xspress3 processor of a PbMoO<sub>4</sub> sample. Even at 3 MHz, the spectra are useful. At 1 MHz, peaks are very well resolved.

Figure 2 presents XRF mapping of a polished thin section of garnet with zoning in yttrium. Acquisition time with the VortexME-4 and the Xspress3 was 45 minutes.



**Figure 1:** Spectra of PbMoO<sub>4</sub> sample, at 3 MHz, 2 MHz, 1 MHz and 200 kHz.



**Figure 2:** Polished thin section of garnet with zoning in yttrium (the purple band). Data collected with 2x2 micron x-ray beam at 18 keV. 1 x 1 mm area, 2 x 2 μm pixels, 10 ms per pixel (45 minute acquisition).

### References

- [1] S. Barkan, V.D. Saveliev, Y. Wang, L. Feng, E.V. Damron, Y. Tomimatsu, “Extreme High Count Rate Performance with a Silicon Drift Detector and ASIC Electronics”, Biological and Chemical Research, Volume 2015, 338-344

# THE NANOMAX BEAMLINE AT MAX IV - A HARD X-RAY NANOPROBE

U. Johansson<sup>1</sup>, D. Carbone<sup>1</sup>, S. Kalbfleisch<sup>1</sup>, T. Stankevic<sup>1</sup>, Z. Matej<sup>1</sup>, P. Westerlind<sup>1</sup>,  
L. Arvidsson<sup>1</sup>, K. Åhnberg<sup>1</sup>, B.N. Jensen<sup>1</sup>, S. Carlson<sup>1</sup>, K. Parfeniukas<sup>2</sup>, S. Giakoumidis<sup>2</sup>,  
U. Vogt<sup>2</sup>, A. Mikkelsen<sup>3</sup>

<sup>1</sup>MAX IV Laboratory, Lund University, Box 118, 221 00 Lund, Sweden

<sup>2</sup>Biomedical and X-Ray Physics, Department of Applied Physics, KTH/Royal Institute of Technology, Albanova University Center, 106 91 Stockholm, Sweden

<sup>3</sup>Synchrotron Radiation Research, Department of Physics, Lund University, Box 118, 221 00 Lund, Sweden

## Abstract

NanoMAX is the name of the first x-ray imaging beamline at the new Swedish synchrotron radiation source MAX IV[1]. It is a hard X-ray undulator beamline for nano-beams and will enable imaging applications exploring diffraction, scattering, fluorescence and coherent diffractive imaging methods.

The beamline will feature two experimental stations for users: One (ES2) with beamsizes in the 100 nm range, well suited for diffractive, fluorescence and coherence experiments in very flexible sample environments. The other experimental station (ES1) will utilize zone plates to reach 10 nm resolution using diffraction and fluorescence methods on nanoscale objects.

The MAX IV multi-bend achromat 3 GeV storage ring is under extensive commissioning and show promising performance. The beamline is completely installed up to the experimental hutch and early commissioning of the undulator, front end and beamline optics has started.

We will present the general ideas for the beamline instrumentation, and in particular discuss the experimental stations design and the initial commissioning work. We aim at opening the NanoMAX beamline for early users early 2017 at the second experimental station.

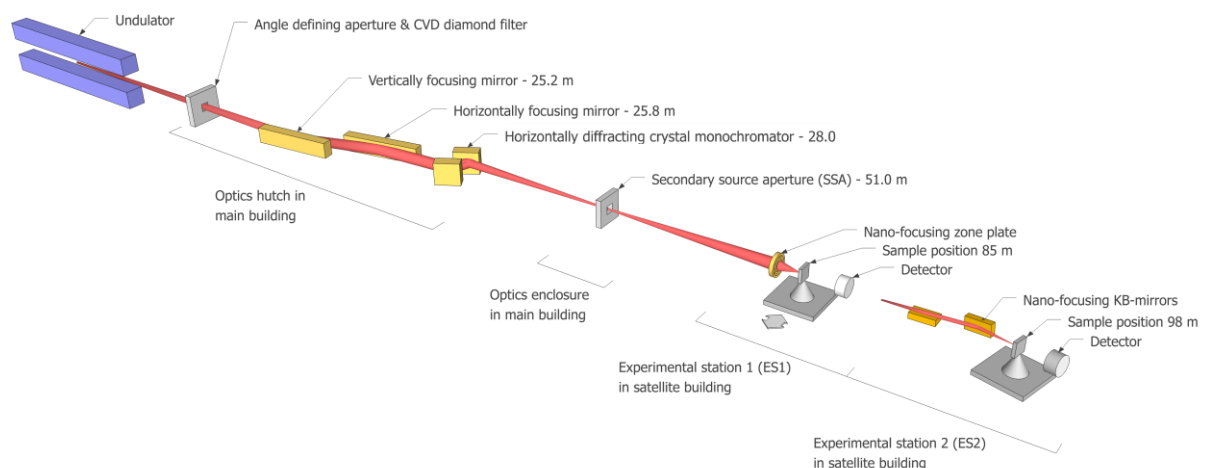


**Figure 1.** Major components of the NanoMAX beamline with two experimental stations.

## References

[1] U. Johansson, U. Vogt, A. Mikkelsen, Proc. SPIE 8851, 88510L (2013).

## COMPARISON OF X-RAY LENSES WITH GRATING INTERFEROMETRY

F.J. Koch<sup>1</sup>, C. Detlefs<sup>2</sup>, T.J. Schöter<sup>1</sup>, O. Márkus<sup>1</sup>, D. Kunka<sup>1</sup>, A. Last<sup>1</sup>, J. Mohr<sup>1</sup>

<sup>1</sup>Karlsruhe Institute of Technology, Eggenstein-Leopoldshafen, Germany

<sup>2</sup>European Synchrotron Radiation Facility, Grenoble, France

### Abstract

Compound refractive X-ray lenses (CRLs [1]) enable X-ray microscopy experiments in the hard X-ray regime, where the currently available zone plate optics become inefficient. CRLs can be fabricated by a variety of techniques, the most common being imprinting, silicon dry etching and X-ray lithography. These techniques are very different, and consequently, different types of lens imperfections are to be expected. We employed X-ray Talbot interferometry at the beamline ID06 of the ESRF to perform at-wavelength metrology of X-ray lenses made from Beryllium and polymer. In this technique, the residuals of a linear fit to the measured phase gradient provide a quantification of the local angular deviation of a lens. Global optical aberrations can be quantified by decomposing the retrieved wavefront phase profile into a set of polynomials adapted to the expected wavefront shape [2], [3].

In our analysis we found that a Beryllium point focus lens offered very high shape accuracy, but showed local errors linked to the deformation of the imprinting tool in the fabrication process and material inhomogeneity. A polymer line focus lens made by X-ray lithography, on the other hand, shows a more homogeneous material and no strongly localized defects, but does not have the same shape accuracy as the Beryllium lens. Figure 1 shows the maps of angular deviation obtained from the two lenses in the same color coding. These results highlight the individual strengths and weaknesses of the fabrication techniques and offer feedback for lens fabrication, which in turn can benefit future X-ray microscopy experiments.

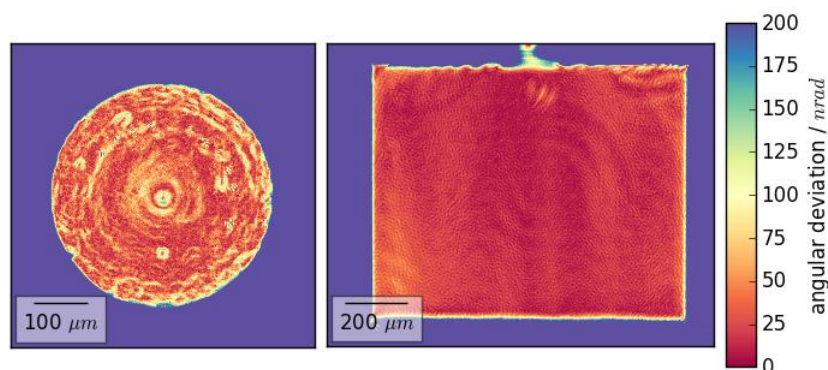


**Figure 1:** Map of angular deviation for a Be point focus lens (left) and a polymer line focus lens (right), from [3]

In order to use the method for routine quality control of a batch of lenses, it would be preferable to take the method to a laboratory based system, and preliminary testing was performed to compare the results at such a setup with the data acquired at the synchrotron.

### References

- [1] A. Snigirev, V. Kohn, I. Snigireva, and B. Lengeler, "A compound refractive lens for focusing high-energy X-rays", *Nature*, vol. 384, no. 6604, pp. 49–51, 1996.
- [2] S. Rutishauser, I. Zanette, T. Weitkamp, T. Donath, and C. David, "At-wavelength characterization of refractive x-ray lenses using a two-dimensional grating interferometer", *Appl. Phys. Lett.*, vol. 99, no. 22, p. 221104, Nov. 2011.
- [3] F. J. Koch, C. Detlefs, T. J. Schröter, D. Kunka, A. Last, and J. Mohr, "Quantitative characterization of X-ray lenses from two fabrication techniques with grating interferometry", *submitted to Optics Express*, 2016.

# DEVELOPMENTS IN STXM INSTRUMENT CONTROL AND DATA FILE FORMAT

B. Watts, J. Raabe

*Paul Scherrer Institute, Villigen, Switzerland*

## Abstract

As the field of scanning transmission X-ray spectro-microscopy (STXM) continues to advance, experiments become more ambitious and increase requirements for the coordination and integration of the many and varied positioners and detectors. Therefore, a new generation of software is being developed that allows the necessary stability, flexibility and extensibility demanded by cutting edge STXM experiments.

The *Pixelator* STXM control software implements a modern, modular design that implements all scan logic in a central server program, with separate modules for interfacing with different types of hardware and hardware control systems. The graphical user interface (Figure 1) runs as a separate client program and is executed on a separate PC from the server in order to maximize system stability.

With the new possibilities afforded by *Pixelator*, a corresponding increase in features is required in the data file format. Therefore, a new STXM file format, NXstxm,[1] based on HDF5 [2] and the NeXus standard [3] has been developed that can be easy to use while also having the flexibility to store the larger volume of more varied data that is now available. For example, NeXus/HDF5 files written by *Pixelator* include values from the X- and Y-interferometer as well as the synchrotron ring current on a per-pixel basis. These data-logging capabilities also extend to arbitrary, user-defined data channels, such as from a separate PC controlling the conditions of a sample environmental cell. This presentation will discuss the design and current implementation status of the *Pixelator* STXM control software and the NeXus/HDF5 STXM data file format.

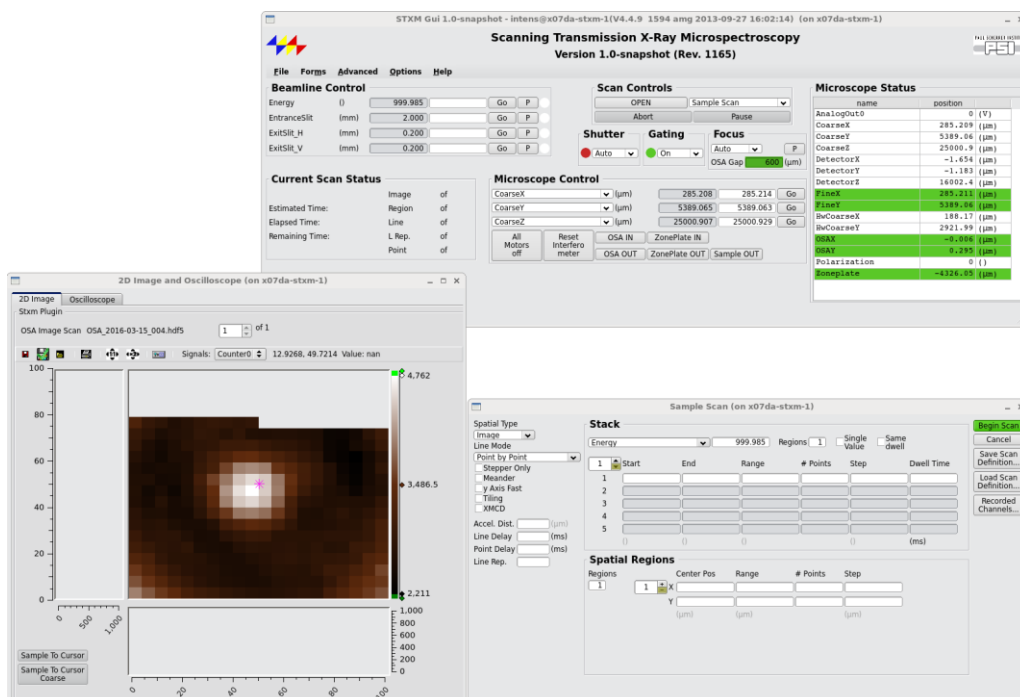


**Figure 1:** The graphical user interface for the *Pixelator* STXM control software.

## References

- [1] B. Watts and J. Raabe, AIP Conf. Proc., 1696, 020042 (2016).
- [2] <http://www.NeXusFormat.org>
- [3] <http://www.hdfgroup.org/HDF5/>



# X-RAY BEAM SHAPER OPTICS VIA DEEP X-RAY LITHOGRAPHY

O. Márkus<sup>1</sup>, S. Georgi<sup>1</sup>, I. Greving<sup>2</sup>, M. Ogurreck<sup>2</sup>, F. Beckmann<sup>2</sup>, E. Kornemann<sup>1</sup>,  
A. Last<sup>1</sup>, J. Mohr<sup>1</sup>

*<sup>1</sup>Institute for Microstructure Technology, Karlsruhe Institute of Technology,  
Kaiserstr. 12, 76131 Karlsruhe, Germany*

*<sup>2</sup>Helmholtz Zentrum Geesthacht, Max-Planck-Str.1, 21502 Geesthacht, Germany*

## Abstract

At high brilliance synchrotron sources the beam size is limited by the low divergence of the beam from the undulator source in vertical direction. This relatively small beam cross section limits the available field of view (FoV) for full field imaging. For many applications a larger FoV is desirable e.g. for medical, or biological samples or in materials science where the sample size is given by the manufacturing process. Covering long samples, several height steps are scanned and the tomograms are stacked, which is time consuming. Furthermore the Gaussian shaped beam profile is not ideal for full field imaging where a more constant intensity over the sample would be of advantage.

To overcome these limitations we developed refractive beam shaping optics, produced via deep X-ray lithography [1] using SU-8, an epoxy based polymer. The designed optics consist of biconvex Fresnel-elements defocusing the beam (fig. 1). The local curvature is tailored to widen the incoming beam and at the same time change the incident Gaussian-like beam profile to a top-hat intensity distribution (fig. 2).

When testing the beam shaper at the P05 beamline of PETRA III (Hamburg, Germany) operated by HZG, we were able to widen up the original beam profile in vertical direction from 1.9 mm to 6 mm. In addition the beam was transformed from a Gaussian-like beam intensity profile to a more top-hat distribution. Due to the fact that we are free to shape the facet of the lens for a certain purpose, it is possible to generate any desired intensity distribution with a suitable designed beam shaper of this type.

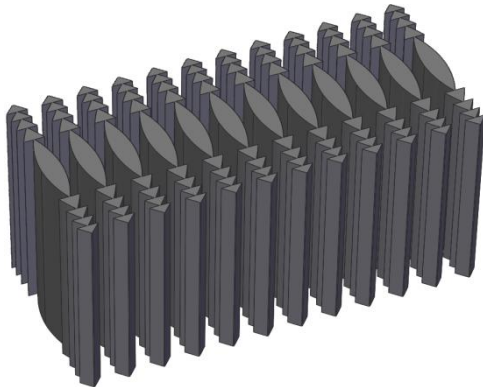


**Figure 1:** Fresnel-type refractive X-ray beam shaper; CAD-sketch.

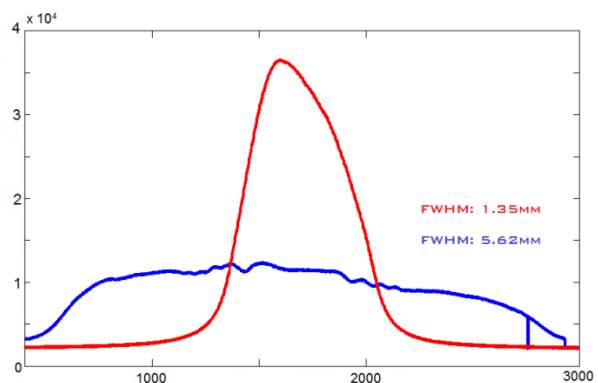


**Figure 2:** The graph shows the intensity profile (FWHM) of the beam without (red) and with (blue) beam shaping optics.

## References

- [1] A. L. Bogdanov et al., *Microelectronic Engineering* 53 (2000) 493-496
- [2] M. Simon et al., *Advances in X-Ray/EUV Optics and Components III*, p. 7077–70771Q–6, 2008

## A TWO-STAGE ADAPTIVE X-RAY FOCUSING SYSTEM USING FOUR PIEZOELECTRIC DEFORMABLE MIRRORS

T. Goto<sup>1</sup>, H. Nakamori<sup>1,2</sup>, S. Matsuyama<sup>1</sup>, H. Hayashi<sup>1</sup>, T. Kimura<sup>3</sup>, K. P. Khakurel<sup>3</sup>, Y. Sano<sup>1</sup>, Y. Kohmura<sup>4</sup>, M. Yabashi<sup>4</sup>, Y. Nishino<sup>3</sup>, T. Ishikawa<sup>4</sup>, K. Yamauchi<sup>1</sup>

<sup>1</sup>Department of Precision Science and Technology, Graduate School of Engineering, Osaka University, 2-1 Yamada-oka, Suita, Osaka 565-0871, Japan

<sup>2</sup>JTEC Corporation, 2-4-35, Saito-Yamabuki, Ibaraki, Osaka 567-0086, Japan

<sup>3</sup>Research Institute for Electronic Science, Hokkaido University, Kita 21 Nishi 10, Kita-ku, Sapporo 001-0021, Japan

<sup>4</sup>RIKEN/SPring-8, 1-1-1 Kouto, Sayo, Hyogo 679-5198, Japan

### Abstract

At synchrotron radiation facilities, various optical devices, such as lenses, zone plates and mirrors, are used for nanofocusing. Usually, these devices are specially designed and fabricated for specific applications. Furthermore, their optical parameters (e.g., numerical aperture (NA) and focal length) are fixed. However, in recent years, adaptive focusing devices that can change such parameters have attracted significant attention. In our previous study, we developed ultraprecise piezoelectric deformable mirrors that can produce nearly diffraction-limited nanobeams [1,2].

In this study, we developed a two-stage adaptive Kirkpatrick-Baez (KB) mirror system [3,4], which consists of the four deformable mirrors, in order to control the NA without changing the position of the final focal plane corresponding to the sample position (Fig. 1). The variable-NA X-ray focusing was demonstrated at BL29XUL (EH3) of SPring-8 at an X-ray energy of 10 keV.

Figure 2 shows the measured one-dimensional intensity profiles at the final focal plane. It was confirmed that the beam size could be varied from 108 to 560 nm (165 to 1434 nm) in the horizontal (vertical) direction by controlling the NA, showing good agreement with an ideal profile.

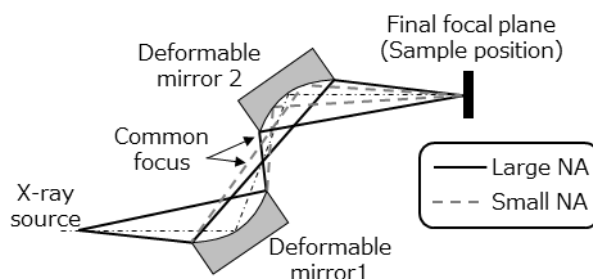


**Figure 1:** Schematic of a two-stage adaptive KB mirror system

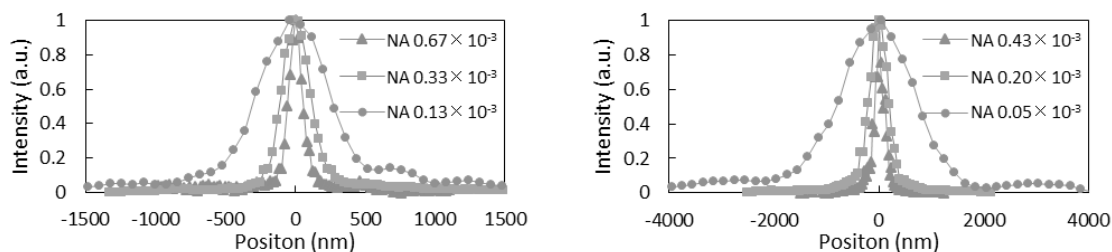


**Figure 2** Measured intensity beam profiles at final focal plane in the horizontal (left) and vertical (right) directions

### References

- [1] H. Nakamori et al., Rev. Sci. Instrum. 83, 053701 (2012).
- [2] T. Goto et al., Rev. Sci. Instrum. 86, 043102 (2015)
- [3] S. Matsuyama et al., Proc. SPIE 8503, 850303 (2012).
- [4] T. Kimura et al., Opt. Express. 21, 8, 9267-9276 (2013)

## THE X-RAY NANOPROBE ENDSTATION AT TAIWAN PHOTON SOURCE

Gung-Chian Yin<sup>1</sup>, Bo-Yi Chen<sup>1</sup>, Huang-Yeh Chen<sup>1</sup>, Chien-Yu Lee<sup>1</sup>, Bi-Hsuan Lin<sup>1</sup>, Shao-Chin Tseng<sup>1</sup>, Shi-Hung Chang<sup>1</sup>, Minghwei Hong<sup>3</sup>, J. Raynien Kwo<sup>2</sup>, Mau-Tsu Tang<sup>1</sup>

<sup>1</sup>National Synchrotron Radiation Research Center, Hsinchu 30076, Taiwan

<sup>2</sup>National Tsing-Hua University, Physics Department, Hsinchu 30076, Taiwan

<sup>3</sup>National Taiwan University, Physics Department, Taipei 10617

### Abstract

The X-ray nanoprobe (XNP) at Taiwan Photon Source (TPS) is to focus hard X-rays down to 40 nm. By the Montel optics[1,2], the matching numerical aperture is increased by a factor of square root 2 than the conventional K-B pair, resulting a fully optimized demagnification ratio even with the moderate length of the present beamline. The focus spot of less than 40nm with 55mm working distance makes the most feasibility for *in-situ* experiments.

The associated endstation provides a wide variety of functions, namely, XRF, XAS, XEOL, projection microscope, CDI, Bragg CDI, and ptychography. This nanoprobe is equipped with on-the-fly scanning capability and high speed position-addressing with multi-axes laser interferometers. A scanning electron microscope (SEM) is installed to precisely locate the sample position relative to incident X-rays. The sample is transferred through load-lock kept under high vacuum ( $1 \times 10^{-6}$  torr) and a cryo-stage with temperature of liquid He is installed.

The current progress of the XNP facility will be presented, including the design of the beamline and preliminary test of the key components such as the Montel mirror holder, cryo sample stage, and the on-the-fly scanning scheme. The beamline will be ready for pilot commissioning by the end of 2016.

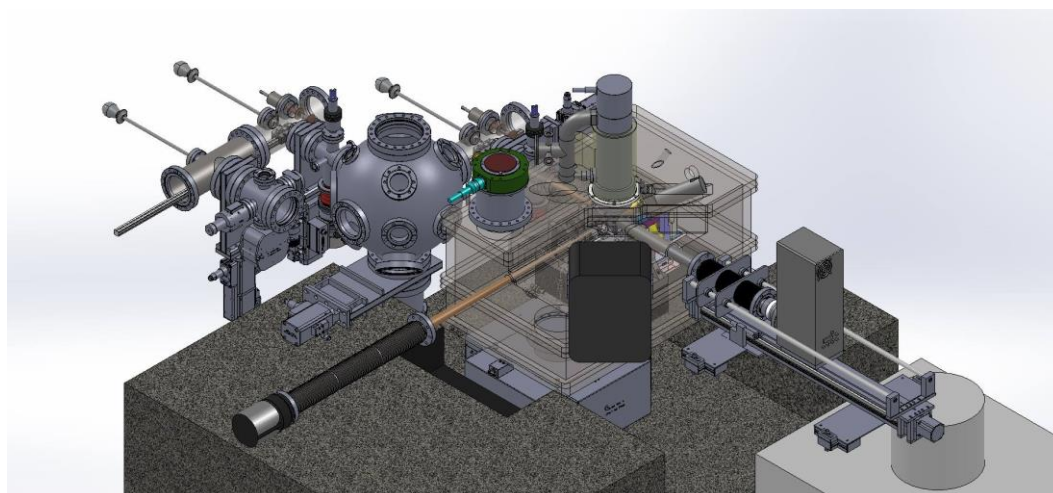


**Figure:** The design of the X-ray nanoprobe endstation at Taiwan Photon Source

### References

- [1] Gene E. Ice, John D. Budai, J.W.L. Pang, Science, 334 (2011) 1234.
- [2] W. Liu, G.E. Ice, L. Assoufid, C. Liu, B. Shi, R. Khachatryan, J. Qian, P. Zschack, J.Z. Tischler, J.-Y. Choi, Journal of Synchrotron Radiation, 18 (2011) 575-579.

## FABRICATION OF HOLOGRAPHIC X-RAY LENSES

M. Baluktsian, K. Keskinbora, U. T. Sanli, G. Schütz

*Max Planck Institute for Intelligent Systems, Heisenbergstr. 3, 70569 Stuttgart, Germany*

### Abstract

An established component in X-ray optics is the Fresnel zone plate (FZP) consisting of alternating opaque and transparent concentric rings. The FZP transmission function is a binary form of a parabolic surface of the computer generated holographic (CGH) lens called the kinoform lens. In contrast to the multiple foci of a standard binary FZP, this special profile, in case of a pure phase plate (no absorption), facilitates a 100 % concentration of the incident light to a single focus. The fabrication of a kinoform lens is challenging and was realized to date by means of various approximation approaches. Recently, we developed a robust and direct gray-scale lithographic method for the fabrication of a lens with a smooth kinoform profile [1]. Gray-scale lithography allows for the realization of nanostructures with surface relief profiles by conversion of exposure gradients into surface topography and is particularly suitable for the fabrication of micro-optics with quasi-3D profiles. Using focused ion beams, it can be realized either by combining ion beam implantation with reactive ion etching [2, 3] or by direct-write focused ion beam milling [1] as shown in Figure 1.

A dramatic improvement in the absolute efficiency by means of circularly symmetric kinoform lenses is yet to be demonstrated. This is partially due to the relatively slow nature of the gray-scale direct-writing, the limited selection of accessible materials with favorable properties for IBL and an even more limited commercial availability of those materials as membranes with desired thicknesses. However, calculations show that the improvement of focusing efficiency can be very dramatic under certain conditions [4] (see Figure 2). Hence, further development of the processes and materials is very promising.

In this work we discuss other potential uses of quasi-three-dimensional structuring from extreme UV to hard X-rays. Various CGHs, such as spiral kinoforms or in principle any tailored illumination pattern enabled by efficient holograms, as well as the materials selection issues are considered.

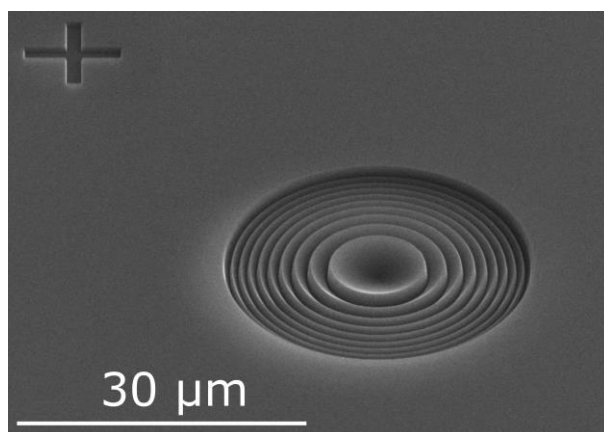


**Figure 1:** A kinoform lens structured in single crystal silicon using our method [1]. The structure is more than 2  $\mu\text{m}$  deep.

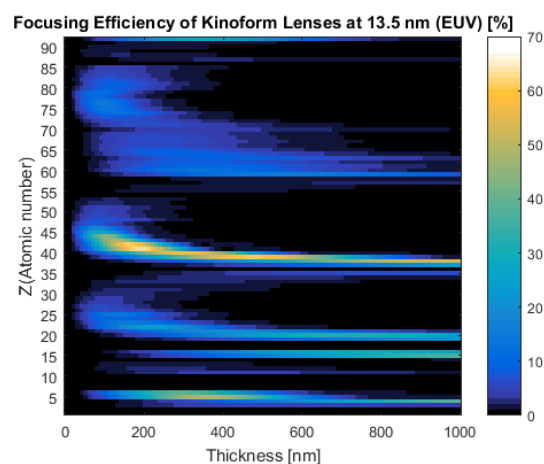


**Figure 2:** Focusing efficiencies of perfect kinoforms consisting of elements from  $Z=2$  to 92 at 13.5 nm wavelength.

### References

- [1] K. Keskinbora, C. Grévent, M. Hirscher, M. Weigand, G. Schütz, *Advanced Optical Materials*, **3** (2015) 792-800.
- [2] M. Erdmanis, I. Tittonen, *Appl Phys Lett*, **104** (2014).
- [3] S. Waid, H.D. Wanzenboeck, M. Muehlberger, M. Gavagnin, E. Bertagnolli, *Nanotechnology*, **25** (2014) 315302.
- [4] K. Keskinbora, U.T. Sanli, C. Grévent, G. Schütz, 2015, pp. 95920H-95920H-95926.

## RECENT DEVELOPMENTS IN TABLE-TOP SXR/EUV MICROSCOPY USING COMPACT GAS-PUFF TARGET SOURCES

A. Torrisi, P. Wachulak, A. Bartnik, L. Wegrzynski, T. Fok, H. Fiedorowicz

*Institute of Optoelectronics, Military University of Technology, Kaliskiego 2 Str., 00-908 Warsaw  
Warsaw, Poland*

### Abstract

Laser-produced plasma sources, emitting short-wavelength radiations, offer an interesting alternative to synchrotrons and free-electron laser installations. By employing table-top Soft X-ray (SXR) and Extreme ultraviolet (EUV) sources it is possible to overpass the limited accessibility and high costs of such large facilities, allowing possibility to perform similar experiments on table-top. It was already demonstrated that a laser-plasma double stream gas puff target source coupled with Fresnel zone plates (FZPs) is a powerful technique suitable for SXR ( $\lambda=0.1-10$  nm) and EUV ( $\lambda=1-120$  nm) microscopy in transmission mode, particularly in the so-called "water window" ( $\lambda=2.3-4.4$  nm) spectral range for nanoscale imaging of biological and inorganic materials.

The SXR and EUV microscopy based on Fresnel optics were performed using a Nd:YAG laser operating at intensities of the order of  $10^{11}$  W/cm<sup>2</sup>, 3 ns pulse duration and 1-10 Hz repetition rate. The source is based on laser-interaction with the gas puff target, which results in plasma formation emitting in the EUV and SXR regions. Such source allows to generate the plasma efficiently, without debris, provide high flux of EUV and X-ray photons. A nitrogen plasma, which emits at  $\lambda=2.88$  nm wavelength, and an argon plasma, emitting at  $\lambda=13.84$  nm, were employed for SXR and EUV experiments, respectively. Thin Ti and Zr filters were employed to spectrally narrow down the plasma emission either, in the "water window", or the EUV spectral range. The filtered radiation illuminates the sample, and a FZP objective was used to form a magnified image in transmission mode, onto a back-illuminated CCD camera.

The SXR/EUV desk-top microscopes based on gas-puff target sources and FZPs allows capturing magnified images of the samples, with 50-60 nm half-pitch spatial resolution and exposure time of few seconds. Herein we would like to present our recent developments and progress in SXR/EUV microscopy, including source and microscope optimization, examples of image acquisition and possible applications.



## NANOPROBE AND SPECTROSCOPY BEAMLINE 5-ID AT NSLS-II

J. Thieme, G. Williams, Y.-C. Chen-Wiegart

Brookhaven National Laboratory, NSLS-II, Building 743, Upton, NY-11973, USA

### Abstract

NSLS-II is a source of synchrotron radiation ideally suited for experiments in need of coherent radiation. With a very low emittance of horizontally 1 nm-rad, vertically 6 pm-rad, a position stability of less than 10% of the source size in vertical and horizontal, and a design goal of 500 mA ring current, it provides an ideal platform for sub- $\mu\text{m}$  focused beam instruments. Beamline 5-ID, the sub-micron resolution X-ray spectroscopy (SRX) beamline has been designed, installed and commissioned as an X-ray fluorescence analytical probe dedicated to spectroscopy experiments with sub- $\mu\text{m}$  and sub-100nm spatial resolution. The scientific emphasis is the study of complex systems with chemical heterogeneity at sub-micrometer and sub-100nm length scales. A horizontally deflecting double crystal monochromator was chosen to provide maximum beam stability while providing very high resolution. The energy range from 4 keV to 25 keV allows for X-ray fluorescence and absorption spectroscopy experiments starting at the K-absorption edge of titanium, extending through the K-edge of rhodium. Utilizing two sets of Kirkpatrick-Baez focusing mirrors, a high-flux mode with sub- $\mu\text{m}$  spatial resolution or a high-resolution mode with sub-100nm resolution can be chosen. At full ring current, the high-flux setup will deliver about  $10^{13}$  phot/sec in a sub- $\mu\text{m}$  spot, the high-resolution setup will deliver a focal spot size of less than 100nm but at a lower flux of approximately  $10^{11}$  phot/sec. The photon flux SRX delivers in a sub- $\mu\text{m}$  spot, ultimately combined with the use of new energy dispersive detectors like the MAIA, will open new possibilities for spectroscopic analysis of major and trace elements in natural and synthetic materials, X-ray fluorescence imaging of their distribution both in 2D and 3D, concurrent  $\mu$ -diffraction measurements, and coherent diffraction imaging experiments. XRF imaging and spectroscopy experiments in cooperation with the academic community and using the high-flux setup have begun in spring 2015, the general user program has started in January 2016. In the coming months, the high-resolution setup as well as the tomography capabilities of the beamline will be commissioned. A detailed description of the status of the SRX beamline will be provided here. Already now, beamtime requests exceed fourfold the time available for experiments, an unambiguous sign for the beneficial impact of such nanoprobe and spectroscopy beamlines. Application examples from environmental and geosciences, material and energy research, and cultural heritage will be presented to substantiate this point.

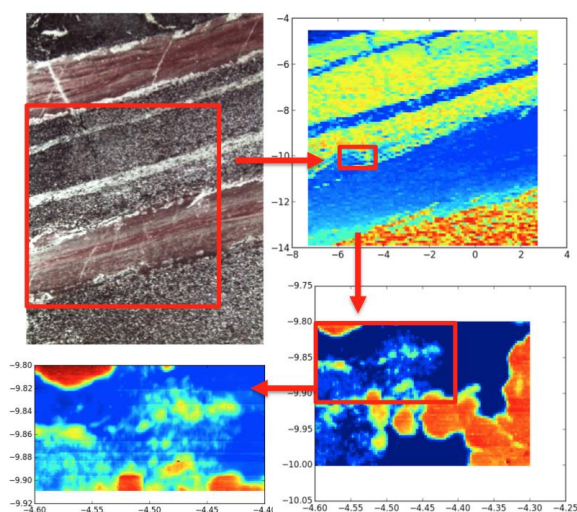


**Figure 2 (left):** XRF image of banded iron formation. Light microscopic image  $16 \times 12 \text{ mm}^2$  (top left), XRF images  $10 \times 10 \text{ mm}^2$  step size  $100 \mu\text{m}$  (top right),  $300 \times 200 \mu\text{m}^2$  step size  $3 \mu\text{m}$  (bottom right), and  $200 \times 100 \mu\text{m}^2$  step size  $1 \mu\text{m}$  (bottom left).

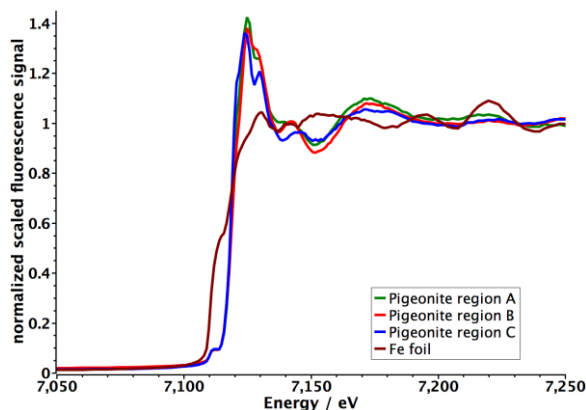


**Figure 1 (top):** XANES spectrum of pigeonite, a mineral found in volcanic rocks and meteorite from Mars and Moon, in comparison to metallic iron.

# HIGH REFLECTANCE CR/V MULTILAYER MIRROR FOR WATER WINDOW APPLICATIONS

Li Jiang, Qiushi Huang, Jiani Fei, ZhongZhang, Zhanshan Wang

*Key Laboratory of Advanced Micro-Structured Materials MOE, Institute of Precision Optical Engineering, School of Physics Science and Engineering, Tongji University, Shanghai 200092, China*

## Abstract

Imaging and spectroscopy in the “water window” ( $\lambda=2.3-4.4\text{nm}$ ) has been long pursued in the fields of biology and material science, driven by the natural contrast between carbon and oxygen, and the high spatial resolution provided by the short wavelength. Significant progress has been achieved in producing high flux and coherent light sources in this wavelength region, using synchrotron or free electron laser [1], and high harmonic generation [2]. Besides the high quality sources, multilayer mirror is another key component for the water window microscope. Due to the short working wavelength, the d-spacing of the multilayer is only 1-2nm. This imposes a severe challenge for the fabrication of such multilayer mirrors. Cr/V multilayer is one of the promising candidate working near the V-L edge ( $\lambda=2.4\text{nm}$ ). To develop high reflectance multilayer mirror for this region, the physical structure inside the multilayer with different layer thicknesses were investigated. Interface engineering was further applied to this metal/metal system which produced a maximum reflectance of 24% near the V-L edge at  $42^\circ$  grazing incidence [3].

## References

- [1] W. Ackermann, G. Asova, V. Ayvazyan, A. Azima, N. Baboi et al, Operation of a free-electron laser from the extreme ultraviolet to the water window, *Nat. Photonics*, 1, 336-342 (2007).
- [2] M.-C. Chen, P. Arpin, T. Popmintchev, M. Gerrity, B. Zhang, et al, Bright, Coherent, Ultrafast Soft X-Ray Harmonics Spanning the Water Window from a Tabletop Light Source, *Phys Rev. Lett.* 105, 173901 (2010).
- [3] Q. Huang, J. Fei, Y. Liu, P. Li, M. Wen, C. Xie, P. Jonnard, A. Giglia, Z. Zhang, K. Wang, Z. Wang, High reflectance Cr/V multilayer with B4C barrier layer for water window wavelength region, *Opt. Lett.* 41(4), 701 (2016).

## REFLECTION ZONE PLATES: FOCUSING AND DISPERSIVE PROPERTIES IN TIME-SPACE SCALE

Alexander Firsov<sup>1</sup>, Alexei Erko<sup>1</sup>, Anatoly Firsov<sup>2</sup>, Frank Siewert<sup>1</sup>, Christoph Braig<sup>1</sup>, Heike Löchel<sup>1</sup>, Alexander Svintsov<sup>2</sup>

*1Helmholtz-Zentrum Berlin für Materialien und Energie GmbH, Institut für Nanometeroptik und Technologie, Albert-Einstein-Str. 15, 12489 Berlin, Germany*

*2Institute of Microelectronics Technology and High Purity Materials RAS, Institutskaya Street 6, Chernogolovka, Moscow Region, 142432, Russia*

### Abstract

In August 2016 the, 30th anniversary of the first publication about the focusing properties of the diffractive element based on the reflection effect from profiled multilayer structure will take place[1]. Later, Bragg-Fresnel diffraction focusing elements based on multilayer structures and crystals were effectively used at the DCI synchrotron radiation source at LURE for fluorescent micro analysis and micro diffraction experiments [2 - 3]. Focusing of a hard x-ray radiation at total external reflection by using the profile of Fresnel zones for the first time demonstrated in [4]. In this report new generation X-ray optical elements and systems for spectroscopy and monochromatization in the soft and hard X-ray range, developed and fabricated at the Helmholtz-Zentrum Berlin (HZB), are reported. These reflection zone plates at total external reflection (RZPs) have been used in optical systems with synchrotron radiation at BESSY II [5, 6], at free electron laser sources and the LCLS in Stanford [7] as well as in laboratory instrumentation such as high harmonic generation sources [8] and scanning electron microscopes [9]. The feasibility of an off-axis X-ray reflection zone plate to perform wavelength-dispersive spectroscopy and on-axis point focusing has been tested [10]. The 2-dimensional and 3-dimensional diffractive optical elements (DOEs), give the unique possibility for spectroscopy and focusing in application to 3rd and 4th generation light sources. Such DOEs are based on the principle of wavelength dispersion in the focal plane of a reflection Fresnel zone plate (RZP). The possibility of a diffractive structure fabrication with a variable depth profile of 4-30 nm with lateral periods <100 nm has been demonstrated. The uniformity and reproducibility of the depth structure vary by less than 0.5 nm within the area of 20 x 80 mm<sup>2</sup>. The obtained characteristics are state-of-the-art and not available elsewhere among the scientific community nowadays.

### References

- [1] V. Aristov, et al., "Focusing properties of shaped multilayer mirrors", JETP Lett., Vol. 44, No. 4, 25 August 1986, p265-267.
- [2] P.Chevallier, et al., "X-ray microprobes" Nuclear Instruments and Methods in Physics Research, B 113, (1996), p. 122-127.
- [3] Al. Firsov, et al., "Application of Bragg-Fresnel lenses for microfluorescent analysis and microdiffraction" , NIM A,399 (1997) 152-159.
- [4] Yu. A. Basov, et al., "Grazing incidence phase Fresnel zone plate for X-ray focusing", Optics Communications, Volume 109, Issues 3–4, 1 July 1994, Pages 324–327.
- [5] A. Erko et al., "Novel parallel vacuum ultra-violet/X-ray fluorescence spectrometer," Spectrochim. Acta B 67, 57–63 (2012)
- [6] K. Holldack et al., "FemtoSpeX: a versatile optical pump–soft X-ray probe facility with 100 fs X-ray pulses of variable polarization," J. Synchrotron Rad. 21, 1090-1104 (2014).
- [7] J. Kern et al., "Methods development for diffraction and spectroscopy studies of metallo-enzymes at X-ray free-electron lasers," Philosophical Transactions of the Royal Society B: Biological Sciences (2014), 369, 1647, 20130590
- [8] J. Metje et al., "Monochromatization of femtosecond XUV light pulses with the use of reflection zone plates," Opt. Express 22, 10747-1760, (2014)
- [9] A Erko et al., "New parallel wavelength-dispersive spectrometer based on scanning electron microscope Optics Express (2014), 22 (14), 16897-16902
- [10] H. Löchel et al., "Femtosecond high-resolution hard X-ray spectroscopy using reflection zone plates," Optics Express 23 (7), (2015), 8788-8799

## G2-LESS GRATING INTERFEROMETER WITH SINGLE PHOTON SENSITIVE HYBRID DETECTORS

Zhentian Wang<sup>1,2</sup>, Matias Kagias<sup>1,2</sup>, Sebastian Cartier<sup>1,2</sup>, Anna Bergamaschi<sup>1</sup>, Roberto Dinapoli<sup>1</sup>, Aldo Mozzanica<sup>1</sup>, Bernd Schmitt<sup>1</sup>, Marco Stampanoni<sup>1,2</sup>

<sup>1</sup>Swiss Light Source, Paul Scherrer Institut, 5232 Villigen, Switzerland

<sup>2</sup>Institute for Biomedical Engineering, University and ETH Zürich, 8092 Zürich, Switzerland

### Abstract

Grating interferometry (GI) [1] can provide valuable diagnostic information in the medical field. However, a number of challenges still hinder its application in clinical settings, for instance, the dose efficiency (analyzer grating G2 blocks half of the photons), the long acquisition times (multiple images due to phase stepping) and the fabrication challenges of G2. In our work we propose a single shot, G2-less grating interferometer based on direct conversion detectors with single photon sensitivity which allows us to tackle the aforementioned limitations. The detector we use – MOENCH [2], features a physical pixel size of  $25\mu\text{m}$  that is suitable for medical imaging but can achieve micrometer resolution by exploiting the charge sharing effect. The interference pattern with pitch of a few  $\mu\text{m}$  can be resolved directly and the absorption and differential phase can be further retrieved from the recorded pattern. The validation of the propose method was performed at the TOMCAT beamline, SLS, Switzerland. Pyramids of 350 to 50  $\mu\text{m}$  with known slopes were used as a sample. Results show that quantitative absorption and differential phase contrast signals can be retrieved. Our approach overcomes the major obstacles regarding dose and flux issues without compromising the sensitivity and resolution of the grating interferometer, therefore presents a promising technique for practical phase contrast imaging in clinical applications.

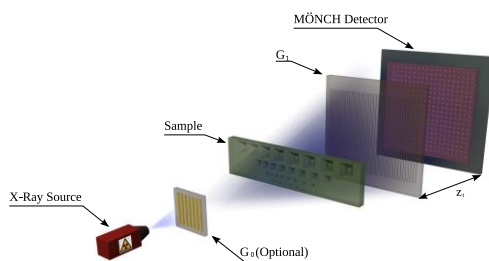


**Figure 1.** Sketch of proposed setup. The setup includes an X-ray source (synchrotron or X-ray tube), an optional source grating G0, the phase grating G1 and the MOENCH detector, which is placed at a Talbot distance from G1.

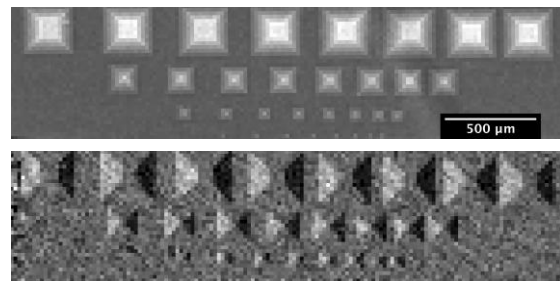


**Figure 2.** Absorption and differential phase contrast images of the pyramids with a pixel size of  $25\mu\text{m}$ .

### References

- [1] F. Pfeiffer et al, *Nature Phys.* (2006)
- [2] S. Cartier et al, *J. Instrum.* 9, C05027 (2014)

## ACHIEVING BUNCH-LENGTH LIMITED TIME RESOLUTION USING A NEW PHOTON COUNTING SYSTEM AT MAXYMUS

Markus Weigand<sup>1</sup>, Jensen Maelfait<sup>2</sup>, Matthias Noske<sup>1</sup>, Iuliia Bykova<sup>1</sup>, Michael Bechtel<sup>1</sup>, Hermann Stoll<sup>1</sup>, Eberhard Goering<sup>1</sup>, Bartel van Waeyenberge<sup>2</sup>, Gisela Schütz<sup>1</sup>

<sup>1</sup>Max-Planck-Institute for Intelligent Systems, Heisenbergstr. 3, 70569 Stuttgart, Germany

<sup>2</sup>Ghent University, Krijgslaan 281, 9000 Ghent, Belgium

### Abstract

Time resolved imaging of magnetic nanostructures has been established as a strength of Scanning transmission X-ray Microscopy (STXM)[1,2], and is the main focus of the MAXYMUS X-ray microscope operated by the MPI for intelligent Systems at the BESSY II synchrotron in Berlin. There, a continuously improved pump-and-probe setup utilizing a FPGA single photon counting and sorting hardware as well as a direct digital synthesis based pump generators was successfully used for sub-ns dynamic imaging of magnetic nanostructures like domain walls [3], spinwaves [4,5], vortex cores [5] or skyrmions [6].

The method provides spatial resolution identical to non-dynamic STXM (<20nm) using XMCD as contrast mechanism, while temporal resolution are strictly limited by the light source itself – at BESSY II, to about 90ps in normal and ca. 15ps in low-alpha operation, with electron bunch phase shift broadening a major contribution to the former.

With increased demand for higher time resolution and only very limited amount of low-alpha beamtime (and brilliance), a completely new detector concept was developed to vastly extend the capabilities beyond the existing design. In addition to the computation power required for realtime correction of electron bunch position, it will also increase the amount of time channels being able to be captured to 16384 and depart from the previously used discriminator based photon detection unit: A 2GHz ADC will be used to directly sample APD output and correctly handle multiple photons per bunch, enabling a significant amount of throughput increase in many experimental situations as well as improved HF noise suppression.

We will present results of a prototype of this FPGA system as well as first results of >20 GHz time resolved low-alpha dynamics.

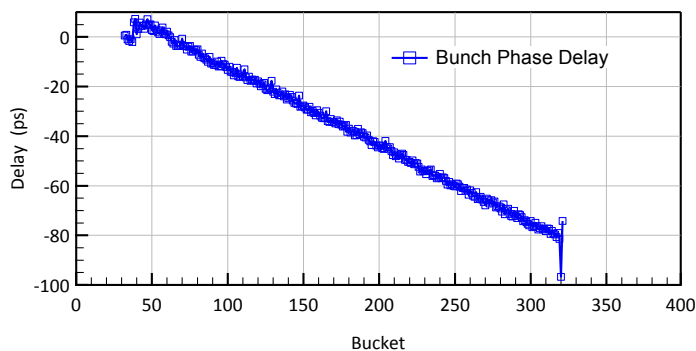


**Figure 1:** Phase shift of BESSY II at 300mA beam current, decreasing time resolution due to effective bunch broadening

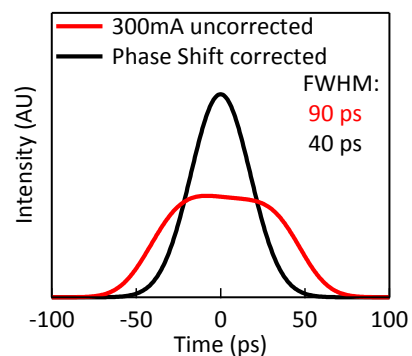


**Figure 2:** Comparison of current and corrected effective bunch width (simulated).

### References

- [1] B. Van Waeyenberge et al., Nature 444, 461-464 (2006)
- [2] Y. Acremann et al, Rev. Sci. Instr. 78, 014792 (2007)
- [3] A. Bisig et al., Nature Communications 4:2328 (2013)
- [4] S. Wintz et al, submitted to Nature Nanotechnology
- [5] M. Kammerer et al., Nature Communications 2:279 (2011)
- [6] W. Woo et al, Nature Materials (2016) Feb 29.



## INTRODUCING HIGH EFFICIENCY IMAGE DETECTOR TO X-RAY IMAGING TOMOGRAPHY

K. Uesugi, M. Hoshino, A. Takeuchi

*Japan Synchrotron Radiation Research Institute /SPring-8, Kouto 1-1-1 Sayo, Hyogo, Japan*

### Abstract

We have been developing x-ray imaging tomography system continuously in SPring-8. The system has now achieved about 140nm of spatial resolution in three-dimension. The measurement time is around 20 minutes for 1800 projections.

Increasing the efficiency of objective zone plate and image detector is essential to get better quality of images. Those affect scan time, radiation damage on the sample, spatial resolution and so on. Concerning the image detector, the signal-to-noise ratio and frame rate are rapidly modified by cutting edge technology such as scientific CMOS (sCMOS) chip. The image detector which commonly used in high energy X-ray region is visible light conversion type. The detector consists of phosphor screen, visible light optics and image device. The most used visible light optics (coupling techniques) are lens- and fiber-couplings (fiber optics plate, FOP). The advantage of FOP system is high numerical aperture [1].

In this experiment, we introduced FOP-sCMOS detector to X-ray imaging tomography with Fresnel zone plate (FZP) optics to get higher efficiency and better image quality.

FOP system (C12849-1015S) is developed by Hamamatsu Photonics. Phosphor screen is 15 $\mu$ m-thick P43 powder. FOP is straight type. Pixel size is 6.5 $\mu$ m/pixel. Lens coupled system used 7 $\mu$ m-thick P43 powder as a phosphor screen. Two AI AF Nikkor 50mm f/1.4D (Nikon) are used tandem lens system. The image device is ORCA Flash 4.0 (Hamamatsu Photonics) which employs the same sCMOS chip to C12849-1015S.

The common experimental conditions are as follows, X-ray energy of 8 keV, exposure time of 250 msec/shot. The undulator gap and effective pixel size for lens and FOP are, 12.2 mm and 12.6mm, 90.4 nm/pixel and 89.7 nm/pixel, respectively. When the undulator gap is 12.6 mm, the beam intensity was 11.5 times smaller than that of 12.2 mm.

Figure 1 and 2 show the X-ray image of a test chart and line profiles. The image obtained by FOP shows higher contrast with small number of X-ray photon. The FOP system has higher contrast (Figure 2). The both CT scan time was about 4 minutes for 900 projections.

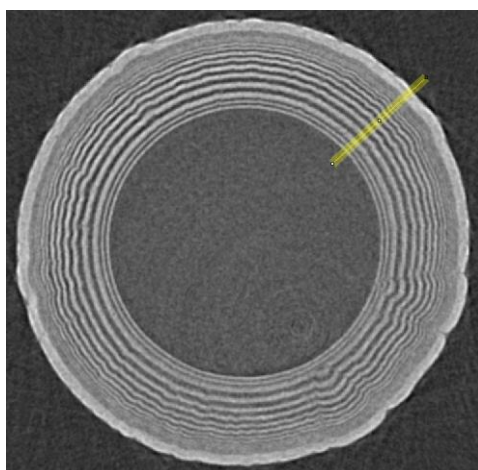


**Figure 1:** CT image of Al-Cu concentric test chart with FOP-sCMOS. The field of view is 45 $\mu$ m x 45 $\mu$ m.

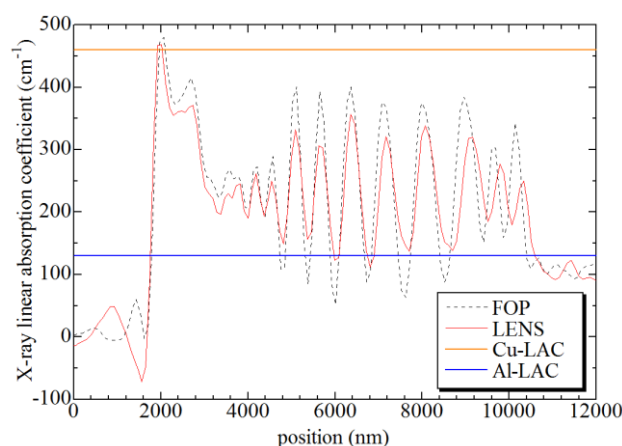


**Figure 2:** Line profiles of the concentric test chart (yellow line in Figure 1).

### References

- [1] K. Uesugi et al., *J. Synchrotron Rad.* (2011). 18, 217–223

## THE NEW PGM BEAMLINE FOR HZB X-RAY MICROSCOPY AT BESSY II

P. Guttman<sup>1</sup>, S. Werner<sup>1</sup>, F. Siewert<sup>2</sup>, A. Sokolov<sup>2</sup>, J.-S. Schmidt<sup>2</sup>, M. Mast<sup>2</sup>,  
M. Brzhezinskaya<sup>3</sup>, C. Jung<sup>3</sup>, R. Follath<sup>4</sup>, G. Schneider<sup>1</sup>

*1Helmholtz-Zentrum Berlin für Materialien und Energie GmbH, Institute for Soft Matter and Functional Materials, Albert-Einstein-Str. 15, 12489 Berlin, Germany*

*2Helmholtz-Zentrum Berlin für Materialien und Energie GmbH, Institute for Nanometer Optics and Technology, Albert-Einstein-Str. 15, 12489 Berlin, Germany*

*3Helmholtz-Zentrum Berlin für Materialien und Energie GmbH, Main Department Scientific-Technical Infrastructure 2, Albert-Einstein-Str. 15, 12489 Berlin, Germany*

*4Paul Scherrer Institute, Beamline Optics Group, 5232 Villigen, Switzerland*

### Abstract

The BESSY II electron storage ring operated by the Helmholtz-Zentrum Berlin (HZB) includes a transmission soft X-ray microscope (TXM) that has been very successful for both tomographic imaging of cells [1,2] and for NEXAFS studies in materials science [3-5]. To significantly enhance the performance of the current HZB TXM, we present here the setup of a newly designed beamline that will enable faster data acquisition together with an extension into the tender X-ray range. Furthermore, within photon energy tuning range, two new important absorption edges, namely sulfur and phosphorus, will become accessible for element-sensitive 3D imaging, in addition to those already available, e.g. at carbon, calcium, titanium and oxygen. Another advantage of this new beamline is that phase contrast X-ray microscopy for thicker specimens will become possible at higher photon energies outside of the “water-window”.

This extensive range of new capabilities will be enabled by a series of key improvements. We will use a plane grating monochromator (PGM) with a highly efficient blaze grating manufactured by the HZB Department of Precision Gratings. Later on, we will incorporate adapted multilayer optical elements and we will exchange the current undulator U41 with a specially designed helical UE30 in-vacuum undulator. This will allow extending the photon energy range up to 2.5 keV. In addition, we have chosen grazing incidence angles of 1° for the pre-mirror M1 as well as for the mirror M3. The mirrors will also be rhodium coated for high reflectivity over the whole photon energy range from 270 eV up to 2.5 keV. In addition to discussing this new beamline design, we will present results of the metrology measurements [6,7] of the new optical elements installed in the beamline, and also the first at wavelength measurements.

### References

- [1] G. Schneider, P. Guttman, S. Rehbein, S. Werner, R. Follath, J. Struct. Biol. 177 (2012), 212-223
- [2] Hagen, C.; Dent, K.C.; Zeev-Ben-Mordehai, T.; Grange, M.; Bosse, J.B.; Whittle, C.; Klupp, B.G.; Siebert, C.A.; Vasishtan, D.; Bäuerlein, F.J.B.; Cheleski, J.; Werner, S.; Guttman, P.; Rehbein, S.; Henzler, K.; Demmerle, J.; Adler, B.; Koszinowski, U.; Schemelleh, L.; Schneider, G.; Enquist, L.W.; Plichtko, J.M.; Mettenleiter, T.C.; Grünwald, K., Cell 163 (2015), 1692-1701
- [3] Guttman, P., Bittencourt, C., Beilstein J. Nanotechnol. 6 (2015), 595-604
- [4] Henzler, K., Heilemann, A., Kneer, J., Guttman, P., Jia, H., Bartsch, E., Lu, Y., Palzer, S., Scientific Reports 5, 17729 (2015)
- [5] Carta, D., Hitchcock, A.P., Guttman, P., Regoutz, A., Khiat, A., Serb, A., Gupta, I., Prodromakis, T., Scientific Reports 6, 21525 (2016)
- [6] Siewert, F.; Buchheim, J.; Zeschke, T.; Brenner, G.; Kapitzki, S.; Tiedtke, K., Nuclear Instruments & Methods in Physics Research A 635 (2011), p. S52 - S57
- [7] A. Sokolov, P. Bischoff, F. Eggenstein, A. Erko, A. Gaupp, S. Künstler, M. Mast, J.-S. Schmidt, F. Senf, F. Siewert, Th. Zeschke, F. Schäfers, Review of Scientific Instruments, accepted

## PRESENT STATUS OF A COMPACT SCANNING TRANSMISSION X-RAY MICROSCOPE AT THE PHOTON FACTORY

Y. Takeichi<sup>1</sup>, H. Suga<sup>2</sup>, N. Inami<sup>1</sup>, T. Ueno<sup>3</sup>, Y. Takahashi<sup>4</sup>, K. Ono<sup>1</sup>

<sup>1</sup>Institute of Materials Structure Science, High Energy Accelerator Research Organization (KEK),  
1-1 Oho, Tsukuba, Japan

<sup>2</sup>Department of Earth and Planetary Systems Science, Hiroshima University,  
1-3-1 Kagamiyama, Higashi-Hiroshima, Japan

<sup>3</sup>National Institute for Materials Science, 1-2-1 Sengen, Tsukuba, Japan

<sup>4</sup>Department of Earth and Planetary Science, the University of Tokyo,  
7-3-1 Hongo, Bunkyo-ku, Tokyo, Japan

### Abstract

Scanning transmission X-ray microscopy (STXM) in the soft X-ray regime is one of the powerful methods which enables us to investigate chemical properties of a sub-100 nm-scale region of interest [1]. At the Photon Factory, Japan, we have developed a compact design of the STXM instrument (cSTXM) that can be installed at a free-port endstation of the soft X-ray spectroscopy beamlines. The design realizes (i) the compactness so that the instrument can be installed to and removed from the beamline, and (ii) the vibration compliance not to affect the spatial resolution determined by the Fresnel zone plate (FZP) [2]. Here, we report the present status and activities of the cSTXM.

The focal distance of the FZP is typically  $\sim 1$  mm, and therefore, the distance between the order sorting aperture (OSA) and the sample is 200–400  $\mu\text{m}$ . When installing the sample, a user should roughly place the sample at the focal position. The cSTXM is now equipped with a side-view microscope camera (Fig. 1) that helps a user to position the sample coarse Z stage in sub-100  $\mu\text{m}$  precision. This also prevents the trouble such as hitting the sample to the OSA.

At present, the cSTXM is operated at BL-13A of the Photon Factory, Japan. The APPLE-II type insertion device ID#13 produces vertical/horizontal linear, circular and elliptical polarization. One can acquire a sequence of polarization dependent measurements for a circular or linear dichroism experiment. Figure 2 shows the magnetic domain structure of a  $\text{SmCo}_5$  specimen obtained by a sequential measurement with right- and left-handed circular polarization at 778.6 eV (Co  $L_3$ -edge).

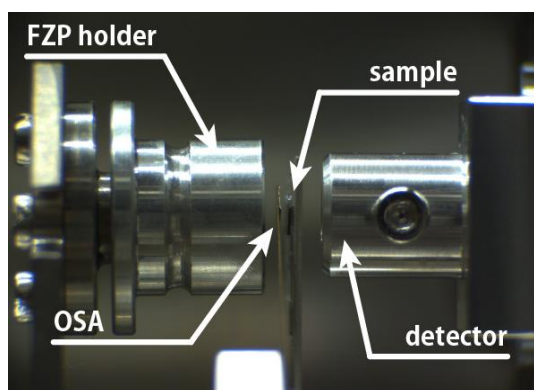


**Figure 1:** Side-view camera image of the cSTXM for sample coarse Z positioning.

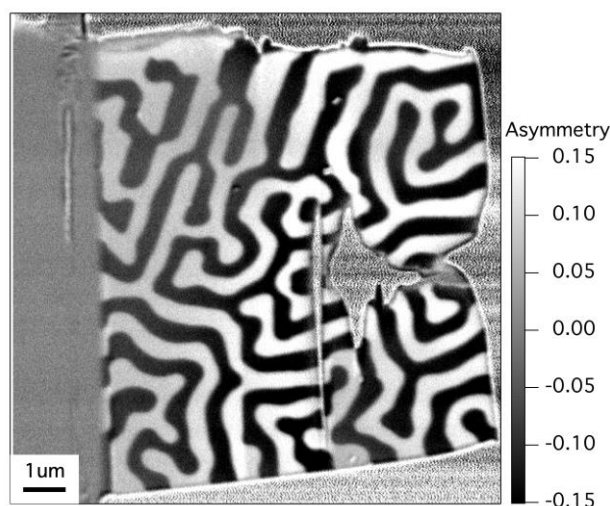


**Figure 2:** XMCD asymmetry image of a  $\text{SmCo}_5$  specimen measured at 778.6 eV.

### References

- [1] A. P. Hitchcock, in "Handbook of Nanoscopy," Vol. 2, Chap. 22 (Wiley-VCH, 2012).
- [2] Y. Takeichi et al., Rev. Sci. Instrum. 87, 013704 (2016).

# SUPER-RESOLUTION IMAGING USING INTERACTION BETWEEN INTERFERENCE FRINGE AND PERIODIC STRUCTURE OF OBJECT

Yoshio Suzuki

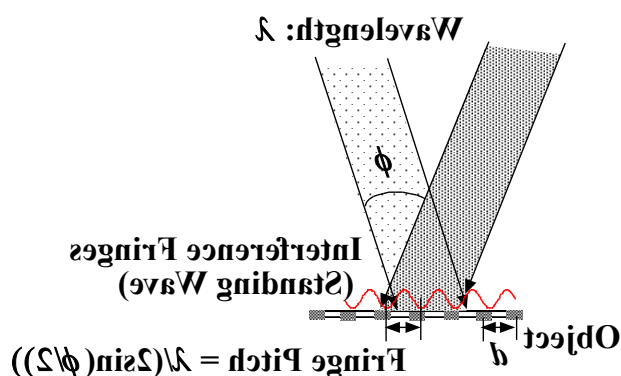
Graduate School of Frontier Sciences, University of Tokyo, Kashiwa, Chiba, 277-8561, Japan

## Abstract

Spatial resolution of projection imaging is generally limited by the resolution of imaging detector and the image blurring due to the diffraction. The practical resolution limit of projection imaging is around 1  $\mu\text{m}$  at present for technical reasons. Higher spatial resolution, of course, can be attained by using image-forming optics, such as Fresnel zone plate, refractive lens, and total-reflection mirror system. However, the fabrication of high-resolution optical system for hard x-rays is still a difficult task at present. We have recently proposed a method for detecting fine structures of object using interaction between standing wave and periodic structures of the object [1]. The technique is a kind of super-resolution imaging, i.e. detection of fine structures beyond the resolution limit of imaging detector.

The principle of the super-resolution imaging is schematically shown in Fig. 1. Two plane waves (wavelength of  $\lambda$ ) are crossed at the object plane with an intersecting angle of  $\phi$ . Then, a standing wave (interference fringe) with a period of  $\lambda/(2\sin(\phi/2))$  is generated on the object plane. When the object has a periodic structure, and its period,  $d$ , is equal to the standing wave period,  $d = \lambda/(2\sin(\phi/2))$ , the existence of the periodic structure can be detected as a modulation of the transmitting beam intensity by scanning the position of standing wave. In our previous experiment, a wavefront-division interferometer with refractive prism was used for generating the standing wave. However, the prism optics has a disadvantage for generation of very short period fringes, i.e. self-absorption loss at the prism. Therefore, in the present experiment, we employed a wavefront-dividing total-reflection-mirror interferometer instead of the prism for generating finer interference fringes.

The experiment was carried out at beamline 20XU of Spring-8. The configuration of interferometer is Lloyd's mirror optics with plane wave illumination. The x-ray energy is 11.5 keV, and x-ray mirror is a 150 mm-long plane mirror. The period of interference fringe can be changed by the glancing angle to the mirror. The scanning of standing wave is carried out by linear translation of the total-reflection mirror. The feasibility study was done using a resolution test chart (XRESO-50HC, NTT-AT) as a model object of periodic fine structures. An example of experimental results is shown in Fig. 2. Fine structure with a period of 100 nm is clearly detected as a modulation of transmitting beam intensity.



QuickTime<sup>®</sup> C<sup>2</sup>  
 TIFFAijÖækAj ëL ïÉÉçÉOÉáÉÄ  
 Ç™Ç±ÇÄEsÉNE´ÉÉÇ%â@ÇÉÇZÇ½Ç...ÇÖiKóvÇ-ÇAB

**Figure 1:** Schematic diagram of standing wave method with two-beam interferometer

**Figure 2:** Intensity modulation of transmitting beam for 100 nm period structure.

## References

- [1] Y. Suzuki, Rev. Sci. Instrum. 86, 043701 (2015).

## HARD X-RAY MULTILAYER ZONE PLATE WITH 25-NM OUTERMOST ZONE WIDTH

Y. Kagoshima<sup>1</sup>, K. Sumida<sup>1</sup>, H. Takano<sup>1</sup>, T. Koyama<sup>2</sup>, S. Ichimaru<sup>3</sup>, T. Ohchi<sup>3</sup>, H. Takenaka<sup>4</sup>

*1Graduate School of Material Science, University of Hyogo,  
3-2-1 Kouto, Kamigori, Ako, Hyogo 678-1297, Japan*

*2JASRI/SPring-8, 1-1-1 Kouto, Sayo, Hyogo 679-5198, Japan*

*3NTT Advanced Technology Corporation,*

*3-1 Morinosato, Wakamiya, Atsugi, Kanagawa 243-0124, Japan*

*4TOYAMA Co., Ltd., 3816-1, Kishi, Yamakita, Ashigarakami, Kanagawa 258-0112, Japan*

### Abstract

We fabricated a multilayer zone plate (MZP) having the outermost zone width of 40.4 nm and achieved its near diffraction-limited focused beam size of 46 nm by using 20-keV undulator beam of BL24XU at SPring-8 [1]. The focusing property was measured by a knife-edge scanning method in dark-field geometry. The method gives us a line spread function (LSF). Since an MZP has a narrow annular aperture, it is difficult to directly measure the two-dimensional focusing property from LSFs. Then, we developed a procedure to reconstruct point spread function (PSF) by applying the tomographic process to LSFs in every radial direction on the focal plane [1].

We have continued upgrading the MZP technology. We presented in XRM2014 the fabrication and the performance test of an MZP with the outermost zone width ( $\Delta r_N$ ) of 30 nm. The focused beam size of about 30 nm was estimated by oscillation peaks observed in the measured LSF according to Rayleigh's criterion [2].

Recently, we have fabricated a new MZP with the smaller outermost zone width. The outermost zone width ( $\Delta r_N$ ) was designed to be 25 nm. Its SEM image is shown in Figure 1. The focal length at 20 keV is 24.5 mm. Figure 2 shows the measured LSF. There appear vibrating structures, which comes from the Airy pattern produced in the focal plane. A half distance between the first minimums was 24.2 nm, which is in relatively good agreement with the diffraction limited focused size of 21.1 nm calculated by taking the annular aperture parameter into account. Thus, it can be concluded that nearly diffraction limited performance was achieved by the MZP with  $\Delta r_N = 25$  nm.

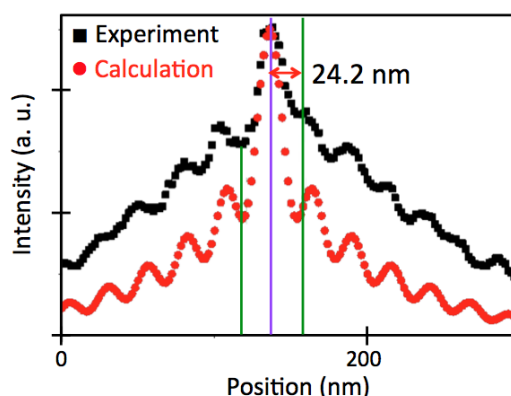
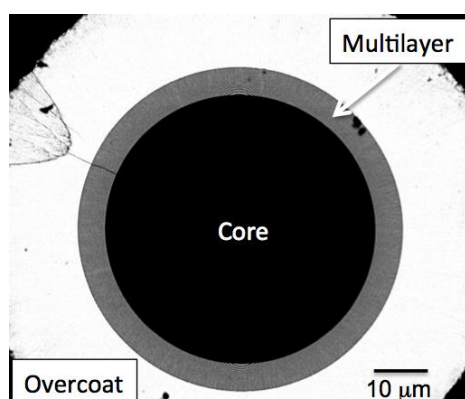


**Figure 1:** SEM image of newly fabricated MZP consisting of MoSi<sub>2</sub>/Si layer pairs. **Figure 2:** Measure LSF of MZP with  $\Delta r_N = 25$  nm.

### References

- [1] H. Takano, S. Konishi, T. Koyama, Y. Tsusaka, S. Ichimaru, T. Ohchi, H. Takenaka and Y. Kagoshima, *J. Synchrotron Rad.* **21**, 446-448 (2014).
- [2] T. Hiroto, H. Takano, K. Sumida, T. Koyama, S. Konishi, S. Ichimaru, T. Ohchi, H. Takenaka, Y. Tsusaka and Y. Kagoshima, *AIP Conference Proceedings* 1696, 020017 (2016).



# DEVELOPMENT OF SOFT X-RAY MICROSCOPE USING WATER WINDOW LPP LIGHT SOURCE

T. Ejima<sup>1</sup>, Y. Kondo<sup>2</sup>, Y. Ono<sup>2</sup>, T. -H. Dinh<sup>2</sup>, T. Higashiguchi<sup>2</sup>, T. Hatano<sup>1</sup>

<sup>1</sup>Institute of Multidisciplinary Research for Advanced Materials, Tohoku University, 2-1-1, Katahira, Aoba-ku, Sendai, Japan

<sup>2</sup>Department of Electrical and Electronic Engineering, Faculty of Engineering and Center for Optical Research and Education (CORE), Utsunomiya University, Utsunomiya, Tochigi, Japan

## Abstract

Wavelength region from 2.3 nm to 4.5 nm is known as Water Window. The light in Water Window wavelength region is transparent in water and is absorbed by carbon and nitrogen atoms, therefore images of bio-cells show absorption contrast in Water Window. Recently, LPP light source using heavy metal target generates broad spectral and high intense light in SX wavelength region [1]. Especially, wavelength regions of the emissions from the plasma using Au, W, Pb, and Bi metal targets are in and around Water Window. Therefore, the LPP light source using these metal targets will become one of SX light sources to observe bio-cells. The purpose of our study is that a SX microscope using the LPP light source with heavy metal targets to explore the optimum conditions of LPP light source in Water Window and to examine observation possibility of hydrated bio-cells by the use of the SX microscope.

In this study, a contact-type microscope using a scintillator plate was developed (Fig. 1 & 2). With the use of the scintillator plate which shows high quantum efficiency and linearity in SX region [2], SX images can be observed instantly by a visible (VI) microscope. As the results of these features, SX images can be directly compared with VI ones.

To demonstrate the performance of the developed microscope, polystyrene beads in water were observed changing the thickness of the water. The diameters of the polystyrene beads in water were 1  $\mu\text{m}$  and 0.4  $\mu\text{m}$ . The thickness of the water was gradually changed from 1.3  $\mu\text{m}$  to 5  $\mu\text{m}$ . The plasma was excited by Nd:YAG laser using a Bi target. The SX light from the LPP light source penetrates the water layer from 1.3  $\mu\text{m}$  to 2.3  $\mu\text{m}$  thick, and the diameter 1  $\mu\text{m}$  of the polystyrene beads was observed.

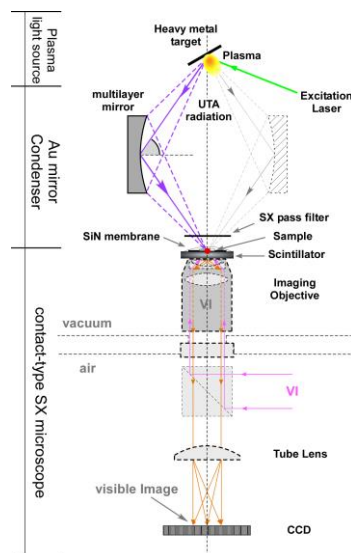


**Figure 1:** Schematic representation of the developed microscope.

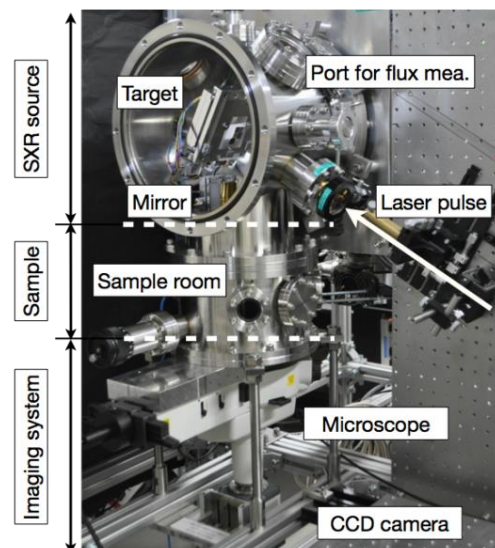


**Figure 2:** View of the developed microscope.

## References

- [1] H. Ohashi, *et al.*, Appl. Phys. Lett. 104, 234107 (2014).
- [2] T. Ejima, *et al.*, CP 1234 "SRI: 10th International Conference on Radiation Instrumentation", 811-814 (2010).

# DESIGN AND FABRICATION OF WOLTER-TYPE 4-MIRROR SYSTEM

N. Watanabe<sup>1</sup>, S. Aoki<sup>1,2</sup>, N. Yamaguchi<sup>2</sup>

<sup>1</sup>Faculty of Pure and Applied Sciences, University of Tsukuba, Tsukuba, Ibaraki, 305-8573, Japan  
<sup>2</sup>CROSS, 1601 Kamitakatsu, Tsuchiura, Ibaraki, 300-0811, Japan

## Abstract

In x-ray microscopy, a Wolter mirror is a 2-mirror system which consists of a combination of axisymmetric hyperboloidal and ellipsoidal mirrors with a common focus as shown in Fig. 1(a) [1]. On the other hand, when a virtual image of an object is formed, a 2-mirror system can be composed of two hyperboloidal mirrors with a common focus as shown in Fig. 1(b). By combining these two types of Wolter mirrors, a 4-mirror imaging optics can be designed. The first Wolter mirror forms a virtual image of an object and the second Wolter mirror forms its real image. The advantage of this 4-mirror system is that the numerical aperture can be approximately doubled compared to a single Wolter mirror as shown in Fig. 1(a) [2].

We designed and fabricated this type of 4-mirror system for x-ray and neutron imaging. The average grazing angle was 5.5 mrad and the magnification ratio was 10. The length of each mirror along the optical axis was about 10mm and the total length of the 4-mirror system was 38 mm. A Pyrex glass 4-mirror system was fabricated by using a replica method [3]. Figure 2 shows the replica of the 4-mirror system. The evaluation of the 4-mirror system is currently under way.

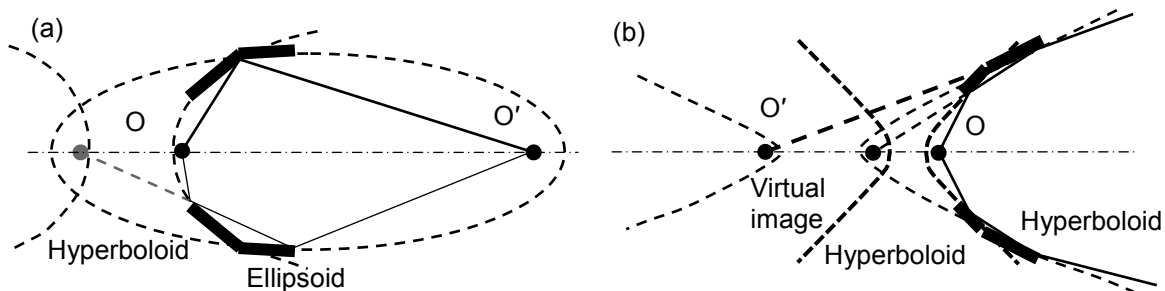


**Figure 1:** (a) A Wolter mirror which forms a real image. (b) A Wolter mirror which forms a virtual image.

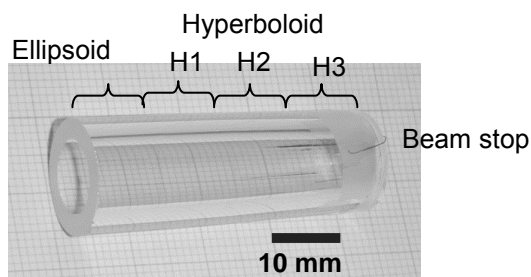


**Figure 2:** The replicated 4-mirror system made of Pyrex glass.

## References

- [1] H. Wolter, *Ann. Phys.* **10**, 94 (1952).
- [2] S. Aoki, N. Watanabe, N. Asami, A. Shimada, *Opt. Rev.* First online: 10 February (2016).
- [3] T. Onuki, K. Sugisaki, S. Aoki, *SPIE* 1720, 258 (1992).

# OBSERVATION OF BIOLOGICAL SAMPLES BY USING AN X-RAY MICROSCOPE WITH A FOUCAULT KNIFE-EDGE

N. Watanabe<sup>1</sup>, S. Aoki<sup>1,2</sup>

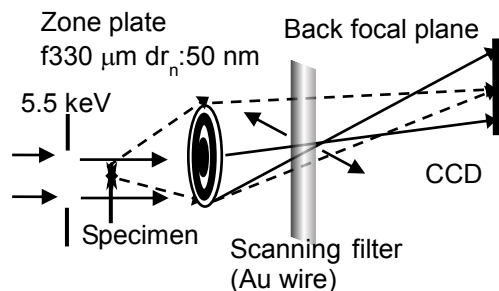
<sup>1</sup>Faculty of Pure and Applied Sciences, University of Tsukuba, Tsukuba, Ibaraki, 305-8573, Japan  
<sup>2</sup>CROSS, 1601 Kamitakatsu, Tsuchiura, Ibaraki, 300-0811, Japan

## Abstract

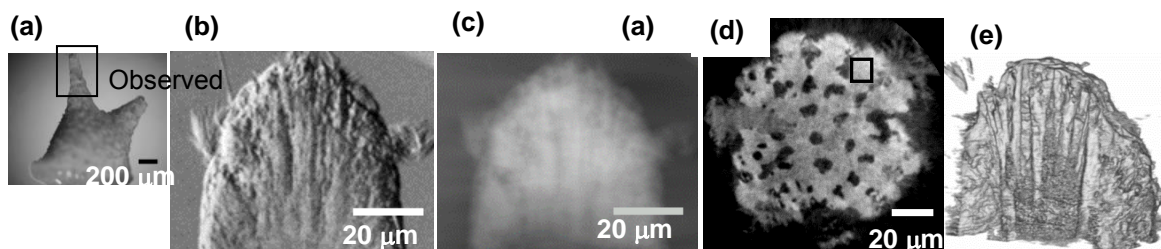
We have been developing a differential phase-contrast microscope at the Photon Factory BL3C, the synchrotron radiation source of the bending magnet. Figure 1 shows the optical system. By introducing a scanning knife-edge filter at the back focal plane of an objective zone plate, relatively quantitative phase imaging and tomography became possible at 5 – 8 keV [1]. As a next step, several biological samples were observed to evaluate the system.

Figure 2 shows images of a distal end portion of a projection of a star sand (a shell of foraminifera). Figure 2(a) is the visible light image. Figure 2(b) is the differential phase image at 5.5 keV, which was calculated from two images recorded by reversing scan direction of the filter. The scan width was 10  $\mu\text{m}$  around the optical axis. Figure 2(c) is the integrated phase image. The 3D phase image was reconstructed from 360 projections over 360 degrees. One of the section image is shown in Fig. 2(d). The average  $\delta$  of refractive index ( $1-\delta$ ) in the black rectangle was  $1.67 \times 10^{-5}$ . Figure 2(e) shows the volume rendering image.

To observe a wide area, a sample scanning and image connection programs were introduced. Figure 3 shows a differential phase image of an ant head. Figure 3(b) shows the  $1.05 \times 1.5 \text{ mm}^2$  area which consists of  $7 \times 15$  field of views. These results shows that this microscope is useful for observation of biological samples.



**Figure 1:** Optical system of a microscope with a knife-edge scanning filter. The filter was scanned about 10  $\mu\text{m}$  during exposure. A differential phase image were calculated from two images with the opposite scanning directions of the filter.



**Figure 2:** X-ray images of a star sand. (a) Visible light image, (b) Differential phase image, (c) Phase image, (d) Section phase image, (e) Volume rendering.

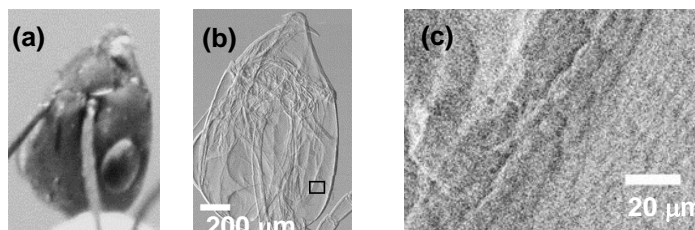


**Figure 3:** X-ray images of an ant head. (a) Visible light image, (b) and (c) Differential phase image

## References

- [1] N. Watanabe, Y. Tsuburaya, A. Shimada, S. Aoki, AIP Conf. Proc. 1696, 020044 (2016).

# NANOFABRICATION OF HIGH RESOLUTION MULTILAYER-FRESNEL ZONE PLATES

U. T. Sanli, K. Keskinbora, C. Grevent, G. Schütz

Max-Planck-Institute for Intelligent Systems, Heisenbergstr. 3, 705679, Stuttgart, Germany

## Abstract

One of the major challenges in X-ray optics is to create optics that can focus hard X-rays down to nanometer resolutions with high diffraction efficiency. The fabrication of such an optic has been a very demanding task because it requires lenses with very high aspect ratios. Among the possible options, multilayer type Fresnel zone plates (ML-FZP) are one of the best suited for accomplishing this challenge, as virtually unlimited aspect ratios can be fabricated through an elegant and a straight forward route [1]. For the fabrication of an ML-FZP we start with a centimeter long glass fiber substrate which has a diameter of 30 microns, and deposit alternating multilayers with atomic layer deposition technique (ALD). The ALD allows angstrom level precision in deposition thickness, and excellent conformality through its sequential, self-limiting surface reactions that take place in the gas phase [2]. This also eliminates the need for rotating the glass fiber that sputtered-sliced ML-FZPs suffer. We can then slice hundreds of ML-FZPs from the deposited glass fiber in the desired thickness *via* a focused ion beam. An SEM image of one of our ML-FZPs is shown in Fig. 1. Being monolithic optics, ML-FZPs are easy to align, have a point focus, and they can be efficient in a very wide X-ray energy range. An efficiency graph as a function of ML-FZP thickness and X-ray energy is shown in Fig. 2 for an  $\text{Al}_2\text{O}_3\text{-SiO}_2$  ML-FZP. With our ML-FZPs, we achieved half-pitch imaging resolution of 15.5 nm. To the best of our knowledge, this is currently the highest imaging resolution reported *via* a multilayer type FZP.

We will also discuss further fabrication routes, strategies and challenges towards efficient focusing of hard and soft X-rays to resolutions below 10 nanometer, through ML-FZPs.

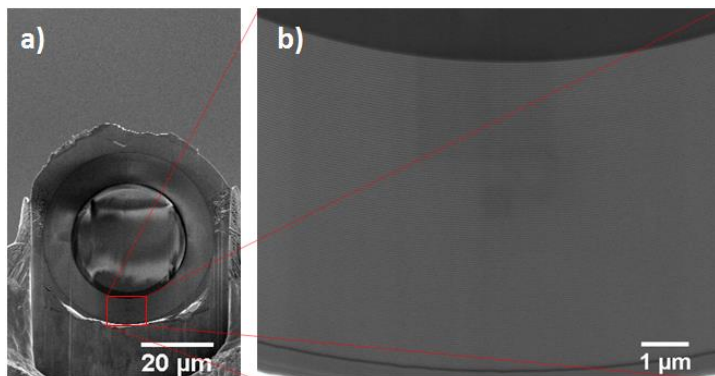


**Figure 1:** a) Overall SEM image of an  $\text{Al}_2\text{O}_3\text{-HfO}_2$  ML-FZP mounted on a TEM grid. The central glass fiber core will be deposited with Pt to act as a beam stop. The FZP has a diameter  $d = 44 \mu\text{m}$ , outermost zone width  $\Delta r = 20 \text{ nm}$  and a deposition thickness of  $6.5 \mu\text{m}$ . b) A high magnification SEM image showing excellent layer and surface quality

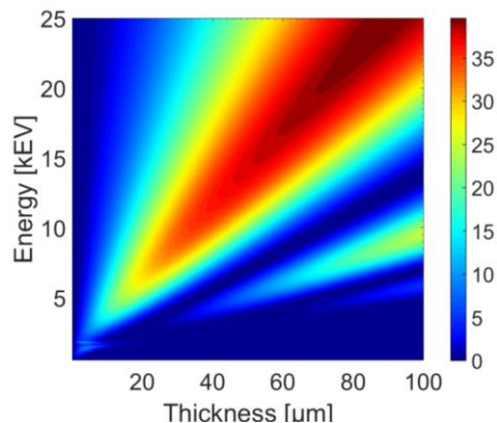


**Figure 2:** Calculated efficiency of an  $\text{Al}_2\text{O}_3\text{-SiO}_2$  ML-FZP as a function of FZP thickness and X-ray energy. Calculations promise very high efficiencies at hard X-rays if required thickness is achieved. The optimum aspect ratio for a  $\Delta r = 20 \text{ nm}$  FZP for 25 keV X-rays would be  $\sim 4000$  according to thin grating approximation.

## References

- [1] M. Mayer, et al., (2011) "Multilayer Fresnel zone plate for soft X-ray microscopy resolves sub-39 nm structures," *Ultramicroscopy*, 111, 1706-1711.
- [2] George, S. M. Atomic layer deposition: an overview. *Chemical reviews* 110, 111-131 (2009).

# THE DEVELOPMENT OF A PARABOLICALLY CURVED MULTILAYER MIRROR FOR AN X-RAY DIFFRACTION SYSTEM

Y. Yao, Z. Zhang, Q. Huang, Z. Wang

*Key Laboratory of Advanced Micro Structural Materials, MOE, Institute of Precision Optical Engineering, School of Physics Science and Engineering, Tongji University, 200092, Shanghai China*

## Abstract

Beam conditioning is one of the most essential parts of an X-ray diffraction system. A parabolically curved multilayer mirror can well collimate the divergent x-ray beam emitted from source.[1] At the same time, it enhances the beam flux comparing to the traditional slit system. The optical performance of such optics has been simulated at first, including the uniformity of the intensity, the divergence of the beam, and the average reflectivity. With a source size of  $100\mu\text{m}$ , The simulated reflection efficiency is 60% and the beam divergence is reduced to 0.6 mrad. To achieve high performance of the optics, the fabrication of a parabolically curved substrate with high quality is a key point. Here, an epoxy replication technique has been used to fabricate the curved substrate.[2] A platinum layer and a periodic multilayer is coated on a supersmooth parabolically curved mandrel first for the separation. Then a regular substrate is bonded to the surface of the mandrel with epoxy to replicate the accurate figure. After that, the deformed substrate is detached together with the separation layers. To achieve a high reflectance, the formed substrate is further coated with a laterally graded multilayer by direct current (DC) magnetron sputtering technology. Both the designed performance and experimental results will be discussed.

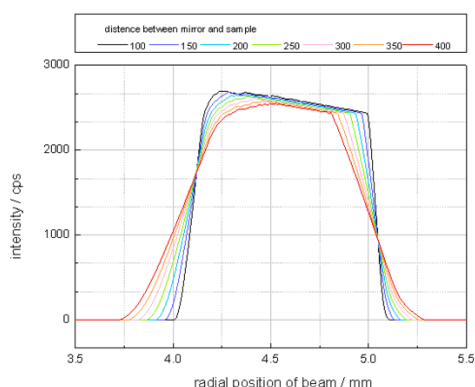


**Figure 1:** The intensity of the collimating beam

## References

- [1] M. Schuster, H. Gobel, *Appl. Phys. Lett.* 28, 00223727 (1995).
- [2] E. Asher, 1988 Los Angeles Symposium--OE/LASE'88, 2-11 (1998).



# IMPROVEMENT OF QUANTITATIVE PERFORMANCE OF IMAGING X-RAY MICROSCOPE BY REDUCING OF EDGE-ENHANCE EFFECT

A. Takeuchi<sup>1</sup>, K. Uesugi<sup>1</sup>, Y. Terada<sup>1</sup>, Y. Suzuki<sup>1,2</sup>

<sup>1</sup>Japan Synchrotron Radiation Research Institute /SPring-8, Kouto 1-1-1 Sayo, Hyogo, Japan  
<sup>2</sup>Graduate School of Frontier Sciences, University of Tokyo, Kashiwa, Chiba 277-8561, Japan

## Abstract

High-resolution x-ray computed tomography (CT) by using imaging x-ray microscope optics with hollow-cone illumination has been developed [1-3], and is now routinely used for various kinds of user experiments at SPring-8. By using a Fresnel zone plate (FZP) as an objective, achieved spatial resolution is approximately 100 nm [4]. For the purpose of quantitative measurement, both a high linearity of image contrast and a large field of view are severely required as well as high spatial resolution. In the present situation, a kind of edge-enhanced pattern (Fig. 1 left) and a periodic pattern noise called as a ringing are still remarkable at the peripheral region of the field of view. This problem is because of a partial coherent illumination and off-axis condition of objective. However, in a FZP optics, neither employing incoherent illumination nor using only a paraxial region are accepted because of necessity of diffraction order sorting. In order to solve this problem, we have newly developed an FZP objective with gradually decreasing zone thickness from the center to the outer regions [5]. Diffraction efficiency distribution of this FZP has a sloped-shouldered shape, that roles like a Gaussian filter in Fourier space. Using this modified FZP, quantitative performance for image contrast was improved by remarkably decreasing edge-enhance contrast (Fig. 1 right). Details of this FZP and noise reduction by using this device will be presented.

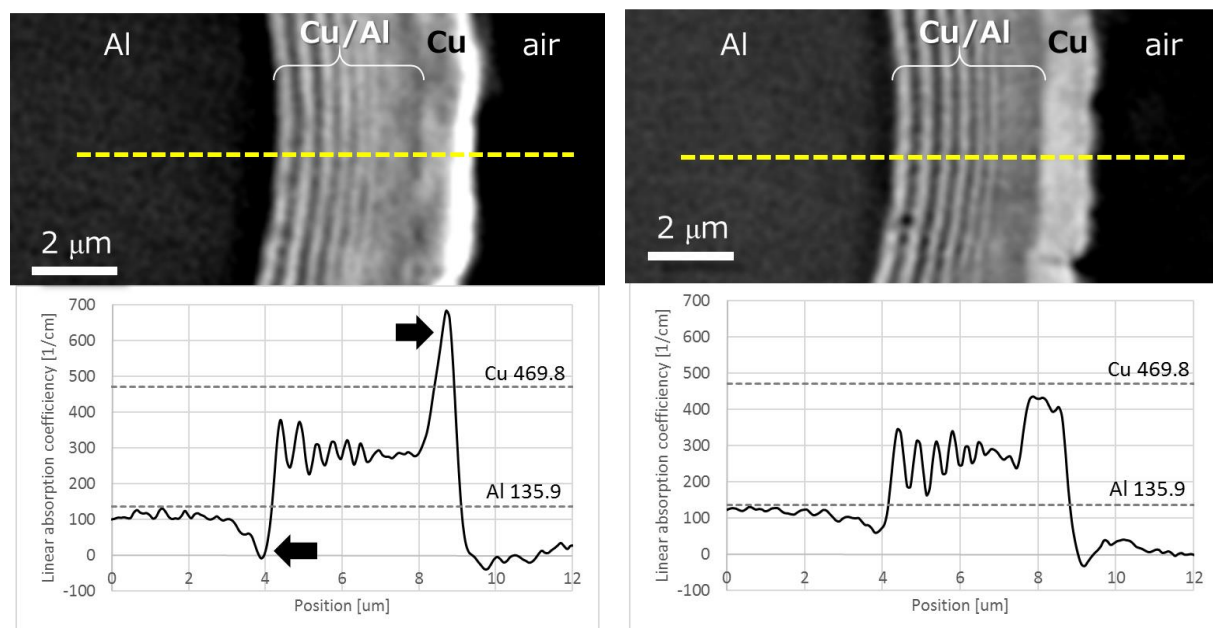


**Figure 1:** CT images (partial view) of concentric Cu/Al test chart and line profiles on broken lines. Left; obtained with normal FZP objective, showing strong edge-enhanced pattern on the boundary of Al/Cu and Cu/air (shown by arrows in the profile). Right; obtained with modified FZP objective. Edge-enhance contrast is remarkably decreased. X-ray energy is 8 keV, voxel size is 83.7 nm, 1800 projection for 180 deg CT rotation, and CT scan time is 30 min.

## References

- [1] A. Takeuchi, K. Uesugi, H. Takano, and Y. Suzuki, *Rev. Sci. Instrum.* 73, 4246 (2002).
- [2] K. Uesugi, A. Takeuchi, and Y. Suzuki, *SPIE* 6318, 63181F (2006).
- [3] A. Takeuchi, K. Uesugi, and Y. Suzuki, *J. Phys. Conf. Series* 186, 012020 (2009).
- [4] R Mizutani, R. Saiga, S. Takekoshi, et. al., *J. Microsc.* 261, 57 (2016).
- [5] A. Takeuchi et al. in preparation.

# OPTICAL DESIGN FOR THE CARNAUBA BEAMLINE AT SIRIUS: ANALYTICAL AND HYBRID RAY TRACING CALCULATIONS

Hélio C.N. Tolentino<sup>1,2</sup>, Harry Westfahl Jr.<sup>1</sup>, Márcio M. Soares<sup>1</sup>, Sérgio A.L. Luiz<sup>1</sup>, Bernd Meyer<sup>1</sup>

<sup>1</sup> Laboratório Nacional de Luz Síncrotron LNLS, CP 6192, 13083-970 Campinas, Brazil

<sup>2</sup> CNRS, Institut Néel, 25 rue des Martyrs, 38042 Grenoble, France

## Abstract

The CARNAUBA beamline [1] is the longest among the first phase SIRIUS beamlines at the LNLS, Brazil. Its main goal is to perform coherent scattering, imaging and spectroscopy with a nano-focused beam in the 2 to 14 keV X-ray energy range. CARNAUBA uses an undulator source (vertical linear polarization) in a low-beta straight section and grazing incidence-focusing mirrors to create, at 145 m from the source, a nanoprobe down to the diffraction limit (fig.1). Designing mirror based optical systems usually starts by estimating the optical layout analytically before running a numerical ray-tracing simulation with eventually wave propagation. These analytical estimates typically employ the approximation where thin lenses replace the mirrors. This approximation is only valid if mirror lengths are much smaller than the distances of the optical element to the source or image. However, in strongly demagnifying mirror systems, as in CARNAUBA, this condition is rarely verified since large mirrors and short working distances are required to increase demagnification and numerical aperture.

We have used simple analytical expressions for geometrical optics outside the thin lens approximation and introduced a correction for the diffraction limit to design and optimize the CARNAUBA optical layout (fig.2). Afterwards, a hybrid ray tracing code has been used to fully take into account the optical layout, errors in the mirrors and the wave character of the propagation. Both calculations fits very well to each other, giving similar results in terms of flux of photons, divergences and nanoprobe sizes [2]. These results certifies the analytical calculations, which has proven to be a valuable and flexible tool in the layout optimization procedure. In addition, it demonstrates the use of the hybrid ray tracing code in an example where wave propagation really matters all along the beamline components.

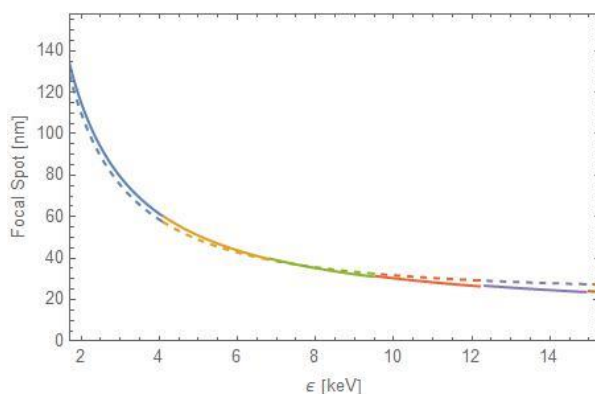


**Figure 1:** FWHM size of the beam on the sample as function of energy (vertical: full line; horizontal: dashed line). A secondary source aperture is used to adjust the horizontal focus size.

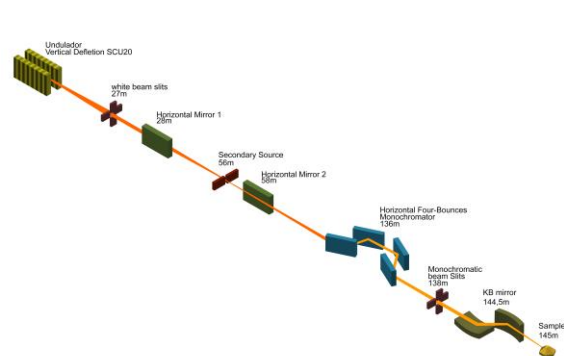


**Figure 2:** Schematic representation of the CARNAUBA beamline layout, indicating the position of the main components.

## References

- [1] H.C.N.Tolentino, et al, CARNAUBA Conceptual Design Report, LNLS Internal documentation (2016)
- [2] H. Westfahl Jr., et al, et al, to be submitted to J. Synchrotron Rad. (2016)

# METAL ASSISTED CHEMICAL ETCHING FOR HARD X-RAY ZONE PLATE FABRICATION

S. Giakoumidis, J. Rahomäki, U. Vogt

*KTH Royal Institute of Technology, Department of Applied Physics, Albanova University Center S-10691, Stockholm, Sweden*

## Abstract

We are developing diffractive x-ray optics (zone plates) for the NanoMAX beamline at MAX IV in Lund. The zone plates are fabricated with metal-assisted chemical etching (MACetch) of silicon instead of the typical industrial dry etching. The high-resolution zone plate optics with high-efficiency are tailored for use at energies around 10 keV. Zone plates with outermost zone width of 45 nm has been fabricated via wet etching silicon, while the aim is to reach down to 10 nm lines.

The main step in device fabrication is metal-assisted chemical etching of silicon [1]. The zone plate pattern is created in a thin gold layer on top of a silicon substrate by e-beam lithography and a standard lift-off process. Then the pattern is transferred into the silicon by wet etching in a solution containing HF, H<sub>2</sub>O<sub>2</sub> and H<sub>2</sub>O. This technique shows clear advantages over dry etching, like faster etching speed, no need of special etching equipment, very high aspect ratios (>35:1) and lower costs. For the final x-ray zone plate, a layer of iridium is deposited on top the fabricated silicon structures by atomic layer deposition. In this work a 45 nm outermost width zone plate has been successfully fabricated in silicon via metal-assisted chemical etching.

We think wet etching of silicon is a very promising technique to be applied in the x-ray optics fabrication area. With fine tuning of the process unique characteristics of very high aspect ratios at small linewidth are possible [2].

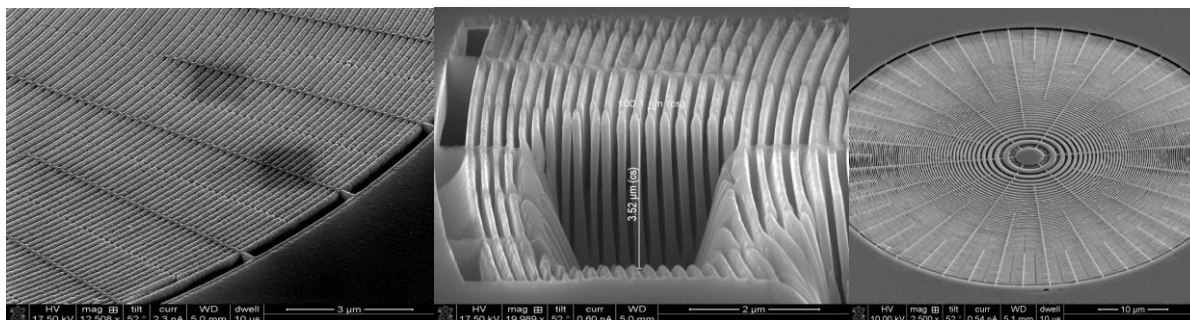


**Figure 1:** Hard x-ray zone plate with 45 nm outermost zone width fabricated in silicon and iridium

**Figure 2:** Very high aspect ratio structures in silicon fabricated by MACetch. 100 nm thick and at least 3.52 µm deep lines.

**Figure 3:** A 45 nm outermost zone width zone plate in silicon as it is seen after etching

## References

- [1] Z. Huang et al., Metal-assisted Chemical Etching of Silicon: A Review, *Adv. Mater.* 2011
- [2] C. Chang, Ann Sakdinawat, Ultra-high aspect ratio high-resolution nanofabrication for hard X-ray diffractive optics, *Nat. Comm.* 2014

# IMPROVED TUNGSTEN NANOFABRICATION FOR HARD X-RAY ZONE PLATES

K. Parfeniukas<sup>1\*</sup>, J. Rahomäki<sup>1</sup>, S. Giakoumidis<sup>1</sup>, and U. Vogt<sup>1</sup>

<sup>1</sup>Department of Applied Physics, KTH Royal Institute of Technology, SWEDEN

\*karolisp@kth.se

## Abstract

We present an improved nanofabrication method of dense high aspect ratio tungsten structures for use in high efficiency nanofocusing hard X-ray zone plates. The main improvement is that the patterned e-beam resist layer is cured by a second, much larger electron dose after development. This step improves pattern transfer fidelity into the hardmask. A 630 nm-thick tungsten zone plate with smallest line width of 30 nm was made and had an efficiency of 2.2% at 8.2 keV photon energy with a focal spot size at the diffraction limit, measured at Diamond Light Source I13-1 beamline.

The design of latest-generation synchrotron radiation facilities allows for an increase in coherence and photon flux at the sample, but current instruments are still limited by the focusing optics. Zone plate optics are circular diffraction gratings with radially decreasing linewidth. The resolution is defined by outermost linewidth, while the efficiency peaks at a certain structure height. Small linewidth and adequate height have been shown in tungsten, but not at the same time. We provide a method for fabricating tungsten structures with an aspect ratio of 21:1 at 30 nm linewidth. [1]

A thin film stack of 5 nm of Cr, 600 nm of W, 25 nm of Cr, and 80 nm of ZEP 7000 is prepared on a 1  $\mu\text{m}$   $\text{Si}_3\text{N}_4$  membrane. The e-beam pattern is exposed using a 100 keV e-beam lithography tool and cold-developed in hexylacetate. The whole area is exposed again at 5 kV with a much larger dose. This improves pattern transfer fidelity (see Fig. 1). The e-beam resist pattern is transferred into the Cr using reactive ion etching with  $\text{Cl}_2/\text{O}_2$  chemistry at +30 °C, and then into W using  $\text{SF}_6/\text{O}_2$  at -35 °C.

We fabricated a zone plate that is 630 nm thick, has a diameter of 200  $\mu\text{m}$ , outermost zone width of 30 nm (see Fig. 2), and a first order focal length of 40 mm at 8.2 keV photon energy. It demonstrated 2.2% total efficiency, measured at Diamond Light Source I13-1 beamline (see Fig. 3). The theoretical efficiency is 11.3%. The main contribution to the lower measured efficiency is decreased density of the sputtered film compared to bulk tungsten. Imperfect vertical profile of the structures also has an effect, seen in radially decreasing efficiency in the zone plate (Fig. 3).

In this work, we presented an improved way to fabricate high aspect ratio tungsten nanostructures. Including a resist curing step into the existing process increased the fidelity of pattern transfer. We showed and characterized a zone plate with a 30 nm outermost zone and an aspect ratio of 21:1. It had a total efficiency of 2.2% at 8.2 keV photon energy with a focal spot size at the diffraction limit.

## ACKNOWLEDGEMENTS

We thank Diamond Light Source for access to I13-1 beamline (proposal no. MT12046), and the Swedish Research Council (grant ID C0242401) and the Knut and Alice Wallenberg Foundation for financial support.

## REFERENCES

[1] K. Parfeniukas, J. Rahomäki, S. Giakoumidis, F. Seiboth, F. Wittwer, C.G. Schroer, and U. Vogt, *Microelectron. Eng.* 152 (2016) 6

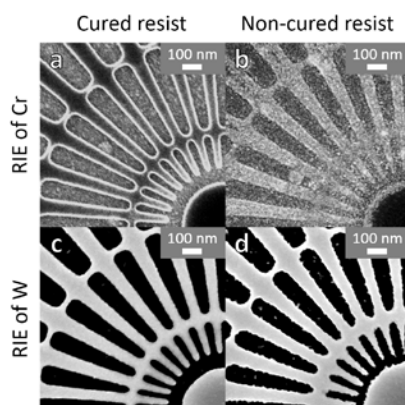


**Fig. 1.** Comparison of pattern transfer quality in test samples using cured and non-cured resists. Top view of hardmask after pattern transfer into the hardmask layer (a) with curing, (b) without curing; after pattern transfer into tungsten (c) with curing, (d) without curing.

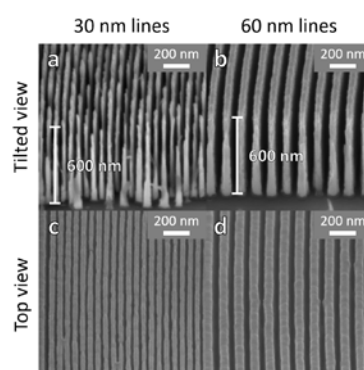


**Fig. 2.** Vertical zone profile with line width of (a) 30 nm and (b) 60 nm. Top view of the zone plate structures at line width of (c) 30 nm, (d) 60 nm.

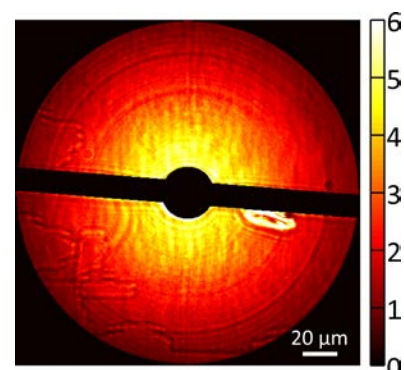


**Fig. 3.** Local zone plate efficiency in percent.

# A FAST ENERGY TUNABLE HARD X-RAY FULL FIELD NANOSCOPE

A. Bonnin<sup>1</sup>, I. Vartiainen<sup>2,3</sup>, R. Mokso<sup>1,4</sup>, C. David<sup>2</sup>, M. Stampanoni<sup>1,5</sup>

*1Swiss Light Source, Paul Scherrer Institute, 5232 Villigen, Switzerland*

*2Laboratory for Micro- and Nanotechnology, Paul Scherrer Institute, 5232 Villigen, Switzerland*

*3Institute of Photonics, University of Eastern Finland, FI-80101 Joensuu, Finland*

*4MAX IV Laboratory, Lund University, P.O. Box 118, 221 00 Lund, Sweden*

*5Institute for Biomedical Engineering, University and ETH Zurich, Gloriastrasse 35, 8092 Zurich, Switzerland*

## Abstract

Since the past 40 years, full-field Transmission X-ray Microscopes (TXM) have been developed for X-ray application in order to reach high resolution. They are well adapted to get 3D information on samples where the contrast between structures have very similar absorption.

Based on the development done in visible-wavelength bright-field microscope, TXM are composed of a condenser optic and an objective Fresnel Zone Plate (FZP) to focus the transmitted X-rays from the sample onto a CCD. Thanks to the improvements brought by Zernike [1] for optical application, phase contrast is achieved by placing a phase shifter at the back-focal plane of the FZP.

The TOMCAT nanoscope is composed of a custom designed beamshaper [2] producing a top-flat illumination in the focal plane [3], a series of Fresnel Zone Plate (FZP) with different diameters on the same frame and the corresponding Zernike phase shifter rings, to use phase contrast (specially for low absorbing material). The new design of our instrument comprises a reduction of the typical artifacts in Zernike phase imaging [4] and the possibility to easily and quickly change the X-ray Energy for the full-field microscope in the energy range of 8-20 keV [5]. This opens the possibility to fine-tune the acquisition energy according to the sample and also to distinguish different materials by K-edge imaging for example.

This instrument has been built in such a way that the sample position remains fixed: for a working energy, the condenser is placed at the appropriate focusing distance and the diameter of the FZP is chosen accordingly. In this way, the magnification is also fixed, i.e. a constant pixel size of 80 nm for all energies. With our new camera, the XSight™ uRapid Camera, a tomography acquisition (about 1000 projections) is now comparable to a standard tomography acquisition at TOMCAT: about 5 min with our Multilayer (energy bandwidth of  $10^{-2}$ ) and about 30 min with the Si111 (energy bandwidth of  $10^{-4}$ ).

Working from 8 to 20 keV, our Full Field TXM setup reaches a spatial resolution down to 150 nm both in absorption and phase contrast mode. Having the capabilities to work at such high energy range opens a wide range of applications from biology application to materials science.

## References

- [1] Zernike F. (1934). *Physica* 1, 689.
- [2] Stampanoni M. et al. (2010). *Physical Review B* 81, 140105.
- [3] Jefimovs K. et al. (2008). *J. Synchrotron Radiation* 15, 106.
- [4] Vartiainen I. et al. (2014). *Opt. Lett.* 39,1601.
- [5] Bonnin A. et al. (2016). Submitted.



# XMI-MSIM: A GENERAL MONTE CARLO SIMULATION OF ENERGY-DISPERSIVE X-RAY FLUORESCENCE SPECTROMETERS

T. Schoonjans<sup>1</sup>, L. Vincze<sup>2</sup>, V.A. Solé<sup>3</sup> and C.Ferrero<sup>3</sup>

*1 Diamond Light Source Ltd, Diamond House, Harwell Science and Innovation Campus, Didcot, UK*

*2 X-ray Microspectroscopy and Research group, Ghent University, Krijgslaan 281, B-9000, Gent, Belgium*

*3 European Synchrotron Radiation Facility, rue Jules Horowitz 6, 38043 Grenoble, France*

## Abstract

Since their inception during the Manhattan project, Monte Carlo simulations have been used for a variety of applications in physics, mathematics, engineering, finance and more. When applied to X-ray fluorescence spectroscopy, it is well known that Monte Carlo simulations are useful for predicting the spectral response of samples irradiated with an X-ray beam of given characteristics. This requires the development of a dedicated computer code that simulates the histories of a large number of individual photons, whose trajectories in the system are modeled as a number of straight steps. At the end of each step, an interaction occurs, leading to a change in direction, energy and polarization state. A photon's trajectory is terminated when it leaves the system, or when the detector captures it. If detection occurs, one count is added to the appropriate channel of a virtual multichannel analyzer.

We have developed a new software package *XMI-MSIM*[1], based on the Monte Carlo code by Vincze et al[2], enhancing and extending it with numerous new features. These include an update of the essential physical data such as cross sections, fluorescence yields and transition rates through linking with the *xraylib*[3] package. Through this dependency, it is now possible to simulate M-lines and cascade effects (radiative and non-radiative). From a software viewpoint, the use of advanced programming techniques such as multithreading and multiprocessing has led to a significant increase in computational efficiency and allows for the deployment on supercomputers, which is recommended when operating in brute-force mode.

Optionally, the code can be called as a plugin from PyMca[4], an open-source tool for XRF spectral analysis, where it serves as an alternative to the default fundamental parameter based quantification procedure. This is accomplished by means of an iterative algorithm in which the simulated line intensities are compared with those experimentally observed, while at every iteration step the simulation input concentrations are adapted until convergence of the line intensities is reached.

The code itself is written in C and Fortran 2003, and makes extensive use of several open source packages. *XMI-MSIM* is available at <http://www.github.com/tschoonj/xmimsim> and is distributed under the GNU General Public License (GPL).

## References

- [1] T. Schoonjans et al. *Spectrochimica Acta B*, 70, 2012, 10-23
- [2] L. Vincze et al. *Spectrochimica Acta B*, 48(4), 1993, 553-573.
- [3] T. Schoonjans et al. *Spectrochimica Acta B*, 66(11-12), 2011, 776-784.
- [4] T. Schoonjans et al. *Spectrochimica Acta B*, 82, 2013, 36-41

# Scattering and absorption of X-rays from a rough surface at extremely small grazing angles

Mingwu Wen<sup>1,2</sup>, Qiushi Huan<sup>1</sup>, Igor V. Kozhevnikov<sup>3</sup>, Zhanshan Wang<sup>1</sup>

<sup>1</sup> MOE Key Laboratory of Advanced Micro-Structured Materials, Institute of Precision Optical Engineering, School of Physics Science and Engineering, Tongji University, Shanghai 200092, China

<sup>2</sup> Max-Planck-Institute for extraterrestrial Physics, Giessenbachstr. 85748 Garching, Germany

<sup>3</sup> Shubnikov Institute of Crystallography, Russian Academy of Sciences, Moscow 119333, Russia

## Abstract

The X-ray scattering technique is a unique instrument to study roughness with a lateral resolution comparable to that of atomic force microscopy (AFM), and, in contrast to AFM, it allows for the investigation of latent interfaces and statistical interrelation (conformity) between the roughnesses of different interfaces. Peculiarities of X-ray diffraction from a rough surface at an extremely small grazing angle of an incident beam are of essential practical importance for the development of optics for existing and future free electron lasers (FELs). In this paper, the interrelation of four diffraction channels (coherent reflectance, coherent transmittance, diffuse scattering in vacuum, and scattering into the matter depth) is analyzed for different limiting cases [1]. Both the Debye-Waller and the Nevot-Croce factors are demonstrated to describe improperly the features of X-ray diffraction at extremely small grazing angles. Transformation of one limiting diffraction regime into another one with variation in the correlation length of roughness is discussed.

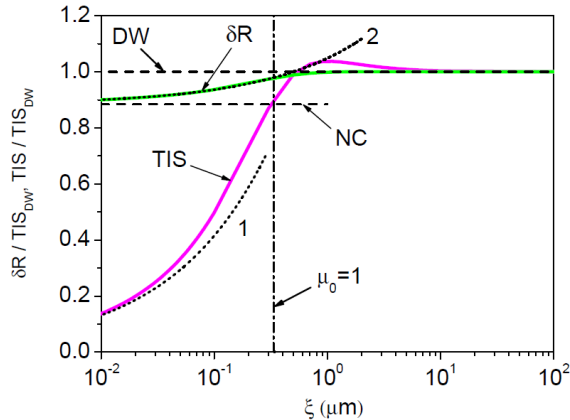


**Figure 1:** The total integral scattering (TIS) and specular reflectance ( $\delta R$ ) of an Au-coated mirror at the photon energy  $E = 3$  keV and with the grazing angle of an incident beam of  $\theta_0 = 50$  mrad versus the correlation length of roughness.

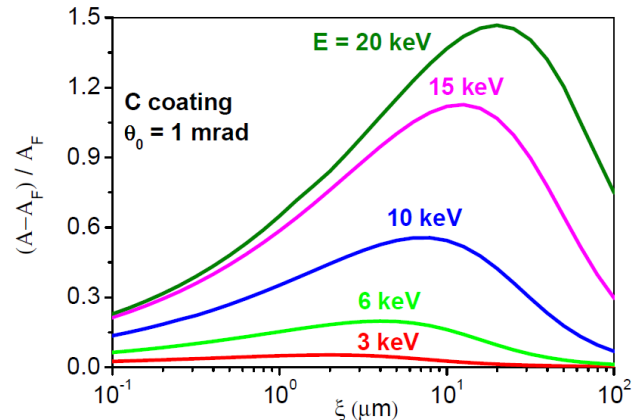


**Figure 2:** The dependence of the relative increase in the absorptivity versus the roughness correlation length of carbon-coated mirror operated at the 1 mrad grazing incidence angle and different photon energies.

## References

- [1] M. Wen, I. V. Kozhevnikov, Z. Wang, *Opt. Express* 23, 24220 (2015).

## Multi-Element SDD Spectrometers for Mapping Applications at High Count Rate

Valeri D. Saveliev<sup>(1)</sup>, Shaul Barkan<sup>(1)</sup>, Liangyuan Feng<sup>(1)</sup>, Yen-Nai Wang<sup>(1)</sup>  
 Elena V. Damron<sup>(1)</sup>, Mengyao Zhang<sup>(1)</sup>  
 and Roger Goldsbrough<sup>(2)</sup>

(1) Hitachi High-Technologies Science America, Inc. 19865 Nordhoff St., Northridge, CA 91324, USA.

(2) Quantum Detectors Ltd. Atlas Building, Fermi Avenue, Harwell Oxford, OX11 0QX, UK

### Abstract

A 3- and 4-element SDD XRF spectrometers (Vortex-ME3 and Vortex-ME4) have been developed for advanced x-ray spectroscopy, such as x-ray fluorescence micro imaging, fluorescence computed microtomography (fCMT), XANES (x-ray absorption near-edge structure) and EXAFS (extended x-ray absorption fine structure).

These multi-element SDD spectrometers are based on 0.5 and 1 mm thick Vortex<sup>®</sup> SDDs, integrated with advanced front-end ASIC preamplifiers, and they feature an excellent energy resolution at extremely short peaking times [1]. The option with unique 1 mm thick SDD provides also significantly increased detection efficiency of x-rays at high energy.

High performance of the multi-element SDD spectrometers could be most fully realized in combination with a modern adaptive processing electronics the Xspress3, developed by Quantum Detectors (Harwell Oxford, UK). Figure 1 presents a result of fCMT measurement at the count rate up to 10 Mcps, undertaken at Argonne National Laboratory, sector 13-D-E, with the Vortex-ME4 and Xspress3. Sample for this measurement is large in one direction and small in the other direction that determinates huge count rate difference in different directions. This measurement was possible due to extremely wide dynamic range of the Xspress3. Other data concerning the design and performance of multi-element SDD XRF spectrometers will be presented.

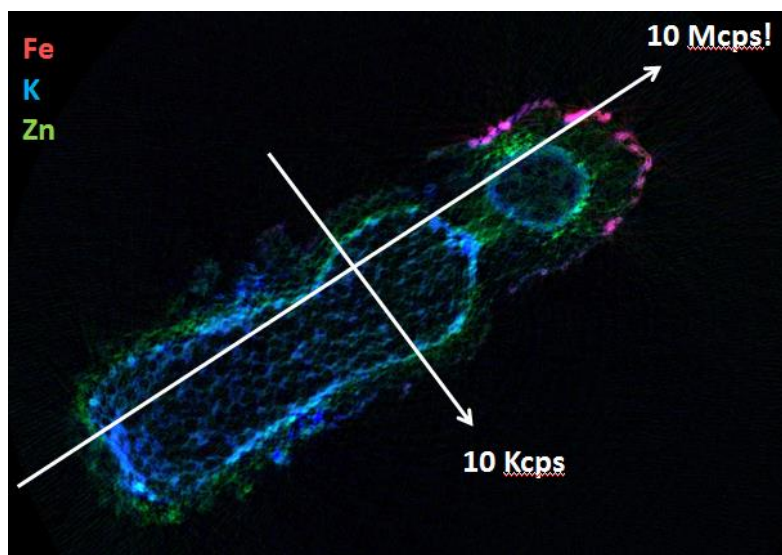


**Figure 1.** The fCMT measurement: Xspress3 with Vortex<sup>®</sup> ME-4.

### References

[1] S. Barkan, V.D. Saveliev, Y. Wang, L. Feng, E.V. Damron, Y. Tomimatsu, "Extreme High Count Rate Performance with a Silicon Drift Detector and ASIC Electronics", Biological and Chemical Research, Volume 2015, 338-344.

## Achromatic full-field X-ray microscope with 50 nm resolution and its applications

S. Matsuyama<sup>1</sup>, S. Yasuda<sup>1</sup>, H. Okada<sup>2</sup>, Y. Kohmura<sup>3</sup>, M. Yabashi<sup>3</sup>,  
T. Ishikawa<sup>3</sup>, K. Yamauchi<sup>1</sup>

<sup>1</sup> Department of Precision Science and Technology, Graduate School of Engineering, Osaka University, 2-1 Yamada-oka, Suita, Osaka 565-0871, Japan

<sup>2</sup> JTEC Corporation, 2-4-35, Saito-Yamabuki, Ibaraki-city, Osaka 567-0086, Japan

<sup>3</sup> RIKEN SPring-8 Center, 1-1-1, Kouto, Sayo-cho, Sayo-gun, Hyogo 679-5148, Japan

### Abstract

Achromatic and high-resolution full-field X-ray microscopes are very promising for realizing spectronanoscopies in the X-ray region [1]. However, there were no suitable imaging optical systems that simultaneously possess high resolution, achromaticity, and practical feasibility.

We developed an achromatic imaging optical system based on total reflection mirrors, which consists of two pairs of imaging mirrors that have elliptical and hyperbolic shapes on a substrate [2]. Such a monolithic structure makes the imaging system highly stable and easy to use. The mirrors were fabricated with a shape accuracy of at least 2 nm. By combining a polycapillary lens and an X-ray camera, a full-field X-ray microscope was constructed at BL29XUL of SPring-8 (Fig. 1). The magnifications in the horizontal and vertical directions are 637 and 196, respectively. The numerical aperture is  $\sim 1.5 \times 10^{-3}$ , and the maximum acceptable X-ray energy is  $\sim 12$  keV.

An image test was performed at an X-ray energy of 9.881 keV using a Siemens star chart made of tantalum with a minimum line width of 50 nm. Bright-field images that clearly exhibited 50 nm features in the innermost region were obtained (Fig. 2). Images with different incident X-ray energies were obtained for further investigation of chromatic aberration. It was found that achromatic imaging is feasible without losing image quality over a wide energy range of 8–12 keV.

Two applications in X-ray absorption fine structure (XAFS) imaging and X-ray fluorescence imaging were attempted. The XAFS imaging of submicron-sized particles was performed by simply changing the input X-ray energy, and the results provided good resolution and clear XAFS spectra. The feasibility of the X-ray fluorescence imaging was only tested so far. Zinc particles with a few micron diameter on a copper mesh were visualized by identifying fluorescence signals of zinc and copper using a charge-coupled device (CCD) camera in single-photon counting mode.

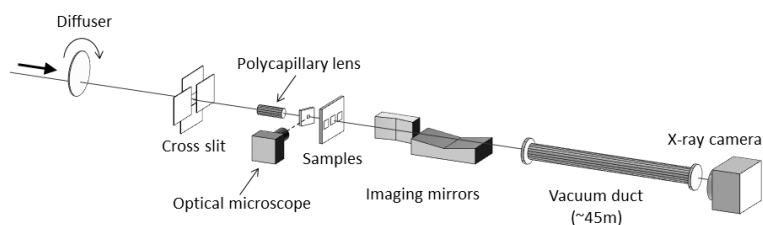


**Figure 1:** Experimental setup of the bright-field imaging system. The microscope was constructed between the first and third experimental hutches at BL29XUL of SPring-8.

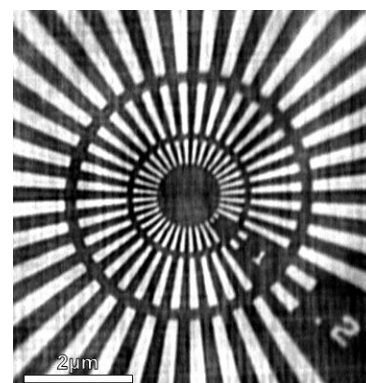


**Figure 2:** Bright-field X-ray image. The 50 nm features in the innermost region are visible.

### References

- [1] S. Matsuyama *et al.*, *Opt. Express* **23**, 9746-9752 (2015).
- [2] S. Matsuyama *et al.*, *Proc. SPIE* **9592**, 959208 (2015).

# CURRENT STATUS OF A HARD X-RAY BEAMLINE AND END-STATION FOR PUMP AND PROBE EXPERIMENTS AT POHANG ACCELERATOR LABORATORY X-RAY FREE ELECTRON LASER FACILITY

S. Kim, J. Park, K. Kim

*Pohang Accelerator Laboratory, Jigokro-127-beongil, Nam-gu, Pohang, Gyeongbuk 790-834, Republic of Korea*

## Abstract

The Pohang Accelerator Laboratory X-ray Free Electron Laser project, a new worldwide-user facility to deliver ultrashort, laser-like x-ray photon pulses, will begin user operation in 2017 after one year of commissioning. Initially, it provides two beamlines for hard and soft x-rays, respectively, and two experimental end-stations for the hard x-ray beamline were constructed at the end of 2015. This article introduces one of the two hard x-ray end-stations, which is for hard x-ray pump-probe experiments, and primarily outlines the overall design of this end-station and its critical components. The content of this article will provide useful guidelines for the planning of experiments conducted at the new facility.

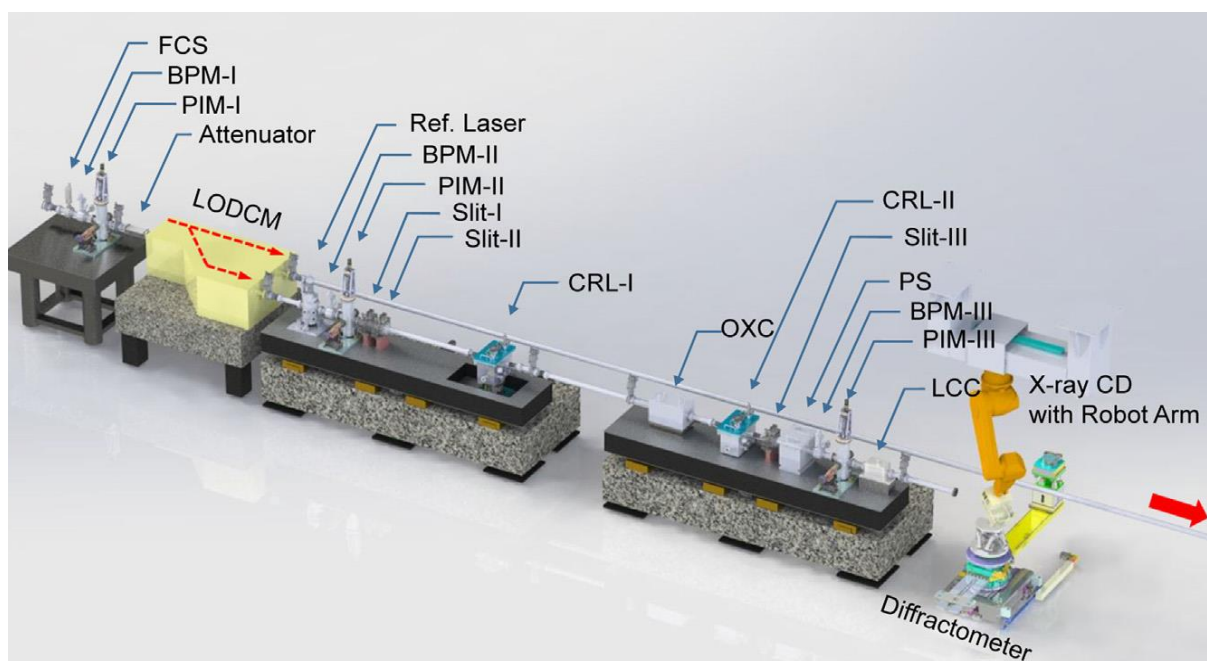


**Figure 1:** HES1 configuration.

## References

- [1] Park J, Eom I, Kang TH, Rah S, Nam KH, Park J, et al. Nucl Instrum Meth A. 810:74-9(2016).



## SUB-MICRON X-RAY FLUORESCENCE MAPPING FACILITY ON THE B16 TEST BEAMLINE AT DIAMOND

I Pape<sup>1</sup>, C Mita<sup>1</sup>, N De Maio<sup>1</sup>, T Geraki<sup>1</sup>, A Malandain<sup>1</sup>, C Strel<sup>2</sup>, K Sawhney<sup>1</sup>

<sup>1</sup>Diamond Light Source, Harwell Science and Innovation Campus Didcot, Oxfordshire, OX11 0DE

<sup>2</sup>Atominstut, Technische Universitaet Wien, Stadionallee 2, 1020 Vienna, Austria

### Abstract

B16 Test Beamline at Diamond Light Source is a general purpose, versatile and flexible beamline where novel experimental set-ups can be realised [1]. Taking advantage of this flexibility, a sub-micron x-ray fluorescence mapping facility has been developed on B16. Focused beams of  $\sim 0.5 \mu\text{m}$  fwhm are generated using a white-beam compatible KB mirror system. A very-high flux focused beam can be provided by using white-beam from the beamline; or a narrow 1% bandwidth beam tuneable in the 8-20 keV energy range can be provided by using beamline's multilayer monochromator. Photon flux in the focal spot with the mono beam is of the order of  $5 \times 10^9$  photons / second. Samples can be raster scanned using piezo motors whilst a four element Vortex spectroscopy detector is used to collect the fluorescence signal. In the last year, the sub-micron mapping facility has been used for several user experiments for studying the elemental distribution in a variety of sample types including biological cells [2], bones and retina samples of animals. Figure 1 shows an example of the elemental distribution in cells. Technical details of the new sub-micron X-ray mapping facility will be presented along with representative results from users' recent experiments.

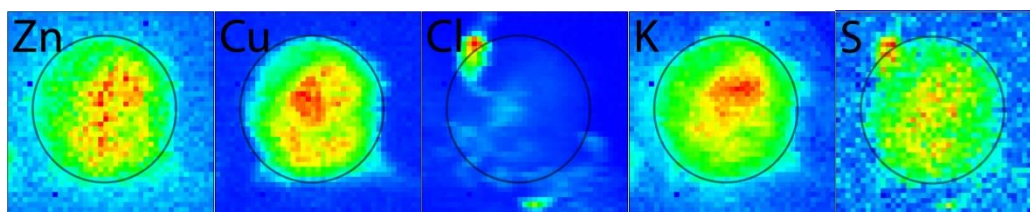


**Figure 1:** Nano XRF image of a cancer cell treated with Cu, measured with a nanobeam of  $400 \times 600$  nm from DIAMOND, Beamline B16, monochromatic excitation with DMM set to 17 keV, Field of view:  $20 \times 20 \mu\text{m}$ .

### References

- [1] K. J. S. Sawhney, I. P. Dolbnya, M. K. Tiwari, L. Alianelli, S. M. Scott, G. M. Preece, U. K. Pedersen and R. D. Walton, AIP Conf. Proc. 1234 (1), 387-390 (2010).
- [2] V. G. Mihucz, F Meirer, Z Polgári, A Réti, G Peponi, D Ingerle, N Szoboszlai, C Strel, J Biol Inorg Chem, pp1-9, DOI 10.1007/s00775-015-1331-x (2016)

# TOMCAT: HIGH TEMPORAL RESOLUTION TOMOGRAPHIC MICROSCOPY OVER SEVERAL LENGTH SCALES

F. Marone<sup>1</sup>, C. M. Schlepütz<sup>1</sup>, A. Bonnin<sup>1</sup>, M. Stampanoni<sup>1,2</sup>

*1Swiss Light Source, Paul Scherrer Institute, 5232 Villigen, Switzerland*

*2Institute for Biomedical Engineering, University and ETH Zurich, Gloriastrasse 35, 8092 Zurich, Switzerland*

## Abstract

Thanks to its versatility, TOMCAT [1], the tomographic microscopy beamline of the Swiss Light Source, enables the volumetric investigation of very diverse specimens ranging from naturally low absorbing fresh biomedical tissues, over a combination of low and high absorbing new materials (foams, fiber, ceramics, alloys, etc.) to rare and delicate fossils. The TOMCAT experimental endstation, equipped with different microscope optics and digital cameras, is very flexible and can accommodate sample sizes from a few microns to a few centimeters achieving spatial resolutions, respectively, from 200 nm with a hard X-ray full-field microscope setup to several microns in parallel geometry.

Latest developments focused on establishing the ultrafast tomography program, pushing the time resolution in 3D up to 20 Hz [2], for spatial resolutions of a few microns. The core of this newest endstation consists of the GigaFRoST [3], an in-house developed system that features continuous data streaming with transfer rates of 7.7 GB/s and thus overcomes limitations imposed by the on-board memory capacity of commercially available CMOS detectors. These enhanced rates, in conjunction with flexible triggering modes, make the GigaFRoST very versatile and adaptable to complex (in-situ and in-vivo) experimental procedures, permitting new investigations of dynamic processes in 3D not possible before.

The temporal resolution has also been significantly improved for the hard X-ray full-field microscope setup [4] delivering a pixel size of 80 nm for microscopic samples (~50  $\mu\text{m}$  field of view). Shorter scan times (< 5 min) together with a better detector (PCO.edge with fiber optic taper), efficient diffractive optics from 8 up to 20 keV, and enhanced component stability greatly contributed to considerably improve the nanotomographic datasets.

Phase contrast phenomena exploiting the partial coherence of the synchrotron beam are increasingly exploited to improve the contrast-to-noise ratio without need for increased dose deposition [3]. Propagation phase methods [5], coupling experimental simplicity, high spatial resolution, and moderate electron density sensitivity, represent often the chosen technique and are compatible with dynamic systems. In addition to absorption and differential phase contrast, grating interferometry [6] also provides complementary information related to the scattering properties of the investigated specimens. This dark-field signal extends the spatial resolution of conventional systems and can give access to unresolved (sub)-micrometer structural variation in large objects [7].

The IT infrastructure (storage, computing cluster and network bandwidth) as well as the reconstruction, data analysis and visualization software are being expanded and upgraded to match the new requirements enforced in particular by the new ultrafast program and therefore enable efficient handling and post-processing, both on-site and remotely, of the large amount of data acquired daily.

## References

- [1] Stampanoni M. et al., SPIE Proc., 2006
- [2] Maire E. et al., Int. J. Fracture, 2016
- [3] Mokso R. et al., J. Phys. D: Appl. Phys., 2013
- [4] Stampanoni M. et al., Phys. Rev. B, 2010
- [5] Paganin D. et al., J. Microscopy, 2002
- [6] McDonald S. et al., J. Synchrotron Rad., 2009
- [7] Kagias M., PRL, 2016

# HIERARCHICAL LENGTH-SCALE SCANNING MULTIMODAL IMAGING AT THE NANOSCOPIUM BEAMLINE OF SYNCHROTRON SOLEIL

A. Somogyi, K. Medjoubi, A. Bergamaschi, V. Le Roux, G. Baranton

*Nanoscopium BL, Synchrotron Soleil, L'Orme des Merisiers, Saint-Aubin - BP 48, 91192 GIF-sur-YVETTE CEDEX, France italic Arial font*

## Abstract

The Nanoscopium 155 m long hard X-ray nanoprobe beamline [1, 2] aims to provide high sensitivity elemental, and structural mapping by scanning multimodal imaging in the 5-20 keV energy range. The typical scientific applications of the beamline cover various fields, such as biology and life sciences, earth- and environmental sciences, geo-biology and bio-nanotechnology. The beamline is especially well suited for studies seeking information about highly heterogeneous systems at multiple length scales. Namely, large overview, moderate spatial resolution multimodal 2D imaging of  $\sim\text{mm}^2$  sample areas can be performed in some minutes [3]. This provides the possibility of choosing regions of interest for higher spatial resolution studies based on the association of major sample morphological features and elemental distributions, which are invisible by optical microscopy. Moreover, we introduced a new analytical strategy for scanning multimodal tomography [2], where as a first step draft elemental distributions and morphology of the whole sample (with up to hundreds  $\mu\text{m}$ 's dimensions) is obtained from multimodal 3D overview tomography performed with limited number of angular projections. This is then used to identify the interesting areas for high resolution multimodal X-ray tomography (Figure 1).

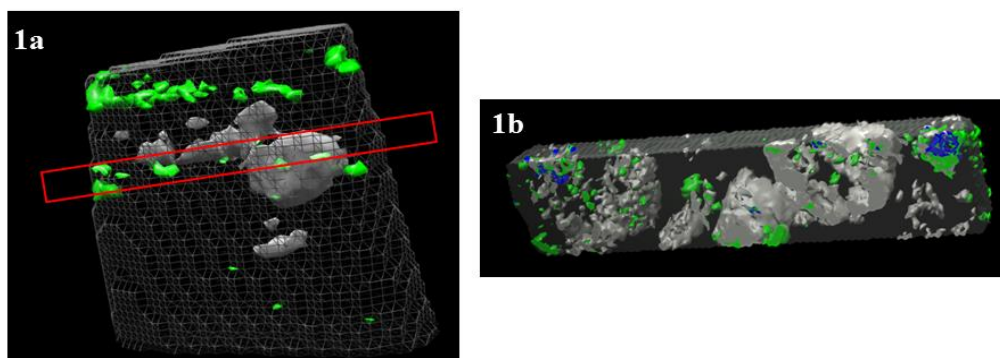


**Figure 1:** **1a)** Volume rendering of the draft Fe (green) distribution and morphology of an Archean rock sample ( $500 \times 750 \times 100 \mu\text{m}^3$ ), grey grid: sample contour from absorption contrast, grey: dark field (DF). **1b)** Higher resolution tomography of the sample region marked by the red rectangle in 1a, transparent: absorption contrast, green: Fe, grey: DF, blue: Zn & Cr distributions [2].

Online processing and analysis of the generated multimodal data is an important issue for routine user experiments. The MMX-I multi-platform open-source freeware [4] was developed for the processing and reconstruction of such large volume, scanning multi-technique X-ray imaging and tomography datasets and is now routinely used by the Nanoscopium users community. The MMX-I software is presented in a separate dedicated presentation [5].

## References

- [1] A. Somogyi, F. Polack, T. Moreno, AIP Conf. Proc. 1234: 395-398. (2010).
- [2] A. Somogyi, K. Medjoubi, et al., J. Synch. Rad. 22, 1118 (2015).
- [3] K. Medjoubi, N. Leclercq, et al., J. Synch. Rad. 20: 293–299 (2013).
- [4] A. Bergamaschi, K. Medjoubi, et al., J. Synch. Rad. 23, (2016) in press
- [5] A. Bergamaschi, K. Medjoubi, C. Messaoudi, S. Marco, A. Somogyi, MMX-I: a data-processing software for multi-modal X-ray imaging and tomography, abstract submitted to XRM2016

## DEVELOPMENT OF X-RAY EXCITED OPTICAL LUMINESCENCE AT THE X-RAY NANOPROBE AT TAIWAN PHOTON SOURCE

Bi-Hsuan Lin<sup>1</sup>, Huang-Yeh Chen<sup>1</sup>, Shao-Chin Tseng<sup>1</sup>, Jian-Xing Wu<sup>1</sup>, Bo-Yi Chen<sup>1</sup>, Chien-Yu Lee<sup>1</sup>, Gung-Chian Yin<sup>1</sup>, Shih-Hung Chang<sup>1</sup>, Kai-Hsiang Lin<sup>2</sup>, Hsu-Cheng Hsu<sup>2</sup>, Wen-Feng Hsieh<sup>3</sup>, Mau-Tsu Tang<sup>1</sup>

*1National Synchrotron Radiation Research Center, Hsinchu 30076, Taiwan*  
*2Department of Photonics and Advanced Optoelectronic Technology Center, National Cheng Kung University, 701 Tainan, Taiwan*  
*3Department of Photonics and Institute of Electro-Optical Engineering, National Chiao Tung University, Hsinchu 30010, Taiwan*

### Abstract

We develop the synchrotron based X-ray excited optical luminescence (XEOL) and time-resolved X-ray excited optical luminescence (TR-XEOL) at the X-ray Nanoprobe (XNP) facility at Taiwan Photon Source (TPS).

Advanced by energy-tunable hard X-rays, the XNP at TPS provides 40nm spatially resolving means for investigating the optical properties of specific elements in the wide band gap semiconductor materials.

A ultrafast streak camera and a photon-multiplier counter (PMC) are synchronized with the pulse structure of the synchrotron ring to study the dynamics of luminescence of the materials with temporal resolution 20 ps ~ 12 ns.

In parallel to the construction of the XNP endstation, demonstrative XEOL experiments were conducted by unfocused X-ray beam at Taiwan Light Source (TLS). Figures 1 and 2 show the morphologies and sizes of ZnO microwires taken by the optical microscopy (OM) and scanning electron microscopy (SEM), respectively. The low temperature (4.2K) and temperature-dependent XEOL with X-ray excited energy below, at and above the Zn K-edge (9.659keV) were used to obtain the further information of the optical mechanisms of these microwires. The temperature-dependent XEOL behavior of the ZnO microwires with X-ray energy at 9.67 keV was shown in Figure 3. The free A excitons, donor bound excitons and their phonon replicas can be seen unambiguously at low temperatures. The design of the XEOL and TR-XEOL at XNP and the demonstrative experimental results will be reported.

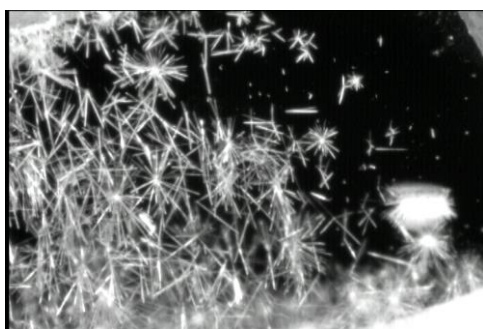


Figure 1: OM image of ZnO microwires.

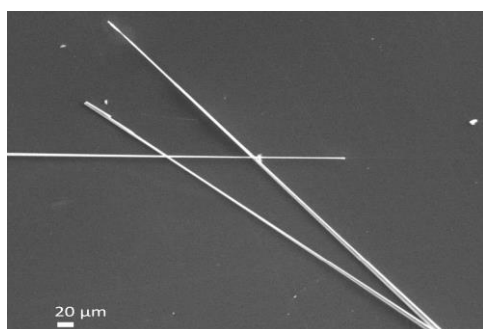


Figure 2: SEM image of ZnO microwires.

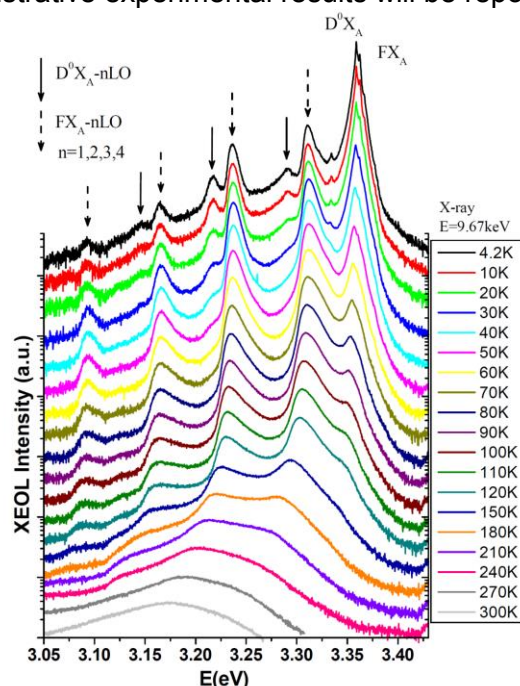


Figure 3: Temperature-dependent XEOL of ZnO microwires.

## XPEEM MICROSCOPY AT THE HERMES BEAMLINE: COMMISSIONING AND FIRST RESULTS

M. Rioult, S. Stanescu, S. Swaraj, A. Besson, and R. Belkhou

*Synchrotron SOLEIL, L'Orme des Merisiers, Saint-Aubin - BP 48, F-91192 Gif-sur-Yvette cedex,  
France*

### Abstract

We present here the first results obtained using the X-ray PhotoEmitted Electron Microscope (XPEEM) installed at the HERMES beamline at synchrotron SOLEIL [1]. The originality of the HERMES beamline is to combine two complementary microscopy methods (XPEEM and STXM) within the same beamline to allow the users to adequately choose the most appropriate instrument for their specific scientific case. Each microscope is installed on a dedicated branch and can operate alternatively and independently.

The XPEEM is based on photon-in/electron-out interactions and is therefore intrinsically a surface-interface microscopy method (probing depth < 10nm), operating in an ultra-high vacuum environment. After few years of functioning at the Nanospectroscopy beamline [2] at the ELETTRA synchrotron (Trieste, Italy), the XPEEM instrument was upgraded prior to its final installation at the HERMES beamline (new cooling stage, motorized/encoded (X,Y, $\theta$ ) manipulator...). The most important upgrade was the installation of a new prototype of hemispherical energy analyzer that opens up the way to perform high-resolution local XPS and ARPES measurements.

The commissioning results of the XPEEM branch will be presented together with the specifications of the X-ray beam in term of flux, size and energy resolution. The beamline allows to achieve very high photon flux (up to  $10^{13}$  photons/s), micro-sized beamspot (< 25  $\mu$ m), high resolving power (> 10,000 within the 70 eV – 2.5 keV range) and hence a high-energy resolution (*e.g.* < 40meV at 400 eV photon energy). The XPEEM microscope performances will also be presented, both in the imaging and local spectroscopy modes. In the LEEM mode, the microscope reaches 6 nm spatial resolution. With the X-ray, spatial resolutions well below 35 nm are routinely achieved.

Finally, some examples of the first user experiments results will be given, together with new additional available capabilities (*in-situ* growth, current injection...).

### References

- [1] R. Belkhou et al., J. Synchrotron Rad., 22, 968-979 (2015)
- [2] <https://www.elettra.trieste.it/elettra-beamlines/nanospectroscopy.html>



## Advanced Lensless Microscopy for Millisecond and Nanometer Scales Using Coherent X-ray Scattering at Taiwan Photon Source

Yu-Shan Huang, Jih-Min Lin, Chun-Yu Chen, Hong-Yi Yan, Chao-Chih Chiu

*National Synchrotron Radiation Research Center, Hsinchu, Taiwan*

### Abstract

The 3 GeV Taiwan Photon Source (TPS) with low emittance 1.6 nm-rad, which provides the extremely brilliant and highly coherent X-ray beams, is being commissioning at the National Synchrotron Radiation Research Centre, Taiwan. The coherent X-ray Scattering (CXS) beamline is one of the seven phase-I beamlines at TPS. This beamline equipped with two in-vacuum undulators provides coherent photon flux greater than  $10^{10}$  photons per second at 6 keV X-rays. The X-ray beam is monochromated by a double crystal monochromator with energy resolution  $2 \times 10^{-4}$  by using Si(111) crystals. Kirkpatrick-Baez (KB) mirrors are used to focus the X-rays down to  $1 \mu\text{m}^2$  in the energy range from 5.6 keV to 20 keV. The sample-to-detector distance can be varied with a range of 0.7-12 m. State-of-the-art detectors of Eiger X 16M and 1M are equipped for data collection of 133/750/3000 Hz frame rates with region-of-interest technique.

Combined the highly coherent X-rays and state-of-the-art detectors, the CXS beamline at TPS provides advanced lensless microscopy for millisecond and nanometer scales using coherent diffraction imaging (CDI) and Bragg CDI techniques. The CXS beamline will open to general users in 2016.



**Figure 1:** Drawing of coherent X-ray scattering beamline at TPS.

## X-RAY IMAGING AND MICROSCOPY AT TAIWAN PHOTON SOURCE: TO SEE AND TO RESOLVE

Mau-Tsu Tang

*National Synchrotron Radiation Research Center, 101 Hsin-Ann Road, Hsinchu, Taiwan*

### **Abstract**

The construction of the third-generation synchrotron facility Taiwan Photon Source (TPS) has been completed successfully. The first synchrotron radiation was coming out from the TPS storage ring on Dec 31, 2014. The 1.6 nm-rad emittance of the light source intensifies the X-ray researches in Taiwan, especially for those fields long hungry for intense and bright photons such like X-ray imaging and microscopy. To emphasize, four out of the seven phase-one beamlines at TPS are associated with abilities of micron – nanometer spatial resolution. In addition, two new soft X-ray microscopy beamlines and one relocated beamline of hard X-ray microscopy from the existing Taiwan Light Source (TLS) are scheduled in the TPS phase-two beamline plan. Integrated with novel X-ray techniques of diffraction, spectroscopy and coherent imaging, these beamlines as a whole will serve for a great diversity of communities from physical sciences to biomedical sciences, domestically and internationally.

The strategy of the X-ray imaging and microscopy at TPS not just aims to see but to resolve as well. Versatile sample environments, such like low/high temperature, high pressure, *in-situ* electrical and chemical cells are developed in individual beamlines. Innovative imaging techniques associated with electron microscope (EM) and fluorescence microscopes (FM) are developed and built in some of the end stations of beamlines, to provide correlative detections and diagnostic other than X-rays. A data center for mass data storage and computing is planned to take full advantage of the resources provided by the National Center for High-performance Computing (NCHC) nearby. Off-line laboratories for sample prior diagnostic and preparation will be set up progressively.

In this presentation, we present the strategic scope of the plan, the present status as well as the scientific opportunities associated with the facility. The technical challenges and developing R&D for X-ray optics, control electronics and sample environments will also be presented.

## IMAGING BEAMLINES FOR MAX IV

A. Lassesson, F. Hennies, Y. Cerenius, J. N. Andersen

*MAX IV Laboratory, Lund University, Lund, Sweden*

### Abstract

Beamlines at MAX IV are developed in close collaboration with the scientific community to ensure that they meet the demands of both existing and future users. The collaboration between MAX IV and users from Swedish and Nordic universities span the entire process from the original definition and scientific case for a beamline into the commissioning phase and the continuous development of a scientific program.

There are currently 14 fully funded MAX IV beamlines at various stages of construction from the early design phases to near completion. The installation of the first insertion devices in the 3 GeV ring during the spring of 2016 marked the beginning of beamline commissioning with light at MAX IV.

MAX IV beamlines are designed to take full advantage of the MAX IV sources including the ultra-low emittance 3 GeV ring which promise very high coherent flux, ideal for imaging applications. For example, NanoMAX will offer micro- and nanofocussing for imaging, diffraction, scattering and fluorescence at 5 - 30 keV. NanoMAX is included in the first beamline construction phase and will be one of the first beamlines to be commissioned. It is expected to enter operation in 2017.

The second phase of beamline construction includes CoSAXS and SoftiMAX which will commence operation in late 2018. Both beamlines will be placed at the 3 GeV ring. CoSAXS will, as a second stage of endstation development, take advantage of the coherent source for coherent diffraction imaging (CDI) at 4 - 20 keV. SoftiMAX will be used for scanning transmission X-ray microscopy (STXM), ptychography, and coherent X-ray imaging (CXI) of soft and hard materials in the soft X-ray regime.

DanMAX, the first Danish beamline at MAX IV, will be dedicated to powder diffraction and tomography. It is the latest addition to the MAX IV beamline portfolio and is currently in the early design phase.

Other, so far unfunded imaging beamlines, will in the future address the needs of the medical imaging community and forestry researchers among others.

We present the imaging beamline portfolio at MAX IV and highlight the possibilities for users at these beamlines with a view to receiving more feedback from the scientific community.

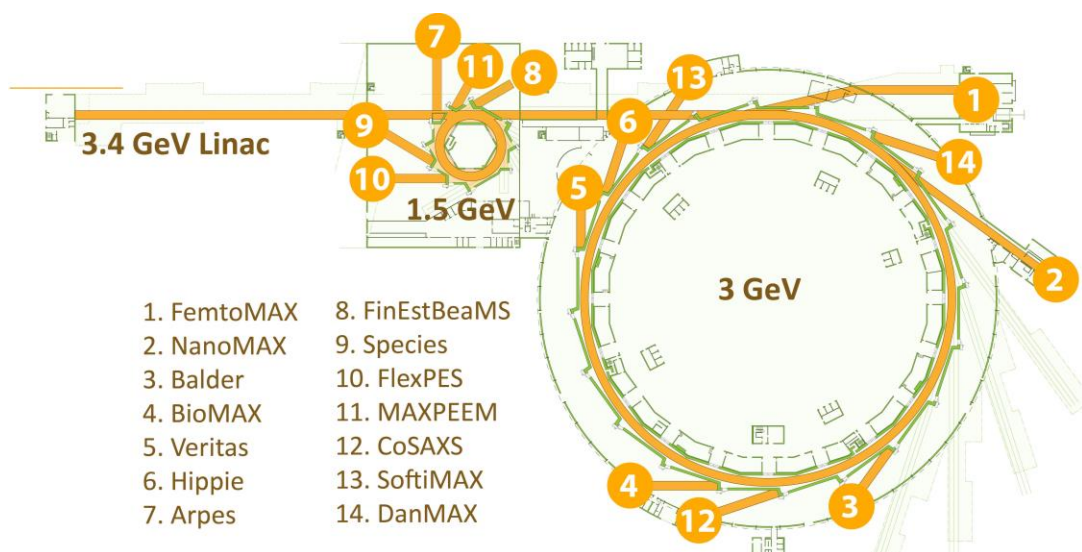


**Figure 1:** The current beamline projects at MAX IV

## POTENTIAL ENVIRONMENTAL APPLICATIONS BY MEDIUM ENERGY MICRO-PROBE BEAMLINE PROPOSED IN SSRF PHASE-II PROJECT

Lina Li, Yanqing Wu, Liansheng Wang

Shanghai Institute of Applied Physics, Chinese Academy of Sciences, Shanghai Synchrotron Radiation, Shanghai 201204, China

### Abstract

There are low levels of pollutants in the environment with a certain potential harmfulness. Using synchrotron radiation method to give an accurate analysis to detect its valence and spatial distribution need to have a certain flux and single atomic testing efficiency. A medium-energy x-ray spectroscopy beamline is proposed in SSRF Phase-II Beamline Project and microscopy method will be realized. In the design indicators, the energy resolution ( $\Delta E/E$ ) is  $2 \times 10^{-4}$  @ 2.5keV and the photon flux is  $1.5 \times 10^{12}$  phs/s @ 2.5keV (after K-B mirror focusing). The focused spot size will be  $6 \times 2 \mu\text{m}^2$  @ 2.5keV (K-B mirror) and  $0.5 \times 0.3 \mu\text{m}^2$  @ 2.5keV (small K-B mirror) respectively. The combination of high-brightness, sub-micron X-ray beams, nondestructive method and high sensitivity detectors are able to analyze environmental pollutants on the micro-scale, especially on sulfur and phosphorus compound, and research their removal mechanism. Similar beamline for microscopy research are Diamond-I13L, APS-2-ID-E and Australian Synchrotron-x-ray microspectroscopy beamline.

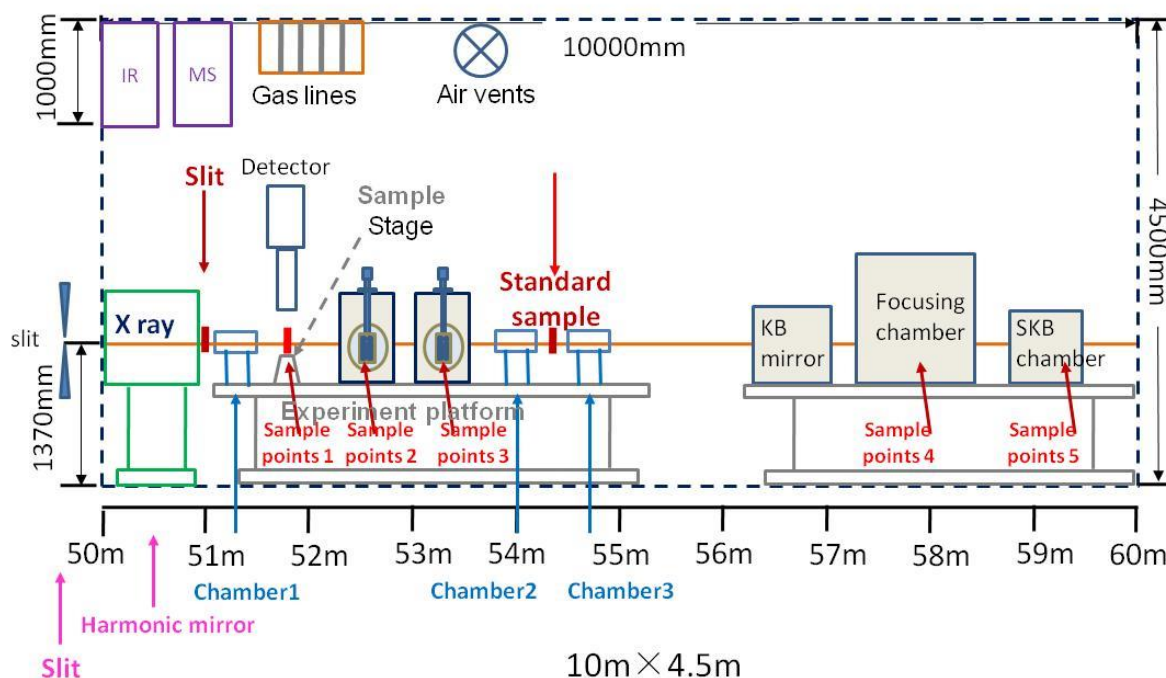


Figure1: Schematic diagram of the end-station at the medium energy beamline

## MEDIUM ENERGY BEAMLINE PROPOSED IN SSRF PHASE-II PROJECT

Liansheng Wang, Lina. Li

*Shanghai Institute of Applied Physics, Chinese Academy of Sciences, Shanghai Synchrotron Radiation Facility, Shanghai 201204, China*

### Abstract

Medium energy beamline is one of the proposed beamlines in SSRF Phase-II Project. There is a micro and nano focus endstation with high flux for  $3 \times 10^{12}$  phs/s@2.5keV from an undulator. Besides, X-ray absorption spectroscopy and X-ray fluorescence spectroscopy will provide users in the energy range of 2.1-16keV. The biological, environmental, and chemical researches can be included. A monochromatized beam is obtained with a double crystal monochromator. Different crystals are used to obtain higher energy resolution ( $\Delta E/E=2 \times 10^{-4}$ @2.5keV) with Si(111) and Si(220). Two focusing mirrors in a Kirkpatrick-Baez configuration provide a focal spot size of about  $5 \mu\text{m} \times 1.5 \mu\text{m}$ , and a small Kirkpatrick-Baez mirror is used to focus beam spot size to  $0.3 \mu\text{m} \times 0.2 \mu\text{m}$ . The small beamsizes allow the mapping of the elemental distribution in the sample. A spacious vacuum chamber provides the necessary environment for the user experiments such as dry and wet samples as well as in-situ and in-operandi studies. The chamber can be easily replaced by a dedicated chamber by a user. Total electron yield measurements, and Si drift detectors will be included for fluorescence detection.

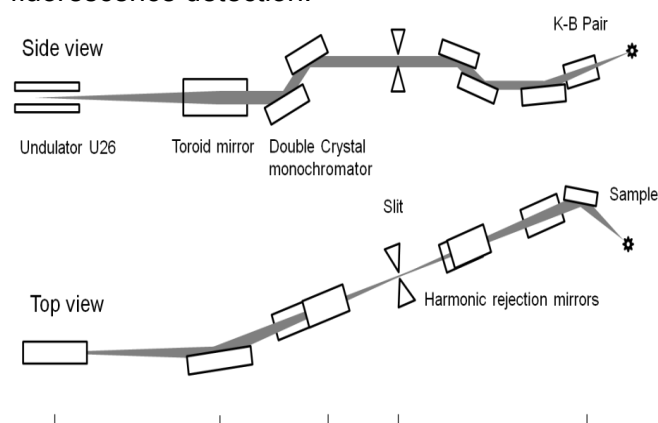


**Figure 1:** Medium energy beamline layout

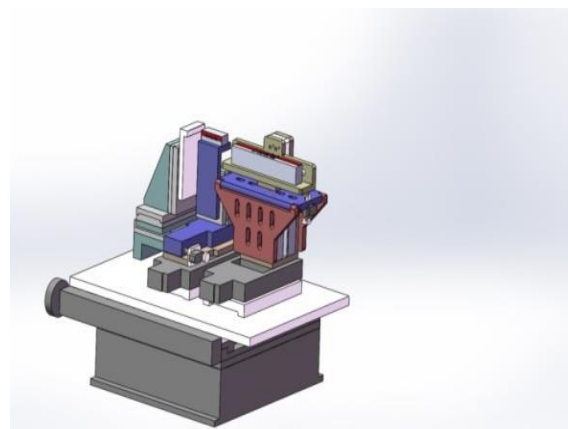


**Figure 2:** Small KB mirror and sample stage system

### References

- [1] Shanghai synchrotron radiation facility phase II medium energy beamline preliminary report.



## A KIRKPATRICK BAEZ-BASED IN-SITU NANOPROBE BEAMLINE AT THE APS MBA LATTICE

Jörg Maser<sup>1</sup>, Barry Lai<sup>1</sup>, Mariana Bertoni<sup>3</sup>, Tonio Buonassisi<sup>2</sup>, Zhonghou Cai<sup>1</sup>, Si Chen<sup>2</sup>, Ross Harder<sup>1</sup>, Curt Preissner<sup>1</sup>, Ruben Reininger<sup>1</sup>, Chris Roehrig<sup>1</sup>, Xianbo Shi<sup>1</sup>, Volker Rose<sup>1</sup>, Deming Shu<sup>1</sup>, David Vine<sup>1</sup>, Stefan Vogt<sup>1</sup>, Bradley West<sup>3</sup>.

<sup>1</sup> Advanced Photon Source, Argonne National Lab, Argonne, IL, United States

<sup>2</sup> Massachusetts Institute of Technology

<sup>3</sup> Arizona State University, Tempe, AZ, United States

### Abstract

An upgrade of the Advanced Photon Source with multibend achromat (MBA) magnetic lattice is proposed and under preliminary design. Such an upgrade would yield a 4<sup>th</sup> generation synchrotron with massively increased brilliance in the hard x-ray range, and almost round x-ray source dimension. This would make the APS supremely suited for coherent techniques such as nanofocusing and coherent diffraction. To exploit the new source properties, we are developing a design for a proposed new flagship hard x-ray microscopy beamline, the In-Situ Nanoprobe (ISN).<sup>[1]</sup> The ISN will use nanofocusing mirrors to focus hard x-rays into a probe of 20 nm size, and use ptychography to achieve sub-10 nm resolution in transmission, as well as “super-resolution” in x-ray fluorescence maps. Use of mirrors as nanofocusing optics will yield a focused flux of  $1.6 \times 10^{11}$  coherent photons/s at 25 keV, and of  $1.8 \times 10^{12}$  coherent photons/s at 10 keV, into an energy band of  $\Delta E/E = 10^{-4}$ . The achromatic mirror optics will enable unique nanospectroscopy capabilities, and allow operation with pink beam. To fully exploit the new source characteristics, the ISN beamline will have a length of approximately 180 m. This will yield large working distances of more than 50 mm at a resolution of 20 nm, critical to deploying a wide variety of *in-situ* environments. The combination of very large focused flux and flux density, nanospectroscopy and large working distance will enable study of complex materials and devices under physically relevant conditions, and characterization through multidimensional parameter spaces, such as temperatures, applied fields, gases and fluids. Examples include photovoltaic systems,<sup>[2]</sup> batteries<sup>[3]</sup> and catalysts, under *in-situ* and *operando* conditions. We will present the conceptual design of the ISN beamline, and discuss initial studies of advanced photovoltaic systems.

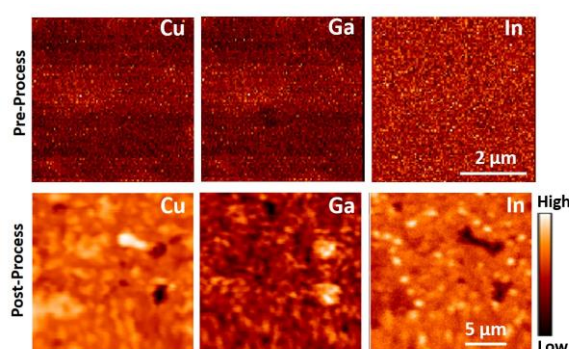


**Figure 1:** XRF maps of Cu, In, and Ga, before and after the precursor reaction process

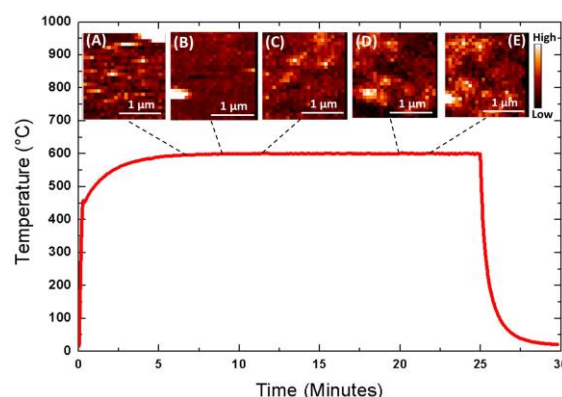


**Figure 2:** Time-temperature profile with example of copper maps taken at two minute intervals. (A) 7 min. (B) 9 m. (C) 11 m. (D) 20 min. (E) 22 m.

### References

- [1] J. Maser, B. Lai, T. Buonassisi, Z. Cai, S.Chen, L. Finney, S.C. Gleber, C.Jacobsen, C.Preissner, C. Roehrig, V. Rose, D. Shu, D. Vine, S. Vogt. Metall. Mater. Trans. A 45 (1), 85-97 (2014). DOI: 10.1007/s11661-013-1901-x.
- [2] M.I. Bertoni, D.P. Fenning, M. Rinio, V. Rose, M. Holt, J. Maser, T. Buonassisi: Energy Environ. Sci., 2011, vol. 4, 4252-4257
- [3] A. Ulvestad, A. Singer, H.-M. Cho, J. N. Clark, R. Harder, J. Maser, Y. S.Meng, O. G. Shpyrko, Nano Lett. 14 (9), 5123-5127 (2014)

## RECENT PROGRESS ON SSRF PHASE-II BEAMLINES

Renzhong Tai

*Shanghai Synchrotron Radiation Facility, Shanghai Institute of Applied Physics, Chinese Academy of Sciences, 239 Zhangheng Road, Pudong District, Shanghai 201204, China*

### **Abstract**

To meet the ever-growing requirements of users' pioneering and cutting-edge researches in interdisciplinary areas, especially the appealing for high spatial resolution, fast temporal resolution and high detection limit, the phase-II project at SSRF has been proposed since 2010 when the Phase-I project was just completed. In Phase-II project, 16 state of the art beamlines will be built, among these some will stress a full of use of brilliance and partial coherence of Shanghai light source in order to pursue higher resolution in space, time and energy. The proposal of the project was approved by Chinese government in 2015. Now we are in the stage of perfecting primary design. It is expected that the construction will be started at the end of this year or the beginning of next year. The building of all the 16 new beamlines will be finished within 5-7 years.

Among these beamlines, Hard X-ray nanoprobe beamline and 3D nano imaging beamline will have very high spatial resolution in 10nm and 20nm for material and life research, respectively. Fast x-ray imaging beamline is dedicated to ultra-fast imaging in 100ps, and dynamic  $\mu$ -CT in seconds for dynamic process research. Medium-energy x-ray spectroscopy beamline will have ability of ppb level chemical sensitivity for environmental researches. Apart from building new beamlines, machine upgrade for light sources, establishment of supporting laboratories for users and beamlines are significant tasks and included in the Phase-II Project as well. With a successful accomplishment of the Phase-II, we anticipate about 40 beamlines are going to serve users from all over the world. Hopefully SSRF will be one of the world centre of synchrotron research.

## HARD X-RAY FLUORESCENCE IMAGING AND MICRO X-RAY ABSORPTION SPECTROSCOPY FACILITIES AT SSRL

S.M. Webb, C.M. Krest (Roach)

*Stanford Synchrotron Radiation Lightsource, Menlo Park, California, USA*

### Abstract

The X-ray fluorescence and micro-spectroscopic imaging facility at the Stanford Synchrotron Radiation Lightsource (SSRL) consists of three beamlines, which cover a wide range of x-ray energies and beam sizes, allowing for the ability to conduct an extensive variety of experiments. As a facility, we cater to a broad range of users including those from the Biological, Environmental, and Material Science communities, which often require different beam line conditions based on sample composition. Needs can range from including varying sample sizes (5 $\mu$ m to 0.5m), varying resolution (<2 $\mu$ m to >200 $\mu$ m), and varying energy ranges (2100eV-20,000eV). These needs have been achieved with the utilization of three beam lines for microfocus activities:

- 1) Beamline 2-3: High spatial resolution (beam size  $\sim$ 2 $\mu$ m), good for spectroscopy/diffraction, accommodates medium to small sample sizes,  $\sim$ 5,000eV to  $\sim$ 20,000 eV, tomography.
- 2) Beamline 10-2: Moderate resolution, (10 $\mu$ m – 200 $\mu$ m), high flux, rapid scanning, accommodates medium to large sample sizes, spectroscopy, ideal diffraction,  $\sim$ 5,000eV to  $\sim$ 20,000eV, tomography, confocal microscopy.
- 3) Beamline 14-3: Low energy ( $\sim$ 2,000 to  $\sim$ 4,500eV), high spatial resolution ( $\sim$ 5 $\mu$ m beam size), good spectroscopy, accommodates small to medium sample sizes, helium sample environment.

These three beamlines are tied together via a cohesive suite of software and similar data acquisition hardware configurations, using Xspress3 detector pulse processing electronics. These data acquisition software also shares the same look and many features as the bulk XAS lines for ease of transition between beamlines. The capabilities of the imaging facility are continuing to expand, as future directions include the addition of zone plates at beamline 10-2 allowing beam sizes < 100nm as well as a hexapod stage to allow for easy changes between optics and thus beam sizes.

# NANOPROBE DESIGN OPTIMISATION: TWO DESIGNS FOR A NANOPROBE BEAMLINE AT THE AUSTRALIAN SYNCHROTRON

M.D. de Jonge<sup>1</sup>, H.H. Harris<sup>2</sup>, D.J. Paterson<sup>1</sup>, M. James<sup>1</sup>, C.G. Ryan<sup>3</sup>

<sup>1</sup>Australian Synchrotron, 800 Blackburn Rd, Clayton, Australia

<sup>2</sup>University of Adelaide, Australia

<sup>3</sup>CSIRO, Research Way, Clayton, Australia

## Abstract

Having recently achieved funding security, the Australian Synchrotron is on a mission to expand capabilities through a suite of new beamlines. The Australian Synchrotron's existing strengths include high-quality SAXS/WAXS, large-beam Imaging and Medical Therapy, and high-pixel rate X-ray Fluorescence Microscopy.

Storage ring parameters will always constrain beamline design, and the Australian Synchrotron's parameters are modest, with horizontal and vertical emittances of  $\eta_x = 57 \text{ nm}\cdot\text{rad}$  and  $\eta_y = 0.8 \text{ nm}\cdot\text{rad}$ , respectively. Here we explore two nanoprobe designs, both based on a total length of 70 m\*, with spot sizes of order 150 nm FWHM\*. Initial findings indicate more efficient flux transport for KB mirror design, largely due to the matching of asymmetric source parameters with the inherently astigmatic focusing of KBs, but also due to the requirement to under-fill the mirror optic contrasted with the requirement to over-fill the ZP optic. However, the ZP optic design facilitates flux / resolution trade-offs down to the ZP resolution, where KB optics are – in the first instance – limited by the vertical source demagnification.

We actively seek comment from those interested in nanoprobe beamline and endstation design and operation.

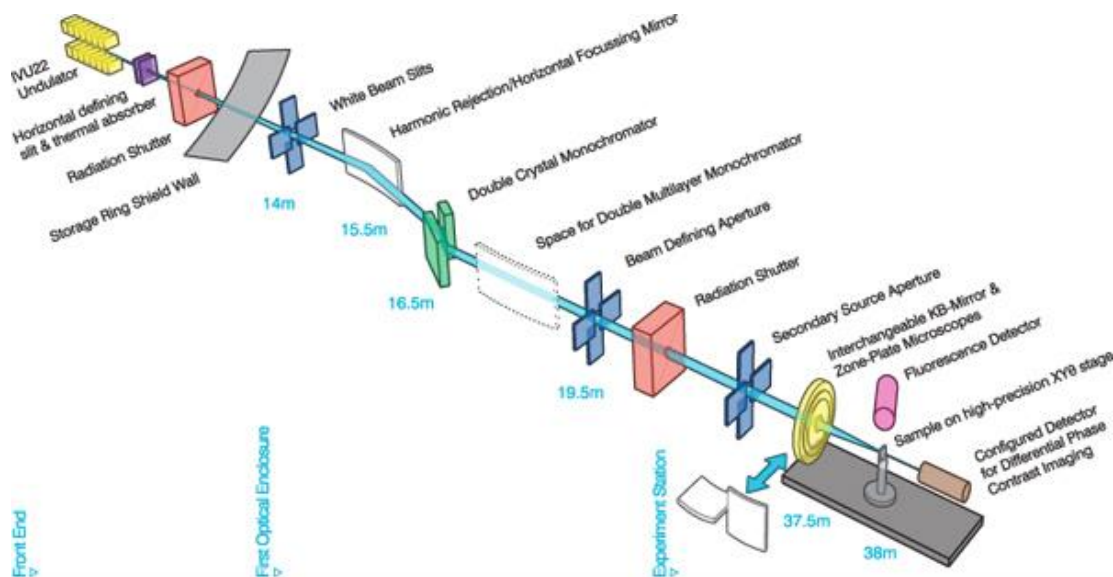


**Figure 1:** The new beamline designs will be based on the existing design of the XFM beamline at the Australian Synchrotron, with a secondary source aperture somewhere along the beamline. In this example, the vertical beam is transported directly from the source to the KB focusing optics, while the horizontal beam is defined by use of a secondary source aperture located in the endstation.

## Notes and References

\* Design targets approximate and subject to change

[1] DJ Paterson et al, AIP Conference Proceedings **1365**, 219 (2011).

[2] R Kirkham et al, AIP Conference Proceedings **1234**, 240 (2010).

## STATUS OF THE TOMOGRAPHY BEAMLINE ANATOMIX AT SYNCHROTRON SOLEIL

T. Weitkamp, M. Scheel, J.-L. Giorgetta, V. Joyet, V. Le Roux, G. Cauchon

*Synchrotron SOLEIL, L'Orme des Merisiers, Saint-Aubin, B.P. 48, 91192 Gif-sur-Yvette, France*

### Abstract

ANATOMIX is a 200-m-long undulator beamline for full-field tomography techniques in the energy range between 5 and 25 keV. It is currently under construction at Synchrotron SOLEIL, the French national light source in the greater Paris region.

ANATOMIX will feature experimental end stations both for parallel-beam microtomography (with a beam size of up to 40 mm width) and for zone-plate transmission X-ray microscopy (down to pixel sizes of 30 nm).

The location of ANATOMIX on a canted straight section of the SOLEIL storage ring brings about specific challenges for the design and operation conditions of the beamline.

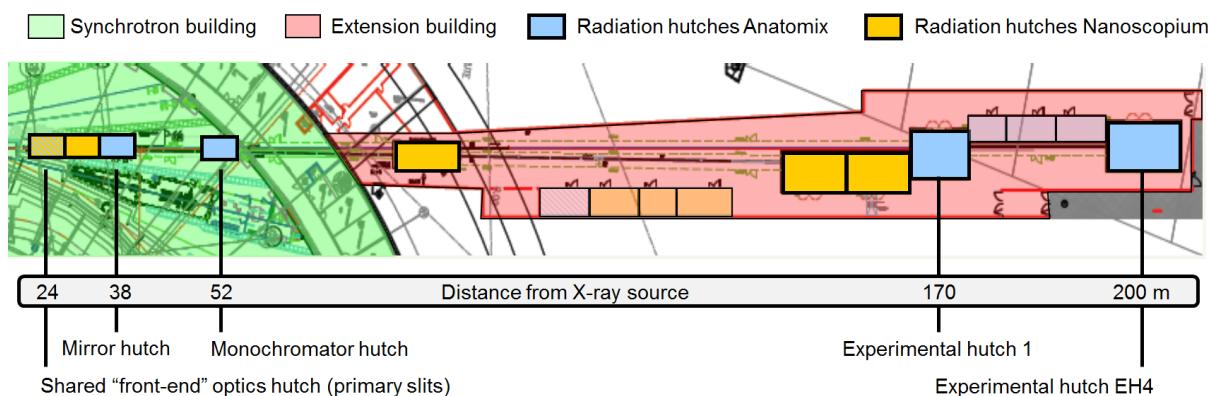


**Figure 1:** Floor plan of ANATOMIX and its neighbor beamline NANOSCOPIUM.

In our poster we will present general design aspects as well as recent progress of the beamline construction.

The construction of ANATOMIX is largely funded by the French National Research Agency (ANR) through the EQUIPEX investment program, project "NanoimagesX", grant no. ANR-11-EQPX-0031. The Nanoscopium consortium comprises 17 partner units from public research and industry.



**Figure 2:** Satellite building for ANATOMIX and its neighbor beamline NANOSCOPIUM.

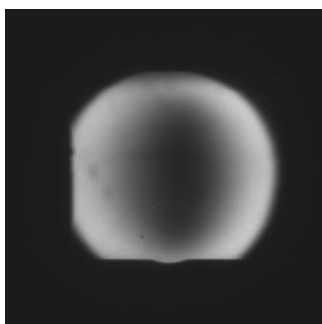


**Figure 3:** First light on energy-selective "DiagOn" imager.



**Figure 4:** Installation of mirrors M1 and M2 in Optics Hutch 3.



## MICRO AND NANO IMAGING AT THE DIAMOND BEAMLINE I13L- IMAGING AND COHERENCE

C. Rau<sup>1,2,3</sup>, U. Wagner<sup>1</sup>, A. Bodey<sup>1</sup>, S. Marathe<sup>1</sup>, S. Cipiccia<sup>1</sup>, X. Shi<sup>1</sup>, D. Batey<sup>1</sup>, I. Zanette<sup>1</sup>,  
M. Zdora<sup>1</sup>, M. Saliba<sup>1,4</sup>, V.S.C. Kuppili<sup>5</sup>, S. Sala<sup>1,5</sup>, S. Chalkidis<sup>5</sup>, P. Thibault<sup>6</sup>

<sup>1</sup>*Diamond Light Source Ltd., Harwell Science and Innovation Campus, Didcot, OX 11 0DE, UK.*

<sup>2</sup>*University of Manchester, School of Materials Grosvenor St., Manchester, M1 7HS, UK.*

<sup>3</sup>*Northwestern University School of Medicine, 303 E. Chicago Avenue, Chicago, IL 60611-3008, USA.*

<sup>4</sup>*Universitaet Zuerich, Winterthurerstr. 190, CH-8057 Zuerich, Switzerland*

<sup>5</sup>*Department of Physics and Astronomy, University College London, WC1E 6BT London, UK,*

<sup>6</sup>*Department of Physics and Astronomy, University of Southampton, Southampton, SO17 1BJ, UK*

### Abstract

The Diamond Beamline I13L is dedicated to imaging on the micron- and nano-lengthscale, operating in the energy range between 6 and 30 keV [1]. For this purpose two independent stations have been built. The imaging branch is fully operational for micro-tomography and in-line phase contrast imaging with micrometre resolution. Grating interferometry will be implemented completing the instrumental capabilities on the micron lengthscale. Currently a full-field microscope providing 50nm spatial resolution over a field of view of 100microns is tested.

On the coherence branch coherent diffraction imaging techniques such as ptychography, coherent X-ray diffraction (CXRD) and Fourier-Transform holography are currently developed. Because of the large lateral coherence length available at I13, the beamline hosts numerous microscopy experiments

The beamline contains a number of unique features. The machine layout has been modified to the so-called mini-beta scheme. New instrumental designs have been employed such as a robot arm for the detector in diffraction experiments and a photon counting detector for diffraction experiments. The imaging branch is operated in collaboration with Manchester University, called therefore the Diamond-Manchester Branchline.

The scientific applications covers a large area including bio-medicine, materials science, chemistry geology etc.. We will present the current status of the beamline and the scientific results achieved during the first years of operation.

### Reference

- [1] C. Rau, U. Wagner, Z. Pesic, A. De Fanis *Physica Status Solidi (a)* **208 (11)**. Issue 11 2522-2525, 2011, [10.1002/pssa.201184272](https://doi.org/10.1002/pssa.201184272)

## ID16A NANO-IMAGING BEAMLINE OF ESRF: A BRIGHT BEAM FOR COHERENT IMAGING AND X-RAY FLUORESCENCE NANOSCOPY

A. Pacureanu<sup>1</sup>, J.C. da Silva<sup>1</sup>, Y. Yang<sup>1</sup>, F. Fus<sup>1</sup>, M. Hubert<sup>1</sup>, S. Bohic<sup>1,2</sup>, P. Cloetens<sup>1</sup>

<sup>1</sup> ESRF – The European Synchrotron, 38000 Grenoble, France

<sup>2</sup> Inserm, U1216, University of Grenoble Alpes, Grenoble, France

### Abstract

Designed for quantitative three dimensional characterization of the morphology and the elemental composition of specimens at the nanoscale, the ID16A-NI beamline of the ESRF produces currently the world's brightest nanofocus. With the endstation situated at 185 m from the source, the beamline is optimized for coherent hard X-ray imaging with very high photon flux ( $10^{12}$  photons/s at  $\Delta E/E \sim 1\%$ ), at the ultimate spatial resolution ( $\sim 20$  nm). The selected energies, 17 keV and 34 keV, are well suited for applications in biomedicine, materials science and nanotechnology. Two coherent imaging techniques, magnified holotomography<sup>[1]</sup> and ptychographic tomography<sup>[2-3]</sup>, provide the distribution of the electron density at length scales ranging from  $\sim 130$  nm down to  $\sim 10$  nm, while keeping a relatively large field of view. Complementary, X-ray fluorescence microscopy delivers label-free highly efficient trace element quantification with detection limit down to subppm level<sup>[4]</sup>.

The instrument attains its unique properties by combining highly performant nanofocusing optics (multilayer coated Kirkpatrick-Baez mirrors) with a carefully designed mechanical device for stable sample positioning and accurate scanning. The samples are measured in vacuum and correlative phase contrast – fluorescence microscopy is feasible. Furthermore, the beamline has been recently upgraded to perform both the fluorescence and phase contrast measurements under cryogenic conditions to preserve the biological samples close to their native hydrated state while performing nanoscale imaging.

The cutting edge capabilities of this instrument enable unprecedented research studies in biomedicine, materials science, environmental sciences and nanotechnology, thus opening new scientific frontiers. We present the specifications and the performance evaluation of the beamline together with unique experimental results from several fields.

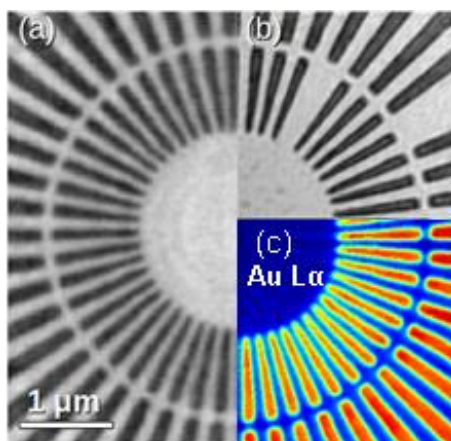


**Figure 1:** Illustration of the three available nano-imaging techniques on a standard sample (Siemens star, inner line measures 50 nm) (a) Holography (b) Ptychography (c) X-ray fluorescence.

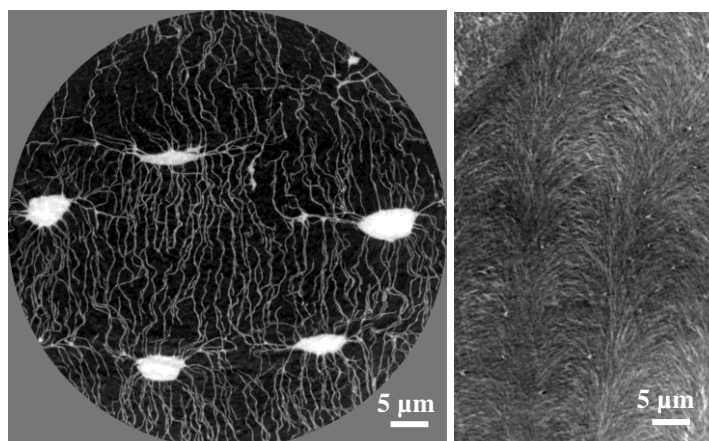


**Figure 2:** Application of magnified holotomography to human bone tissue (a) Osteocyte cell network (lacunae interconnected via canaliculi). Image represents the maximum intensity projection over  $12 \mu\text{m}$ . (b) Collagen fibres in the bone mineralized matrix. For visibility, regions of interest have been cut out from reconstructed slices.

### References

- [1] R. Mokso, P. Cloetens, E. Maire, W. Ludwig, J.Y. Buffiere, *Appl. Phys. Lett.*, **90**, (2007).
- [2] M. Dierolf et al., *Nature* **467**, (2010).
- [3] M. Stockmar, M. Hubert et al., *Optics Express* **23**, (2015).
- [4] Bohic S. et al., *Journal of Structural Biology*, **177**, (2012).

## LABORATORY CRYO SOFT X-RAY TOMOGRAPHY WITH A SIMPLE ROBUST LASER PLASMA LIGHT SOURCE

F. O'Reilly<sup>1,2</sup>, G. Wielgoszewski<sup>2</sup>, J. Howard<sup>2</sup>, F. McGrath<sup>2</sup>, R. Byrne<sup>2</sup>, A. Mahon<sup>2</sup>,  
O. Hammad<sup>2</sup>, T. McEnroe<sup>2</sup>, T. McCormack<sup>1</sup>, G. O'Sullivan<sup>1</sup>, E. Sokell<sup>1</sup>, P. Dunne<sup>1</sup>,  
N. Kennedy<sup>1</sup>, K. Fahy<sup>2</sup>, P. Sheridan<sup>2</sup>

*1 University College Dublin, School of Physics, Dublin, Ireland*

*2 SiriusXT Ltd, Science Centre North, Belfield, Ireland*

### **Abstract**

Great progress has been made over the last decade in developing cryo soft x-ray tomography as an imaging technique on synchrotron based microscopes. Workflows have improved which allow non-synchrotron researchers to access the technique, and significant expertise has been developed in correlating SXT and fluorescence data. Here we report on the development of a new lab based microscope, based on a laser plasma source, that aims to deliver synchrotron performance in a system that will turn SXT into an affordable and efficient laboratory tool. We show data on source performance and images of test samples.

## SOFTIMAX: A BEAMLINE FOR COHERENT SOFT X-RAY MICROSCOPY, IMAGING AND SCATTERING AT MAX IV

K. Thånell, J. Schwenke, W. Grizolli and R. Sankari

Research with coherent X-rays has experienced a tremendous boost in the last decade, as sources with considerable coherent photon flux have become available. The MAX IV 3 GeV ring will provide a very high *average* coherent flux, especially towards longer wavelengths (lower photon energy). This is an ideal situation for imaging applications built around the use of spatially coherent light waves: coherent imaging, scattering and scanning microscopy with soft X-rays. These techniques produce microscopic images of a sample, which at the same time can hold chemical, electronic, magnetic and/or structural information, depending on the details of the experiment.

The SoftiMAX beamline will have two branchlines: the first one is for scanning transmission x-ray microscopy (**STXM**) as well as nanoscale imaging through ptychography, both by using a Fresnel zone plate as the last optical element. The branchline will have an energy range from 275 to 2500 eV, and thereby provide access to both the carbon K-edge and sulphur K-edge. The mirror system is adapted to provide high throughput in this wide energy range by choice of mirror coatings and shallow incidence angles, yet simultaneously provides higher order suppression around the carbon K-edge. Full control over the polarization is provided by the 48 mm EPU, based on the APPLE-II design, giving access to measurements of magnetic moments or bond orientation. A wide range of research fields: from materials science to life and environmental science is foreseen.

The second branch line has a Kirkpatrick-Baez refocusing scheme, providing a focus of  $20 \times 20 \mu\text{m}^2$  or less and will host a variety of Coherent X-ray Imaging and Scattering (**CXI&S**) techniques, where a specimen is typically illuminated without X-ray “lenses”, such as the zone plate. These coherent scattering based approaches are characterized by a higher freedom with respect to sample environments (temperature, magnetic or electric fields), and as such the end station will have a modular character. Several closely related techniques such as coherent diffraction imaging, holography, near-field ptychography, but also resonant soft X-ray scattering, have been established in recent years and are increasingly used for imaging e.g. in nanoscale (magnetic) materials and life sciences. These methods will, to some degree, be possible at the CXI&S end station. At the same time, the CXI&S branchline will provide a platform to develop novel imaging concepts using coherent x-ray beams.

The layout, concepts and expected performance of the beamline and its stations are presented.

## CARNAÚBA: THE COHERENT X-RAY NANOPROBE BEAMLINE FOR THE BRAZILIAN SYNCHROTRON SIRIUS/LNLS

Hélio C. N. Tolentino<sup>1,2</sup>, Carlos A. Perez<sup>1</sup>, Márcio M. Soares<sup>1</sup>, Flávio C. Vicentin<sup>1</sup>, Dalton Abdala<sup>1</sup>, Douglas Galante<sup>1</sup>, Verônica de C. Teixeira<sup>1</sup>, Douglas H. C. de Araújo<sup>1</sup>, Harry Westfahl Jr.<sup>1</sup>,

<sup>1</sup> Laboratório Nacional de Luz Síncrotron LNLS, CP 6192, 13083-970 Campinas, Brazil.

<sup>2</sup> Université de Grenoble Alpes and CNRS, Institut Néel, BP 166, 38042 Grenoble, France.  
helio.tolentino@lnls.br

### Abstract

The Coherent x-Ray NANoprobe Beamline (CARNAÚBA) will deliver the smallest nanoprobe among the first phase SIRIUS beamlines at the LNLS, Brazil. CARNAÚBA [1] uses an undulator source with vertical linear polarization in a low-beta straight section and grazing incidence-focusing mirrors to create a nanoprobe at 145 m from the source. The beamline optic provides high brilliance at an achromatic focal spot down to the diffraction limit diameter of  $\sim 30$  nm with a working distance of  $\sim 6$  cm in the 2 to 14 keV range. These characteristics are crucial for studying nanometric samples in experiments involving complex stages and environments. CARNAÚBA will tackle scientific studies in areas of sound importance, as in life, geological, environmental and materials science. Its nanoprobe will allow answering many questions regarding the nature of these heterogeneous samples, such as the local composition, chemistry, atomic structure, crystal orientation, strain, among other important characteristics. The CARNAÚBA beamline aims to perform raster scans using x-ray fluorescence, x-ray absorption spectroscopy, x-ray diffraction and coherent x-ray imaging techniques. Moreover, these methods will be extended to three dimensions with computed tomography. We will present the design characteristics and expected performance, as well a few prototype instruments that are under construction.

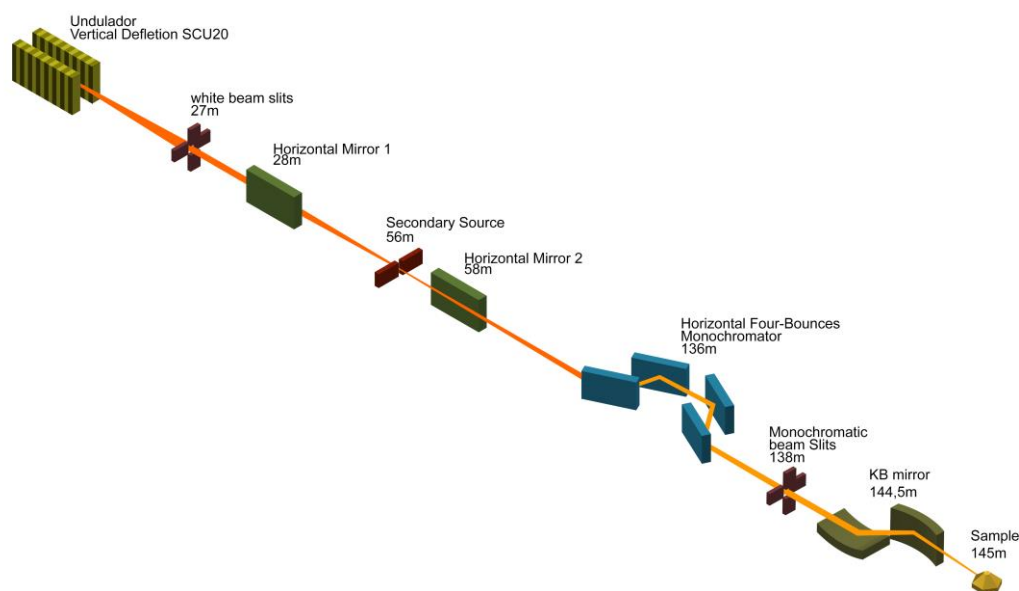


**Figure 1:** Schematic representation of the CARNAUBA beamline layout

### References

- [1] H.C.N.Tolentino, et al, CARNAUBA Conceptual Design Report, LNLS Internal report (2016)



## CATERETÊ: THE COHERENT AND TIME-RESOLVED X-RAY SCATTERING BEAMLINE AT THE SIRIUS/LNLS

Florian E. Meneau, Carla C. Pólo, Tiago A. Kalile, Sérgio A. L. Luiz, Bernd C. Meyer, Joacir E. dos Santos, Jean Rinkel, and Harry Westfahl Jr.

*Laboratório Nacional de Luz Síncrotron LNLS-CNPEM, CP 6192, 13083-970 Campinas, Brazil  
Florian.meneau@lnls.br*

### Abstract

The Cateretê beamline will be located at SIRIUS-CNPEM, the new low emittance Brazilian synchrotron light source under construction. The beamline will be dedicated to coherent X-ray diffractive imaging (CXDI) and time-resolved scattering (TR-SAXS) experiments. It will be designed to provide a compact, versatile and ultra-stable platform, which will allow to image biological specimens such as parasite cells, yeast spores, chromosomes and viruses and will also extend the imaging possibilities to larger biological specimens, up to 30  $\mu\text{m}^2$  with unprecedented resolution of few nm. The high coherent Hard-X-ray flux of Cateretê will enable to perform *in situ* 3D CXDI experiments with a particular focus on operando measurements for catalysis. The coherent beam size will range from one to tenth of microns with the possibility to be sub-micron by using zone plate focusing device. The proposed microscope will enable diverse CDI schemes (plane-wave, Bragg, Fresnel and ptychography). The Cateretê design and the latest wave-propagation simulations of the partially coherent beam will be presented. The Cateretê design is targeted to offer the largest coherent X-ray beam at the sample position, 73 x 40  $\mu\text{m}^2$ , with a coherent flux of  $10^{13}$  ph/s. The beamline will be operating in the 3 to 20 keV energy range using a large in-vacuum Medipix pixel detector (55 x 55  $\mu\text{m}^2$ ) for imaging biological and nanomaterials. The sample-to-detector distance will be remotely controlled and variable from 50 cm up to 8 m, enabling to carry out ultra-SAXS in the pinhole geometry,  $q_{\text{min}} \sim 1 \cdot 10^{-4} \text{ \AA}^{-1}$ . Finally, yet importantly, pink beam operation is envisaged for time-resolved experiment requiring extremely large flux.

## CONFOCAL X-RAY FLUORESCENCE MICROSCOPY AT THE ADVANCED PHOTON SOURCE SECTOR 20

Y. Zou, Finfrock<sup>1</sup>, Dale L. Brew<sup>2</sup>, Steve M. Heald<sup>2</sup>

*<sup>1</sup>Science Division, Canadian Light Source, Saskatoon SK, CA*

*<sup>2</sup>X-ray Science Division, Advanced Photon Source, Argonne National Laboratory, Argonne IL, USA*

### Abstract

X-ray fluorescence (XRF) is a powerful technique for elemental analysis in part owing to its minimal sample preparation requirements and sub-ppm-sensitivity. However, conventional XRF imaging generally requires thin samples, which is not always desirable or possible, e.g. for brittle samples or when non-destructive analysis is required. Non-destructive 3-D confocal XRF microscopy allows spatial discrimination of XRF photons in all three dimensions and enables high resolution x-ray spectroscopy, such as XANES, to be performed directly on a small region of interest within large samples. Polycapillaries are the most common collection optics used for a confocal XRF microscopy, but limit the technique to depth resolution of upwards of 10 microns at 10keV. The polycapillary in use at sector 20-ID, with a working distance of 10mm, gives a resolution of 30 $\mu$ m at 17.3keV. The new confocal XRF microscopy capability at sector 20-ID, enabled by CHESS micro-channel arrays (CCA), [1] improve depth resolution from 30  $\mu$ m to 2 - 5  $\mu$ m. CCAs provide both an improvement in resolution and, in addition, invariant spatial resolution with the x-ray fluorescence energy. This capability has applications in environmental science, biology, and anthropology. Recent experiments include studies on mineral inclusions, human teeth, fish embryos, plants, and cultural artifacts. The sector 20-ID microscopy station is a KB mirror based microprobe providing a focus in the range 2-8 microns, and we can match the beam sizes to the CCAs spatial resolutions. Recent software development enabled quick (fly) scanning in both ROI and full spectrum mode, which cuts down scan time overhead to a minimum. This poster presents detailed current capabilities of the confocal technique at Sector 20-ID and sample data.

### Acknowledgements

Sector 20 facilities at the Advanced Photon Source, and research at these facilities, are supported by the US Department of Energy - Basic Energy Sciences, the Canadian Light Source and its funding partners, and the Advanced Photon Source. Use of the Advanced Photon Source, an Office of Science User Facility operated for the U.S. Department of Energy (DOE) Office of Science by Argonne National Laboratory, was supported by the U.S. DOE under Contract No. DE-AC02-06CH11357. This research has been performed using optics provided by Cornell High Energy Synchrotron Source "CHESS". CHESS is supported by the NSF & NIH/NIGMS via NSF award DMR-1332208.

### References

- [1] David N Agyeman-Budu, Sanjukta Choudhury, Ian Coulthard, Robert Gordon, Emil Hallin, Arthur R Woll, "Germanium Collimating micro-Channel Arrays For High Resolution, High Energy Confocal X-ray Fluorescence Microscopy," Accepted for publication in the Proceedings of ICXOM 2015, arXiv:1607.01476.

## SUB-CELLULAR ELEMENTAL IMAGING OF EPITHELIAL OVARIAN CANCERS AND THEIR POTENTIAL AS A TISSUE CLASSIFIER

M. Lankosz<sup>1</sup>, M. Grzelak<sup>1</sup>, D. Krauze<sup>1</sup>, M. Brzyszczyk<sup>2</sup>, M. Czyzycki<sup>1,4</sup>, P. Wrobel<sup>1</sup>, D. Adamek<sup>3</sup>, L. Chmura<sup>3</sup>

*1AGH-University of Science and Technology, Faculty of Physics and Applied Computer Science, 30-059 Krakow, Poland,*

*2Jagiellonian University, Faculty of Physics, Krakow, Poland*

*3Jagiellonian University, Faculty of Medicine, Krakow, Poland*

*4IAEA, Wagramer Str. 5, A-1400 Vienna, Austria*

### Abstract

The ovarian surface epithelial tumors are a heterogenic group of neoplasms in which a wide spectrum of clinical behavior can be observed. The carcinogenesis of the above is a multistep process in which varied genetic pathways can be triggered. This raises the question of possible molecular or elemental differences between various ovarian tumors and creates a need for investigation. The proposed studies will help to know if concentrations of minor- and trace elements in the malignant tissues can be used for differentiation and/or classification (diagnosis) of ovarian tumors. The samples designed to elemental  $\mu$ -imaging were taken intraoperatively from ovarian tumors of different types and degree of malignancy. Among the samples analyzed, there were tumors with different degrees of malignancy (benign tumor, borderline tumor, malignant and control tissue). X-ray fluorescence  $\mu$ -spectroscopy was applied for chemical elemental analysis. The samples for cellular analysis were cryo-sectioned to a thickness of 20  $\mu\text{m}$  and then placed on X-ray-transparent ultralene foil and freeze dried. The measurements were performed on beamline FLUO (ANKA, Karlsruhe). The beam was monochromated to 17,2 keV and then focused with glass capillary to  $10 \times 15 \mu\text{m}^2$ . Significant amounts of elements such as P, S, Cl, K, Ca, Fe, Cu, Zn, Br and Rb were present in all neoplastic tissues analyzed. Multivariate methods, i.e., Multivariate Discriminant Analysis (MDA), were applied to the grouping and classification of ovarian tissue samples based on their elemental content. It was found that S, K, Cl, Fe, Zn and Br are the most significant elements in the general discrimination of tumor type. The distribution of the samples in the plane of the two discriminant functions is illustrated in Fig. 1. It was found, that trace elements could be used to correctly identify cancerous tissue and effectively classify the ovarian cancer stage. Tissue material for the sub-cellular experiment was cryo-sectioned to slices of 5  $\mu\text{m}$  thick, mounted on a square silicon nitride membrane window on silicon frame and stored frozen at temperature of liquid nitrogen. The experiment was performed at beamline ID21at ESRF. The 7,3 keV X-ray focused to the spot size of ca.  $0.5 \times 0.9 \mu\text{m}^2$  was used. Such elements as P, S, Cl, K, Ca, Fe were present in all neoplastic tissues analyzed. The maps of Fe, S and P distribution in malignant and control tissues are presented on Fig. 2. The higher concentration of Fe, S and P in cancer cells in comparison to control area was observed.

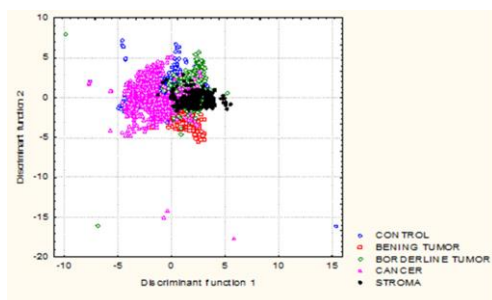


**Figure 1:** The scatter plot of observations in the space of discriminant variables for different types of ovarian cancer

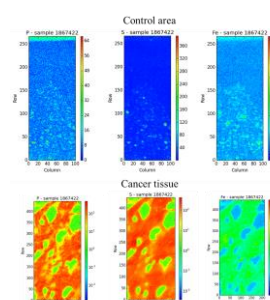


**Figure 2:** SR-XRF maps of P, S and Fe distribution in cancer tissue and control sample.

# DETERMINATION OF CARBON-TO-NITROGEN RATIO IN THE FILAMENTOUS AND HETEROCYSTOUS CYANOBACTERIUM *ANABAENA* SP. PCC 7120 WITH SINGLE-CELL SOFT X-RAY IMAGING

T. Teramoto<sup>1</sup>, M. Yoshimura<sup>2</sup>, C. Azai<sup>3</sup>, K. Terauchi<sup>3</sup>, T. Ohota<sup>2</sup>

<sup>1</sup>College of Science & Engineering, Ritsumeikan University, Shiga, 525-8577, JAPAN

<sup>2</sup>SR center, Ritsumeikan University, Shiga, 525-8577, JAPAN

<sup>3</sup>College of Life Sciences, Ritsumeikan University, Shiga, 525-8577, JAPAN

## Abstract

The natural and anthropogenic conversion of unreactive N<sub>2</sub> to more reactive nitrogen compounds is one of the main issues for ecosystem and food production [1]. Some cyanobacteria are versatile organisms capable of both oxygenic photosynthesis and biological nitrogen fixation, and attract much attention as a potential producer for the industrial nitrogen. The filamentous cyanobacterium *Anabaena* sp. PCC 7120 is a representative of them [2]. It forms a filament of “vegetative cells” responsible for oxygenic photosynthesis; when starved for reactive nitrogen compounds, it differentiates a specialized cell for nitrogen fixation, called “heterocyst”, out of about ten vegetative cells. The heterocyst differentiation is believed to be triggered by a high carbon-to-nitrogen ratio (C/N ratio) of the vegetative cell. However, the C/N ratio change in the single differentiating cell had never been observed so far.

In this study, we applied the soft X-ray microscopy to determine the C/N ratio of individual *Anabaena* sp. PCC 7120 cells. The cells grown on a nitrogen-depleted plate were suspended in pure water and tightly packed between two silicon nitride membranes. The absolute positions of each heterocyst were determined by optical and fluorescence microscopy. The soft X-ray microscopic observation was performed at the wavelengths ( $\lambda$ ) of 2.98 and 3.11 nm at BL12 end station in the Ritsumeikan SR Center. The specification of the soft X-ray microscope setup was described in detail elsewhere [3]. Figure 1 shows the resultant absorbance images; the heterocysts, enclosed in red circles in the panel (a), appeared to have higher absorbance than the surrounding vegetative cells. By statistical analysis of the images from repetitive observations, histograms of element-specific absorbance of vegetative cells and heterocysts were obtained (figure 2).

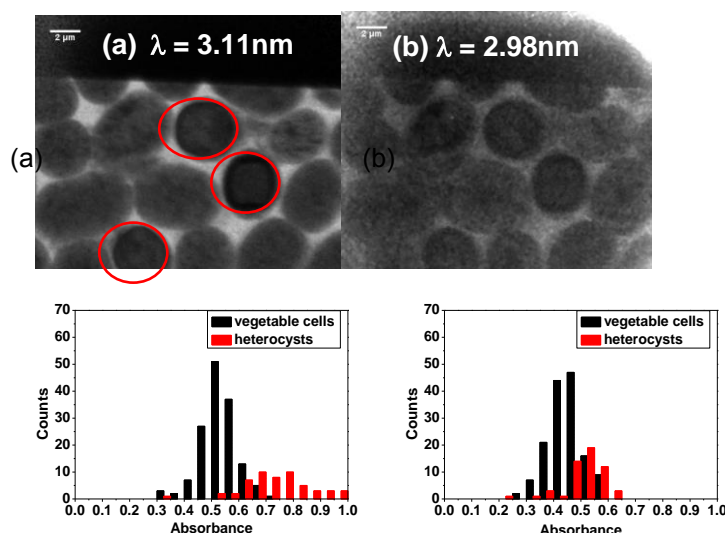


**Figure 1:**  
Soft X-ray microscopic images of *Anabaena* sp. cells at  $\lambda = 3.11 \text{ nm}$  (a) and  $2.98 \text{ nm}$  (b)

**Figure 2:**  
Histograms of the absorbance of each vegetative cell (black bars) and heterocyst (red bars) at  $\lambda = 3.11 \text{ nm}$  (a) and  $2.98 \text{ nm}$  (b)

## References

- [1] J.N. Galloway *et al.*, *Biogeochem.*, 70, 153 (2004)
- [2] A.M. Muro-Pastor and W. Hess, *Trends Microbiol.*, 20, 548 (2012).
- [3] K. Takemoto *et al.*, *JPCS*, 463, 012009 (2013)

# QUANTITATIVE STUDY OF MAMMALIAN CELLS BY SCANNING TRANSMISSION SOFT X-RAY MICROSCOPY

K. Shinohara<sup>1</sup>, T. Ohigashi<sup>2</sup>, S. Tone<sup>3</sup>, M. Kado<sup>4</sup>, A. Ito<sup>1</sup>

*1School of Engineering, Tokai University, Kitakaname, Hiratsuka-shi, Kanagawa 259-1292, Japan*  
*2UVSOR Synchrotron, Institute of Molecular Science, Myodaiji, Okazaki-shi, Aichi 444-8585, Japan*  
*3 Dept. of Biochem., Kawasaki Medical School, Kurashiki-shi, Okayama 701-0192, Japan*  
*4National Institutes for QST, Umemidai, Kizugawa-shi, Kyoto 619-0215, Japan*

## Abstract

Biological application of X-ray microscopy has been extensively developed in imaging the localization of electron dense materials at high resolution. Nevertheless its application to quantitative distribution of biological molecules remains to be studied, though it has long been expected with the observation by soft X-ray spectromicroscopy [1, 2, 3]. In this report, we studied soft X-ray images of mammalian cells and chromosomes quantitatively.

Cultured CHO cells at interphase and at mitotic phase were collected by trypsinization and by blowing the surface of cells in culture grown in the presence of colcemid, respectively. Cells were fixed with Carnoy solution or glutaraldehyde and dropped on the commercially available formvar membrane. Cells and molecules such as DNA and histone were observed with scanning transmission X-ray microscope (STXM) installed at BL4U, UVSOR-III, Okazaki, Japan. The results were analyzed using aXis2000 program. For quantitative analysis, we use NEXAFS spectra of DNA and histone at N-edge, since nucleic acids and proteins are major components of cells containing nitrogen and were clearly separated at  $1s-\pi^*$  transition.

Figure 1 shows the optical density image for an interphase cell obtained with STXM. The absorption spectrum for a whole field was calculated and shown as spect1 in Figure 2. Contribution of DNA on spect1 was subtracted by adjusting the DNA spectrum to spect1 in the OD difference between peak (at 399.6 eV) and valley (at 398 eV) and the resulting spectrum was named as spect2. In the same way, contribution of histone on spect2 was subtracted by adjusting the histone spectrum to spect2 between peak (at 401.5) and valley (at 398). Residual spectrum was named as spect3 and suggested that there may be some molecule(s) containing nitrogen other than nucleic acid and protein. Detailed study for local area is in progress.

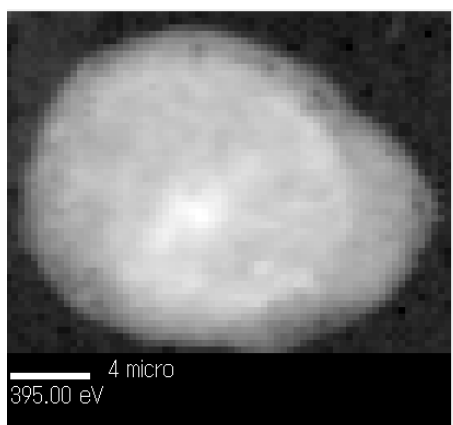


**Figure 1:** Optical density image of an interphase CHO cell fixed with Carnoy solution and observed at 395 eV

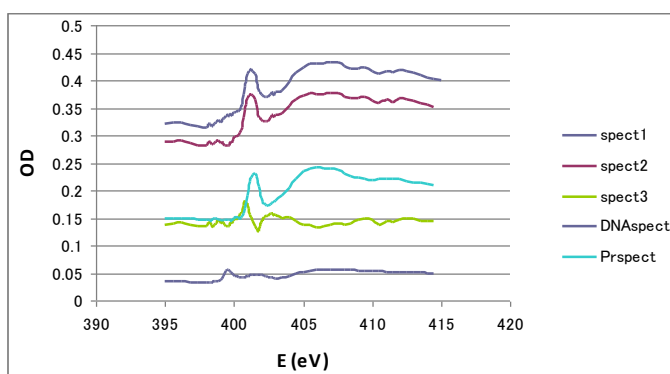


**Figure 2:** Overall averaged spectra of the cell shown in Figure 1 (spect1), DNA spectrum was subtracted from spect1 (spect2), histone spectrum was subtracted from spect2 (spect3). Quantity adjusted DNA (DNAspect) and histone (Prspect) spectra were also included.

## References

- [1] H. Ade et al, Science 258, 972 (1992).
- [2] Zhang et al, J. Struct. Biol. 116, 335 (1996).
- [3] Yangquanwei et al, Nanoscale Res. Lett. 8, 463 (2013).



# AMYLOID PLAQUES ARE A SITE OF REDOX-ACTIVE IRON FORMATION AND CALCIUM MINERALISATION IN ALZHEIMER'S DISEASE TISSUES AS REVEALED BY X-RAY SPECTROMICROSCOPY

J. Everett<sup>1</sup>, V. Tjendana<sup>2</sup>, T. Tyliczszak<sup>3</sup>, J. Dobson<sup>4</sup>, J.F. Collingwood<sup>2</sup> and N. D. Telling<sup>1</sup>

<sup>1</sup>ISTM, Keele University, Stoke-on-Trent, Staffordshire ST4 7QB, UK

<sup>2</sup>School of Engineering, University of Warwick, Coventry, CV4 7AL, UK

<sup>3</sup>Advanced Light Source, Lawrence Berkeley National Laboratory, Berkeley, California, 94720, USA

<sup>4</sup>J. Crayton Pruitt Family Department of Biomedical Engineering & Department of Materials Science and Engineering, University of Florida, Gainesville, Florida 32611, USA

## Abstract

Metals play a pivotal role in multiple processes within the human brain, therefore maintaining metal homeostasis is essential for brain tissue wellbeing. However, mounting evidence indicates disruptions in iron and calcium homeostasis to contribute to the development of the neurodegenerative disorder Alzheimer's disease (AD) [1]. Despite the cause(s) of these disruptions being unclear, recent findings implicate the AD peptide  $\beta$ -amyloid ( $A\beta$ ) in the deleterious handling of metals in AD.  $A\beta$ , the major constituent of AD senile plaques, acts as a metalloprotein and is capable of sequestering calcium [2,3]. Furthermore,  $A\beta$  has been shown to convert benign redox-inactive iron phases into toxic redox-active phases *in vitro* [4,5]. Yet, despite these observations, the role played by iron and calcium dysregulation in human AD tissues remains unknown.

Here x-ray spectromicroscopy is employed to examine pathological amyloid plaque material extracted from the grey matter of two AD subjects. Through this approach, high resolution (ca. 25 nm) speciation-dependent maps were obtained revealing amyloid plaques to *consistently* contain high levels of iron and *two* distinct calcium phases. Further to this, x-ray absorption spectroscopy performed over the iron  $L_{2,3}$ -absorption edge revealed amyloid plaques to harbour *redox-active* iron forms.

These data implicate  $A\beta$  in the disruption of calcium homeostasis and the formation of toxic chemically-active iron phases within human AD tissues, a finding which may influence future methodologies aimed at the diagnosis and treatment of AD. The identification of iron forms specifically associated with AD pathology may act as a biomarker for AD diagnosis using non-invasive techniques such as MRI. Additionally, "pathological" iron phases could provide a target for therapeutics designed to alleviate iron toxicity, whilst maintaining benign iron stores required for brain function. Finally, the observation of two distinct calcium phases within  $A\beta$  plaques indicates a process of calcium biomineralisation to be occurring within AD tissues which could again be utilized as a MRI marker for AD ( $A\beta$ ) diagnosis.

## References

1. Barnham, K.J. *et al.* *Curr. Opin. Chem. Bio.* 12, 222–228 (2008).
2. Watt, F. *Cell. Mol. Biol.* 42, 17-26 (1996).
3. Lovell, M.A. *et al.* *J. Neurol. Sci.* 158, 47-52 (1998).
4. Everett J. *et al.* *J. R. Soc. Int.* 11, 20140165 (2014).
5. Everett J. *et al.* *Inorg. Chem.* 53, 2803-2809 (2014).

## ZINC DISTRIBUTION IN HUMAN BONE: SR-MICRO X-RAY FLUORESCENCE IMAGING OF OSTEOPOROTIC SAMPLES

M. Rauwolf<sup>1</sup>, A. Turyanskaya<sup>1</sup>, A. Roschger<sup>2\*</sup>, J. Prost<sup>1</sup>, R. Simon<sup>3</sup>, I. Pape<sup>4</sup>, M. Radtke<sup>5</sup>, O. Scharf<sup>6</sup>, T. Schoonjans<sup>5†</sup>, A. Guilherme Buzanich<sup>5</sup>, K. Sawhney<sup>4</sup>, P. Wobrauschek<sup>1</sup>, P. Roschger<sup>2</sup>, J.G. Hofstaetter<sup>7,2</sup>, C. Strelli<sup>1</sup>

<sup>1</sup>Atominstytut, TU Wien, Stadionallee 2, 1020 Vienna, Austria

<sup>2</sup>Ludwig Boltzmann Institute of Osteology at the Hanusch Hospital of WGKK and AUVA Trauma Centre Meidling, 1st Med. Dept., Hanusch Hospital, 1140 Vienna, Austria

<sup>3</sup>Karlsruhe Institute of Technology (KIT), ANKA synchrotron radiation source, Hermann-von-Helmholtz-Platz 1, 76344 Eggenstein-Leopoldshafen, Germany

<sup>4</sup>Diamond Light Source Ltd, Harwell Science & Innovation Campus, Didcot, Oxfordshire, Great Britain

<sup>5</sup>Federal Institute for Materials Research and Testing (BAM), 12489 Berlin, Germany

<sup>6</sup>IFG Institute of Scientific Instruments GmbH, Berlin, Germany

<sup>7</sup>Orthopaedic Hospital Vienna-Speising, 1130 Vienna, Austria

### Abstract

Zn is known to be located in the reactive centers of various enzymes, which play a major role in the mineralization process at sites where new bone formation occurs. In addition, elevated Zn levels are supposed to increase the proliferation rate of osteoblasts [1] and may lead to a stimulation of bone formation in vitro and in vivo [2]. Consequently, Zn seems to play an essential role in bone formation and mineralization through various pathways. We thus expected Zn levels to be altered at sites of extensive bone formation like in the case of fracture healing.

We measured the same areas on human bone samples with both a scanning confocal synchrotron radiation induced micro X-ray fluorescence (SR- $\mu$ XRF) at the FLUO beamline (ANKA) and a full-field Color X-ray Camera at the BAMline (Bessy II) setup in order to find the ideal SR- $\mu$ XRF imaging method to investigate trace element distributions in bone samples. As zinc is a trace element of special interest in bone, the setups were optimized for Zn detection. The setups were compared concerning count rate, required measurement time and resolution. We could show that the ideal method is depending on the element of interest. While for Ca (a major constituent of the bone with a low energy of 3.69keV for K) the Color X-ray Camera provided us with a higher resolution in the plane, for Zn (a trace element in bone) only the confocal SR- $\mu$ XRF was able to sufficiently image the distribution.

Biopsies of healing osteoporotic fractures (Vertebral compression fractures (VCFs)) were investigated in regard to their Zn distribution. The samples were measured with a confocal SR- $\mu$ XRF setup with a 10  $\mu$ m x 15  $\mu$ m resolution at the FLUO beamline at ANKA. As we found increased Zn levels, which seemed to be accumulated in narrow structures between bone packages we also investigated thin cuts (4  $\mu$ m thick) of two sample areas with a higher resolution of 1  $\mu$ m x 1  $\mu$ m (monochromatic beam with E= 17 keV) at B16 at Diamond SR facility.

We will present the advantages and disadvantages of all three SR- $\mu$ XRF setups (ANKA FLUO beamline, Bessy II BAMline, and Diamond B16) for imaging elemental distributions in bone with a focus on Zn. We will also show the distribution of Zn in healing VCFs.

### References

- [1] H.-J. Seo, Y.-E. Cho, T. Kim, H.-I. Shin, I.-S. Kwun, *Nutr. Res. Pract.* 4 (2010) 356–61
- [2] A. Ito, H. Kawamura, M. Otsuka, M. Ikeuchi, H. Ohgushi, K. Ishikawa, K. Onuma, N. Kanzaki, Y. Sogo, N. Ichinose, *Mater. Sci. Eng. C.* 22 (2002) 21–25

\* Now at Max Planck Institute of Colloids and Interfaces, Department of Biomaterials, Potsdam, Germany

† Now at Diamond Light Source Ltd, Harwell Science & Innovation Campus, Didcot, Oxfordshire, Great Britain

## EXPLOITATION OF $\mu$ XRF SPECTROMETER FOR BIO-IMAGING

A. Turyanskaya<sup>1</sup>, M. Rauwolf<sup>1</sup>, L. Pernecky<sup>1</sup>, J. Prost<sup>1</sup>, T.A. Gruenewald<sup>2</sup>, M. Meischel<sup>2</sup>,  
H. Lichtenegger<sup>2</sup>, S.E. Stanzl-Tschegg<sup>2</sup>, A.M. Weinberg<sup>3</sup>, P. Wobrauschek<sup>1</sup>, C. Strel<sup>1</sup>

*1TU Wien, Atominstitut, Vienna, Austria*

*2University of Natural Resources and Life Sciences (BOKU), Vienna, Austria*

*3Department of Orthopaedics and Orthopaedic Surgery, Medical University Graz, Graz, Austria*

### Abstract

Micro X-ray fluorescence spectrometry ( $\mu$ XRF) is a powerful tool for determination of spatial distribution of major, minor, and trace elements within a sample.

The  $\mu$ XRF setup at Atominstitut (ATI) was designed in house and is suited for the detection of wide range of elements [1,2]. The Rh-low power tube (20W) offers excellent excitation conditions for both light and heavy elements. The 30mm<sup>2</sup> Si(Li) detector, LN<sub>2</sub> cooled, with ultrathin polymer window (UTW), as well as operation under vacuum conditions are suited for analysis of light elements, e.g. magnesium. To focus the primary beam on the sample a polycapillary optics (full lens) is used; the beam size determined for Cu-K $\alpha$  - 50x50 $\mu$ m<sup>2</sup>.

In confocal configuration, which is assembled by installing another x-ray polycapillary optics (half lens) in front of the detector, a depth-defined measurement is obtained, allowing the determination of the spatial distribution of elements within a sample in three dimensions [3]. The beam size determined for Cu-K $\alpha$  in the system with confocal set-up - 50x50x50 $\mu$ m<sup>3</sup>.

The ATI  $\mu$ XRF setup has also an advantage of being a transportable system, therefore allowing to use synchrotron radiation as a source for experiments, thus shortening considerably the required measurement time and/or enabling to scan larger areas.

The samples under investigation - rat bone tissue with implanted pins, made of a biodegradable alloy, were collected at given time points between 1 and 18 months after implantation, and thin sections (range of 150-550 $\mu$ m) were then embedded into PMMA [4]. The scans were performed in the areas, engaging the interface implant/bone and surrounding bone tissue. The obtained elemental maps of magnesium and yttrium (the constituents of the implants) and calcium (the primary mineral component of the bone) in non-confocal and confocal setups, provide us with the relevant information on the degradation process.

### References

- [1] P. Wobrauschek, B. Frank, N. Zöger, S. Strel, N. Cernohlawek, C. Jokubonis, H. Hoefler, Micro XRF of light elements using a polycapillary lens and an ultra thin window silicon drift detector inside a vacuum chamber, *Adv. X-Ray Anal.* 48 (2005) 229–235.
- [2] S. Smolek, C. Strel, N. Zoeger, P. Wobrauschek, Improved micro x-ray fluorescence spectrometer for light element analysis., *Rev. Sci. Instrum.* 81 (2010) 053707.
- [3] S. Smolek, B. Pemmer, M. Fölser, C. Strel, P. Wobrauschek, Confocal micro-x-ray fluorescence spectrometer for light element analysis., *Rev. Sci. Instrum.* 83 (2012) 083703.
- [4] T. Kraus, S.F. Fischerauer, A.C. Hänzi, P.J. Uggowitz, J.F. Löffler, A.M. Weinberg, Magnesium alloys for temporary implants in osteosynthesis: In vivo studies of their degradation and interaction with bone, *Acta Biomater.* 8 (2012) 1230–1238.

# AN INTEGRATED APPROACH TO UNRAVEL THE INTERPLAY BETWEEN STRUCTURAL AND CHEMICAL PROPERTIES OF SUBSTANTIA NIGRA NEURONS IN THE ELDERLY

A.D. Surowka<sup>1</sup>, M. Töpperwien<sup>2</sup>, M. Bernhardt<sup>2</sup>, J.D. Nicolas<sup>2</sup>, M. Osterhoff<sup>2</sup>, T. Salditt<sup>2</sup>, D. Adamek<sup>3</sup>, M. Szczerbowska-Boruchowska<sup>1</sup>

<sup>1</sup>AGH University of Science and Technology, Faculty of Physics and Applied Computer Science, Al. Mickiewicza 30, 30-059 Kraków, Poland

<sup>2</sup>Institut für Röntgenphysik, Georg-August-Universität Göttingen, Friedrich-Hund-Platz 1, Göttingen, Germany

<sup>3</sup>Jagiellonian University, Faculty of Medicine, Department of Neuropathology, Krakow, Poland.

## Abstract

Human dopaminergic system in general, and the substantia nigra (SN) neurons in particular are implicated in the pathologies underlying the human brain ageing [3]. The interplay between the structure and elemental composition of SN neuron bodies has recently gained in importance as metals: Fe, Cu, Zn, Ca were found to trigger oxidative-stress-mediated aberration in their molecular assembly due to concomitant protein aggregation and lipid peroxidation [1-2]. In the present study, we demonstrate an integrated approach for the analysis of structure, assembly, and metals' accumulation in two distinct areas of SN: in the neuromelanine neurons and neuropil. By using the highly brilliant source PETRA III and the Kirkpatrick-Baez nano-focus, we could afford to ultra-fast dynamic scanning at the sub-neuronal resolution down to 500 nm. Elemental analysis with combined X-ray Fluorescence (SRXRF) and X-ray Phase Contrast Imaging (XPCI) allowed for unbiased quantification of the spectroscopic data by determination of the electron density. Based on the raw SRXRF spectra, we could find P, S, Cl, K, Ca, Fe, Cu and Zn to accumulate predominantly in the SN neurons. However, upon the mass thickness correction, the concentration of Cl became significantly less focalized. Concomitant Small Angle X-ray Scattering (SAXS) experiments, thorough computation of the dark field and differential phase contrast, have demonstrated these tissue compartments are made of unordered matter, whilst the SN neurons and neuropil have radically higher density. In all, the results show up the combined SRXRF-PPCI-SAXS experiments can serve as a unique tool for understanding the interplay between the chemical and structural properties that may drive the biochemical age-related processes occurring in the human dopaminergic system.

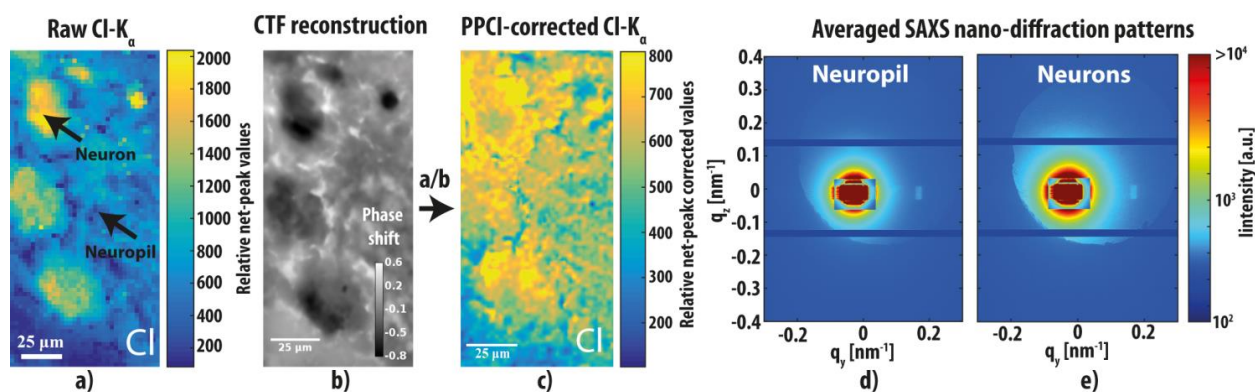


**Figure 1:** a) Raw (uncorrected) values of net-peak values of C, b) CTF-based phase reconstruction for the areas shown in Fig a; c) The corrected distribution of Cl-K $\alpha$ ; d) e) Averaged SAXS nano-diffraction patterns for neuropil and neurons, respectively.

## References

- [1] A.D. Surowka, P. Wróbel, D. Adamek, E. Radwańska, M. Szczerbowska-Boruchowska. *Metallomics*, 2015,7; 1522-1531. doi: 10.1039/C5MT00154D
- [2] Surowka AD, Adamek D, Radwańska E, Szczerbowska-Boruchowska M. *Neurochem Int*. 2014 30;76C:12-22. doi: 10.1016/j.neuint.2014.06.014.
- [3] Szczerbowska-Boruchowska M, Krygowska-Wajs A, Adamek D. *J Phys Condens Matter*. 2012, 20; 24(24):244104. doi: 10.1088/0953-8984/24/24/244104.

## X-RAY SCATTERING AND NANOPROBE XRF REVEALS ULTRASTRUCTURAL ORGANIZATION IN MELANOSOMES

T. Gorniak<sup>1</sup>, T. Haraszti<sup>2</sup>, A.R. Buck<sup>1</sup>, T. Senkbeil<sup>1</sup>, C. Rumancev<sup>1</sup>, S. Stuhr<sup>1</sup>, M. Priebe<sup>3</sup>, T. Salditt<sup>3</sup>, H. Suhonen<sup>4</sup>, Y. Yang<sup>4</sup>, R. Heine<sup>5</sup>, V.M. Garamus<sup>6</sup>, M. Grunze<sup>5</sup>, M.G. Anderson<sup>7</sup>, A. Rosenhahn<sup>1</sup>

<sup>1</sup> Analytical Chemistry - Biointerfaces, Ruhr-University Bochum, Bochum, Germany

<sup>2</sup> Max Planck Institute for Intelligent Systems, Stuttgart, Germany

<sup>3</sup> Institute for X-ray physics, University of Göttingen

<sup>4</sup> ESRF, Grenoble, Cedex, France

<sup>5</sup> Karlsruhe Institute of Technology, Karlsruhe, Germany

<sup>6</sup> Helmholtz Zentrum Geesthacht, Geesthacht, Germany

<sup>7</sup> The University of Iowa, Iowa city, IA, USA

### Abstract

Melanosomes are highly specialized organelles that produce and store pigment melanin, thereby fulfilling essential functions within their host organism. Besides having obvious cosmetic consequences – determining the color of skin, hair and the iris – they contribute to photochemical protection from ultraviolet radiation, as well as to vision (by defining how much light enters the eye). Though melanosomes can be beneficial for health, abnormalities in their structure can lead to adverse effects. We exploited the high structural sensitivity and penetration depth in conjunction with the powerful element sensitivity of X-rays to shed further light on the structure of melanosomes. The complementary information from SAXS of large, suspended melanosome ensembles was compared to scattering from single, vitrified specimens<sup>1</sup>. The experiments revealed a melanosomal sub-structure whose surface and bulk properties differ in two commonly used inbred strains of laboratory mice. Whereas melanosomes in C57BL/6J mice have a well-defined surface and are densely packed with 40-nm units, their counterparts in DBA/2J mice feature a rough surface, are more granular and consist of 60-nm building blocks. The fact that these strains have different coat colors and distinct susceptibilities to pigment-related eye disease suggest that these differences in size and packing are of biological significance. In addition to the structural analysis by scattering, X-ray nanoprobe fluorescence analysis was applied to survey the nanoscale distribution of metals within purified organelles<sup>2</sup>. Cu is known to be associated with eumelanin and its predominant occurrence in the shell of the melanosomes is a proof of the long discussed ‘casing model’, predicting that melanosomes contain a pheomelanin core surrounded by a eumelanin shell.

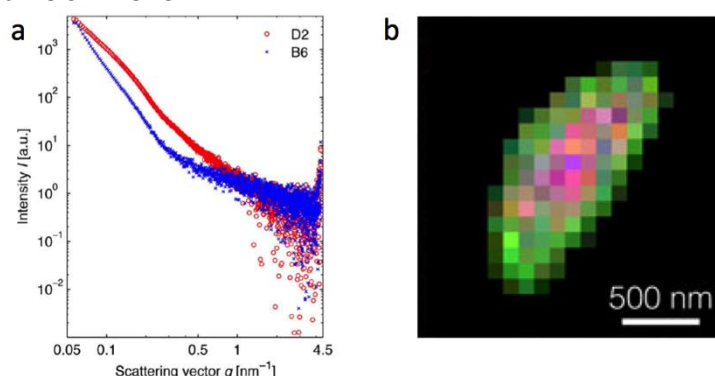


**Figure 1:** (a) SAXS reveals an enhanced granularity for D2 phenotype<sup>1</sup> (b) Cu concentration within organelles serves as intrinsic marker to reveal the core-shell organization of melanosomes<sup>2</sup>.

### References

- [1] T. Gorniak, T. Haraszti, V. M. Garamus, A. R. Buck, T. Senkbeil, M. Priebe, A. Hedberg-Buenz, D. Koehn, T. Salditt, M. Grunze, M. G. Anderson and A. Rosenhahn, *PLoS ONE*, 2014, **9**, e90884.
- [2] T. Gorniak, T. Haraszti, H. Suhonen, Y. Yang, A. Hedberg-Buenz, D. Koehn, R. Heine, M. Grunze, A. Rosenhahn and M. G. Anderson, *Pigment Cell & Melanoma Research*, 2014, **27**, 831-834.



## INVESTIGATING TISSUE SURROUNDING MULTI-CHANNEL COCHLEAR IMPLANT ELECTRODE ARRAYS WITH X-RAY FLUORESCENCE MICROSCOPY

K. M. Spiers<sup>1</sup>, T. Cardamone<sup>2</sup>, J. B. Furness<sup>2,3</sup>, J. C. M. Clark<sup>4</sup>, J. F. Patrick<sup>5</sup>, G. M. Clark<sup>6</sup>

<sup>1</sup>Deutsches Elektronen-Synchrotron DESY, Hamburg, Germany, <sup>2</sup>Department of Anatomy and Neuroscience, University of Melbourne, Australia, <sup>3</sup>Florey Institute of Neuroscience and Mental Health, Australia, <sup>4</sup>Department of Anatomical Pathology, Austin Hospital, University of Melbourne, Australia, <sup>5</sup>Cochlear Corporation, Sydney, Australia, <sup>6</sup>Centre for Neural Engineering, University of Melbourne, Australia

### Abstract

X-ray fluorescence microscopy (XFM) analysis was performed on temporal bone thin sections taken posthumously from a patient who had been the recipient of three multi-channel cochlear implant electrode arrays. The arrays were sequentially denoted UOM, CI-22 and CI-24; the latter two arrays replaced their predecessor upon failure, and the third array was removed posthumously [1]. Each array consisted of Pt ring electrodes, around an insulated core carrying the Pt/Ir lead wires, which electrically stimulated cells within the cochlea to enable hearing. The longest period an array had remained in place was 24 years.

The fixed and decalcified temporal bones were sectioned (5  $\mu\text{m}$ ) for histological analysis of the cochlea (Fig 1A). Fibrous connective tissue, active fibroblasts and small regions of heterotopic bone were identified. The fibrous tissue was associated with dark particulate material which was not identifiable, but likely to be Pt.

An XFM study [2] confirmed the particulate material as Pt, and revealed sub-micron Pt particles not previously observed (Fig 1B). A further XANES imaging investigation (Fig 1C, D) indicated the larger particles were metallic Pt(0) and corresponded to higher concentrations, while the spectra of the sub-micron, lower concentration Pt deposits demonstrated an edge shift and spectral characteristics of oxidized Pt. The oxidation state of the Pt may provide insight as to the particles' deposition mechanism (ie flaked off the electrode, or released by electrolysis). However, possible chemical changes due to fixatives and other treatments applied to the sample must be considered.

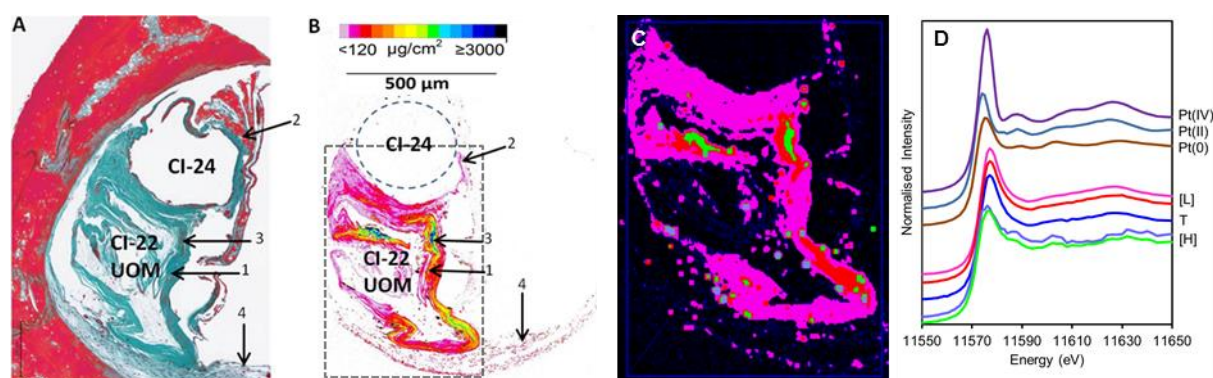


**Figure 1A:** Masson Trichrome stain of human cochlea from UOM patient. **B:** XFM image of an adjacent section to Fig 1A. Pt areal density on a linear colour scale for  $>120 \mu\text{g}/\text{cm}^2$  Pt. Arrows in Fig 1A,B: (1) capsule of UOM and CI-22 arrays; (2) capsule of CI-24 with bone formation; (3) site of visible Pt particle; (4) sub-micron Pt particles incorporated into the spiral ligament. **C:** Region (rectangle in B) investigated with XANES mapping; colours correspond to spectra shown in D. **D:** Pt XANES spectra for standards: Pt(0) (foil), Pt(II)Cl, Pt(IV)Cl, and extracted spectra for coloured regions in C: [L] and [H] Low and High Pt concentrations; T: Total area (blue rectangle in C).

### References

- [1] Clark G. M. et. al., Cochlear Implants International, 15: S1-S15 (2014)
- [2] Spiers, K. et. al., Cochlear Implants International, DOI: 10.1080/14670100.2016.1157943



## DYNAMICAL X-RAY IMAGING AT A COMPACT LIGHT SOURCE

R. Gradl<sup>1</sup>, M. Dierolf<sup>1</sup>, K. S. Morgan<sup>1,4</sup>, B. Günther<sup>1,3</sup>, L. Hehn<sup>1,2</sup>, E. Eggl<sup>1</sup>, C. Jud<sup>1</sup>, B. Gleich<sup>1</sup>, K. Achterhold<sup>1</sup>, F. Pfeiffer<sup>1,2</sup>

<sup>1</sup> Department of Physics and Institute of Medical Engineering, Technical University of Munich, James-Franck-Str. 1, 85748 Garching, Germany

<sup>2</sup> Department of Diagnostic and Interventional Radiology, Klinikum rechts der Isar, Technical University of Munich, Ismaninger Straße 22, 81675 München, Germany

<sup>3</sup> Max-Planck-Institute for Quantum Optics, Hans-Kopfermann-Str. 1, 85748 Garching, Germany

<sup>4</sup> School of Physics, Monash University, Clayton, Victoria 3800, Australia

### Abstract

Since their discovery X-rays have strongly influenced a variety of scientific domains. In particular their property to penetrate matter has been used to visualize the inner structures of opaque objects. Fundamental steps for a significant contrast enhancement in X-ray imaging have been achieved by the transfer of the phase-contrast imaging principle from visible light to X-rays together with the large improvement in X-ray beam quality through the construction of synchrotrons. However these large-scale facilities have limited beam time, are high in cost and are not available for routine applications. Accordingly, the development of affordable and compact sources with sufficient flux and coherence is important to enable laboratory experiments which were previously limited to synchrotrons.

This gap between laboratory sources and synchrotrons is now filled with the installation of the Munich Compact Light Source (MuCLS). The MuCLS, with a size of about 5 m x 2 m, can deliver a highly coherent, quasi-monochromatic X-ray beam between 15 keV and 35 keV, with flux up to 1e10 ph/s [1, 2].

As shown in Fig. 1 the MuCLS consists of three major parts: The source itself produces X-rays via inverse Compton scattering by colliding an intense laser beam with an electron beam. This X-ray beam is guided to two end-stations. One is placed about 3 m after the interaction point and the second is 15 m away. In this report, the focus lies on the front experimental hutch that is equipped with a setup for propagation-based phase-contrast imaging and high-resolution micro-tomography.

One of the intended applications of this setup is *in vivo* dynamical lung and airway imaging in small-animal models. This will provide an important tool in better understanding and treating pulmonary diseases such as emphysema and cystic fibrosis. To be fast enough to image every breath and to achieve high-quality propagation-based phase contrast to render the lungs and airways visible, a sufficiently coherent X-ray beam with high flux is necessary. Therefore, these experiments have so far been limited to synchrotron facilities. However, the X-ray beam properties at the MuCLS enable a high frame rate combined with micron-scale resolution over a centimeter-sized field of view in a laboratory environment. The first biomedical phase-contrast measurements at the CLS show promising results [3, 4].

This presentation describes the modalities available in the front experimental hutch at the MuCLS and presents first results obtained with the high-resolution setup.

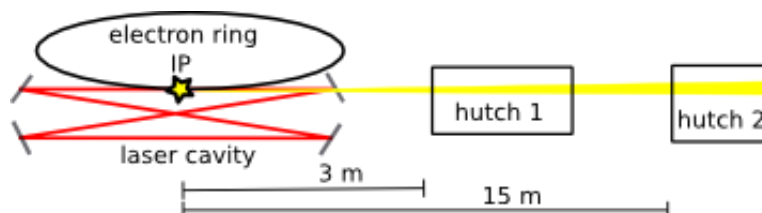


**Figure 1:** The X-ray beam is produced at the Interaction Point (IP) of the laser and electron beams and then guided into hutch 1 and hutch 2.

### References

- [1] E. Eggl et al., (submitted 2016).
- [2] The MuCLS was developed by Lyncean Technologies Inc.; [www.lynceantech.com](http://www.lynceantech.com)
- [3] S. Schleede et al., PNAS 109 (44), 17880, (2012).
- [4] E. Eggl et al., PNAS 112 (18), 5571, (2015).

## THE DEVELOPMENT OF A TOMOGRAPHIC X-RAY FLUORESCENCE MICROSCOPY AT THE 2-ID-E BEAMLIN

Luxi Li, Olga Antipova, Si Chen, Doga Gursoy, Stefan Vogt

*Advanced Photon Source, X-ray Science Division, Argonne National Laboratory, 9700 S. Cass Ave., Lemont, IL 60439 USA*

### Abstract

The X-ray Fluorescence Microscopy (XFM) has been an indispensable technique to determine the elemental distribution, especially for trace element mapping. It provides a nondestructive approach to the projective elemental mapping of samples, especially biological and medical materials. Recently, 3D element mapping has been performed on Diatoms [1] and Zebrafish embryos [2] with the tomographic XFM approach at the 2-ID-E beamline at the Advanced Photon Source (APS). Due to the low efficiency of the fluorescence emission, the tomographic XFM is limited to the sample thickness or the attenuation of the sample materials. In this work, we will present the current development of the tomographic XFM at the 2-ID-E microprobe beamline at APS. The absorption correction to the measured fluorescence signals will also be discussed for the data processing strategies. The application of the tomographic XFM is not restricted to biological and medical samples. It also presents great potential in material sciences and industrial studies.

### References

- [1] M. D. de Jonge, *et al*, Proc. Natl. Acad. Sci. USA 107, 15676 (2010).
- [2] D. Bourassa, *et al*, Metallomics 6, 1648 (2014).

# HIGH-RESOLUTION SUBCELLULAR IMAGING AT THE ESRF NEW NANOIMAGING BEAMLINE: DECIPHERING INTRACELLULAR TARGETS OF ANTICANCER DRUGS IN BREAST CANCER CELLS

Florin Fus<sup>1,2</sup>, Peter Cloetens<sup>1</sup>, Siden Top<sup>3</sup>, Yang Yang<sup>1</sup>, Alexandra Pacureanu<sup>1</sup>, Julio Cesar da Silva<sup>1</sup>, Anne Vessi re<sup>3</sup>, G rard Jaouen<sup>3</sup>, Sylvain Bohic<sup>1,2</sup>

<sup>1</sup>ESRF – The European Synchrotron, 38000 Grenoble, France

<sup>2</sup>Inserm U1216, Team Synchrotron radiation and Medical research, University of Grenoble Alpes, Grenoble, France

<sup>3</sup>Sorbonne Universit s, UPMC Univ Paris 06, UMR 8232, IPCM, Paris, France

## Abstract

The new state-of-the-art Nano-Imaging beamline ID16A-NI at ESRF offers unique capabilities for X-ray imaging at nanometer scale delivering a highly coherent, very intense nanofocused beam ( $> 5 \times 10^{11}$  ph/s at  $\Delta\lambda/\lambda \sim 10^{-2}$ ) at high energies ( $\sim 30$  nm at 17 keV). It is particularly well suited for the investigation of biological samples at high spatial resolution, e.g. the detection and quantification of trace elements <sup>[2]</sup>, such as metals in metal-based drugs in cancer treatment. Triple negative breast cancer tumors, responsible for a high rate of mortality, are a major challenge for breast oncologists since no targeting therapy is currently available for them. Jaouen's group has developed<sup>[1]</sup> ferrocenyl metal-based drug candidates that can target both hormone-dependent and independent breast cancer cells at low  $\mu$ M range showing encouraging anticancer effects. Our aim is to identify the targeted intracellular compartments where these compounds are active as a main step towards explaining their action mechanisms.

Osmium derivatives of the ferrocenyl based drug were imaged in MDA-MB-231 breast cancer cell line (2  $\mu$ M of Os-diOH and Os-OHTAM for 30 min) using both X-ray fluorescence and phase imaging at 17 keV. Various sample preparation techniques were explored. First chemically fixed cells (2% PFA for 30 min at room temperature) were imaged in 2D (fluorescence at 50 nm and phase imaging at 10 nm pixel size) to reveal the quantitative elemental distribution. Then we imaged 200 nm thin sections prepared by high pressure freezing for fixation followed by cryo-substitution and resin embedding. Finally X-ray fluorescence tomography scans of the entire cells were performed at 150 nm step size, after the endoplasmic reticulum had been labeled using ER-tracker bleue-white DPX live cell dye.

The 2D fluorescence maps of entire cells consistently revealed a pattern of high Os concentration alongside the nuclear membrane, localization further confirmed by the 3D fluorotomography data. This work confirms the potential to reveal structural information at unprecedented resolution.

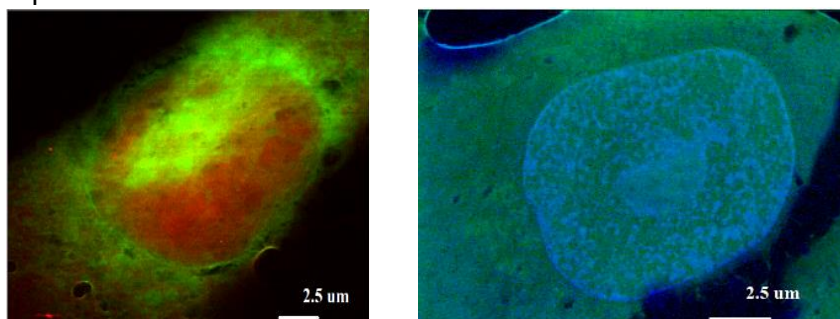


**Figure 1:** Fluorescence maps of breast cancer cells at 50 nm pixel size. Left: Superimposed Zn (red) and Os (green) distributions. Right: 200 nm thick section, Cl (green) and P (blue) distributions

## References

- [1] Hillard, E. A.; Vessieres, A.; Jaouen, G., Ferrocene Functionalized Endocrine Modulators as Anticancer Agents. In *Medicinal Organometallic Chemistry*, Jaouen, G.; Metzler-Nolte, N., Eds. Springer Verlag, 2010; Vol. 32, pp 81-118.
- [2] Bohic S. et al., Biomedical applications of the ESRF synchrotron-based microspectroscopy platform, *Journal of Structural Biology*, 177 (2012) 248-258

## THE BIONANOPROBE: PRESENT AND FUTURE

S. Chen<sup>1</sup>, B. Lai<sup>1</sup>, Jörg Maser<sup>1</sup>, Chris Roehrig<sup>1</sup>, T. Paunesku<sup>2</sup>, Q. Jin<sup>3</sup>, Junjing Deng<sup>4</sup>, K. Brister<sup>5</sup>, C. Jacobsen<sup>1,2,3</sup>, G. Woloschak<sup>2</sup>, S. Vogt<sup>1</sup>

<sup>1</sup>Advanced Photon Source, Argonne National Lab, Argonne, IL 60439, USA

<sup>2</sup>Department of Radiation Oncology, Northwestern University, Chicago, IL 60611, USA

<sup>3</sup>Department of Physics and Astronomy, Northwestern University, Evanston, IL 60208, USA

<sup>4</sup>Applied Physics, Northwestern University, Evanston, IL 60208, USA

<sup>5</sup>Synchrotron Research Center, Northwestern University, Argonne, IL 60439, USA

### Abstract

The Bionanoprobe (BNP) is a hard x-ray fluorescence nanoprobe installed at the Advanced Photon Source (APS) at Argonne National Lab. The BNP is dedicated to studying trace elements, particularly metals, in whole and fully hydrated biological cells at cryogenic temperatures. It is the first such instrument worldwide with a robotic sample transfer system (Fig 1) for cryogenic specimens. We have demonstrated spatial resolution down to 30 nm for 2D imaging [1] and fluorescence tomography capabilities [2].

We will first describe the instrument and its capabilities. In most cases we work with biological specimens deposited or cultured on silicon nitride windows, which are then plunge frozen. We have demonstrated UV sterilization of cryogenic specimens [3]. Recent results on the comparison of cryo versus conventional chemical fixation and drying protocols will be summarized. Cryo light microscopy is used to evaluate and select specimen regions prior to x-ray examinations using the BNP, and a cryo confocal light microscope is currently under development for correlative studies. We use either differential phase contrast or ptychography [4] to obtain complementary information on the ultrastructure of cells since lighter elements are not easily detected using x-ray fluorescence. Example applications using these combined capabilities will be discussed.

Biological systems are hierarchically organized, with features from such as exosomes with sub-10 nm in size to the macroscopic size scales of tissues and organs. However, the current BNP only provides a window into features from 30 nm to a few hundred microns. Studies requiring incident energies above 20 keV are very challenging due to significant

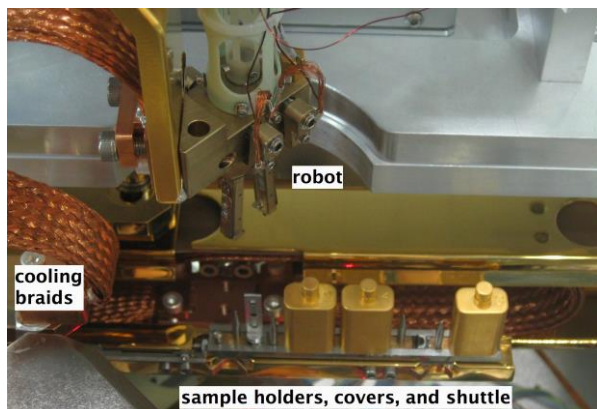


**Figure 1:** Robotic sample transfer system at the Bionanoprobe handling frozen samples at the temperature range of liquid nitrogen.

reduced photon flux and low efficiency of zone plates at high energies. With the advent APS Upgrade, the brilliance of the light source will massively increase in particular at high energies. Coupled with advanced zone plate nanofocusing techniques, the BNP will allow probing cellular ultrastructures at the level of 10 nm across large tissues of millimeters in size. Studies of high atomic number elements will be enabled: elements such as Se, Ru, Cd, and Pt are important for both life and environmental sciences; Au is traditionally used as a label for immunocytochemistry applications in life sciences.

### References

- [1] S. Chen *et al.*, *J. of Synchrotron Rad* **21**, 66 (2014).
- [2] Y. Yuan *et al.*, *ACS Nano* **7**(12), 10502 (2013).
- [3] Q. Jin *et al.*, *PLoS One* **10** (2), e0117437 (2015).
- [4] J. Deng *et al.*, *Proc Natl Acad Sci USA*, 201413003 (2015).



## SUB-MICRON X-RAY FLUORESCENCE IMAGING OF BIOLOGICAL SAMPLES AT 2-ID-E AT THE ADVANCED PHOTON SOURCE

O. Antipova<sup>1</sup>, L. Li<sup>1</sup>, T. Paunesku<sup>2</sup>, L. Nonn<sup>3</sup>, C. Roehrig<sup>1</sup>, S. Vogt<sup>1</sup>

*1Advanced Photon Source, Argonne National Laboratory, Argonne IL, USA*

*2Department of Radiation Oncology, Northwestern University, Chicago, IL 60611, USA*

*3Department of Pathology, University of Illinois at Chicago, Chicago, IL 60611, USA*

### Abstract

Synchrotron-based hard x-ray fluorescence microscopy is a great tool for studying the distribution of elements, such as S, P, K, Fe, Zn, Cu, and others in many-micrometer-thick specimens with sub-micron spatial resolution, part-per-million detection sensitivity, and the ability to acquire tomographic datasets [1]. Samples (biological tissue sections, cells, crystals, etc.) are raster-scanned with x-ray beam and x-ray fluorescence signal is recorded for each pixel. The elemental content is measured using the characteristic fluorescence of atoms excited by the x-ray beam. This information in addition to other biochemical methods help understanding a variety of biological processes, such as embryo development, cancer spreading mechanisms and cells response to treatments [2].

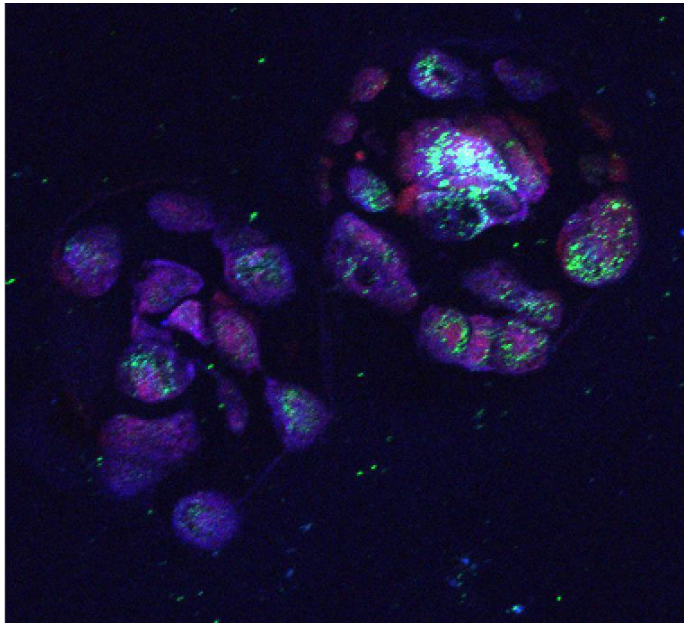


**Figure 1:** Colocalization of Zn (blue), P (red) and Fe (green) in human prostate organoids, designed to study effect of miR-183-96-182 on Zn homeostasis and prostate health [3].

### References

- [1] T. Paunesku, S. Vogt, J. Maser, B. Lai, G. Woloschak. X-ray fluorescence microprobe imaging in biology and medicine. *J Cell Biochem.* 99(6) (2006).
- [2] D. Mustafi, J. Ward, U. Dougherty, M. Bissonnette, J. Hart, S. Vogt, G.S. Karczmar. X-ray fluorescence microscopy demonstrates preferential accumulation of a vanadium-based magnetic resonance imaging contrast agent in murine colonic tumors. *Mol Imaging.* 14 (2015).
- [3] B. Mihelich, E. Khramtsova, N. Arva, A. Vaishnav, D. Johnson, A. Giangreco, E. Martens-Uzunova, O. Bagasra, A. Kajdacsy-Balla, L. Nonn. The miR-183-96-182 cluster is overexpressed in prostate tissue and regulates zinc homeostasis in prostate cells. *J Biol Chem* 286(52):44503-11 (2011).

## TWO-DIMENSIONAL SINGLE CRYSTAL DIAMOND COMPOUND REFRACTIVE X-RAY LENS

O. Antipova<sup>1</sup>, S.V. Baryshev<sup>2</sup>, S. Stoupin<sup>1</sup>, S. Antipov<sup>2</sup>

<sup>1</sup>X-ray Science Division, Argonne National Laboratory, Lemont, IL  
<sup>2</sup>Euclid Techlabs LLC, Bolingbrook, IL

### Abstract

The next generation light sources such as diffraction-limited storage rings and high repetition rate X-ray free-electron lasers will generate x-ray beams with significantly increased brilliance. These future machines will require X-ray optical components that are capable of handling higher instantaneous and average power densities while tailoring the properties of the X-ray beams for a variety of scientific experiments. Single crystal diamond is the most suitable material for this application, because it is radiation hard, has an appropriate combination of absorption coefficient and index of refraction, and the best available thermal properties. Recently we fabricated and tested two-dimensional (2D) single crystal diamond refractive X-ray lens [1]. The lenses were manufactured using femto-second laser micromachining and tested at the Advanced Photon Source (APS) of Argonne National Laboratory. In this paper, we present realization and testing of a compound refractive lens (CRL) [2], i.e. a stack of two-dimensional diamond lenses.

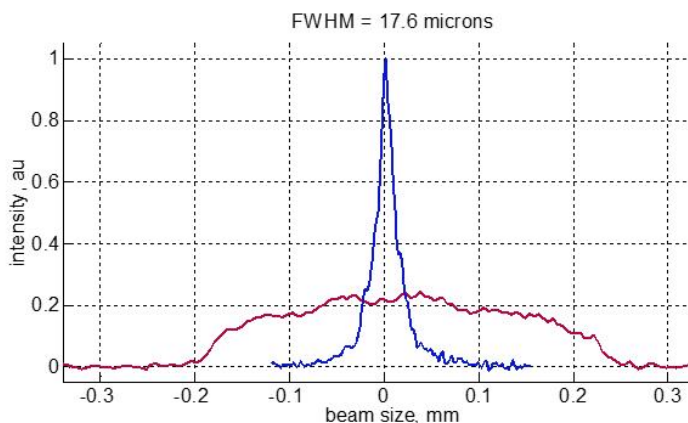
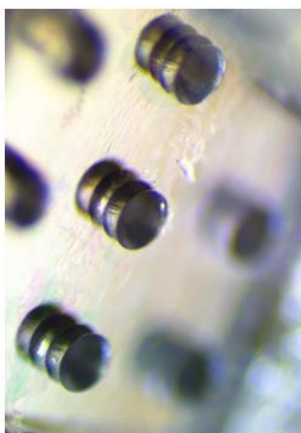


**Figure 1:** Left: a diamond CRL, a stack of three 2D refractive lenses. Right: knife edge scan. Blue – lens in, Red – lens out.

Recently, a 1D diamond CRL has been demonstrated [3]. To form a 2D diamond CRL, three 2D refractive lenses were stacked together and tested using an undulator radiation at the Biophysics Collaborative Access Team at APS (see Figure 1 for main results).

### References

- [1] S. Antipov, S.V. Baryshev, J.E. Butler, O. Antipova, Z. Liu, S. Stoupin, <http://arxiv.org/abs/1506.04016>
- [2] A. Snigirev, V. Kohn, I. Snigireva, and B. Lengeler, *Nature* 384, 49 (1996)
- [3] M. Polikarpov et al., *J. Synchrotron Rad.* 22, 23 (2015).



## SPATIALLY RESOLVED SMALL-ANGLE X-RAY SCATTERING OF MECHANO-SENSITIVE NANOMETER-SIZED LIPOSOME

H. Deyhle<sup>1</sup>, M. Buscema<sup>1</sup>, S. Matviyukiv<sup>1</sup>, T. Pfohl<sup>1</sup>, A. Zumbuehl<sup>2</sup>, B. Müller<sup>1</sup>

<sup>1</sup>Biomaterials Science Center, University of Basel, 4123 Allschwil, Switzerland

<sup>2</sup>Department of Chemistry, University of Fribourg, 1700 Fribourg, Switzerland

### Abstract

The development of atherosclerosis is related to the accumulation of white blood cells and the proliferation of intimal-smooth-muscle cells that lead to a fibro-fatty plaque. This leads to a thickening of the vessel wall, and a consequent constriction of the vessel lumen, hindering blood flow. In severe cases, it can block the blood flow leading to heart attack or stroke. To counter the constriction in case of infarct, vasodilator drugs are often employed. A systemic administration of these substances leads to an undesired drop in blood pressure.

Recently, a formulation for mechano-sensitive vesicles was proposed [1]. The vesicles are loaded with a vasodilator. Taking advantage of the altered blood flow conditions in a constriction [2], namely increased shear stress, the release of the drug is triggered locally.

To characterize the behavior of the liposomes under varying flow conditions, microfluidics in combination with small-angle X-ray scattering (SAXS) were performed at the beamline ID 02 (European Synchrotron Radiation Facility, Grenoble, France). The experiments were performed at 12.5 keV photon energy at specimen-detector distances of 1, 5, and 10 m. By tuning the flow rate of the solution containing the vesicles, shear rates similar to those found in diseased coronary arteries can be reproduced, and the response of the liposomes can be monitored. By changing the diameter of the micro-channels, different shear rates can be obtained on the same device. Necessary flow rates can be calculated using numeric simulations with the finite element method (FEM, cf. Fig. 1). Figure 2 shows a schematic of the experimental SAXS setup. The microfluidic device is scanned through the X-ray beam at several positions along the micro-channel. In this way, possible changes in shape and size as well as alignment as a function of shear and time evolution can be detected.

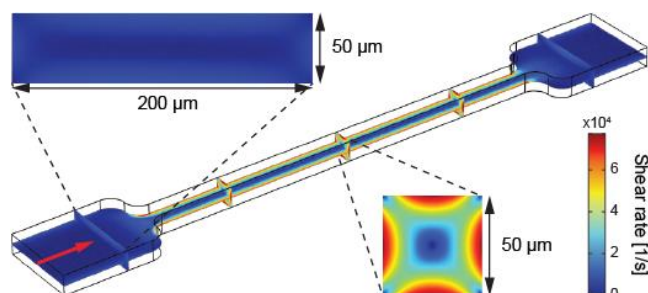


**Figure 1:** Simulation of the shear rate in water through a  $50\ \mu\text{m} \times 50\ \mu\text{m}$  channel at a flow rate of  $1\ \mu\text{L/s}$ .

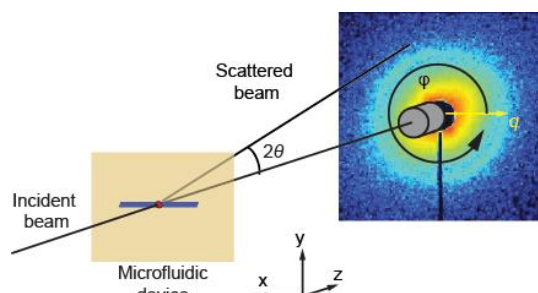


**Figure 2:** Schematic setup of the SAXS experiment.

### References

- [1] M. N. Holme et al., Nature Nanotech. 7, 536 (2012).
- [2] M. N. Holme et al., Nature Prot. 9, 1401 (2014).

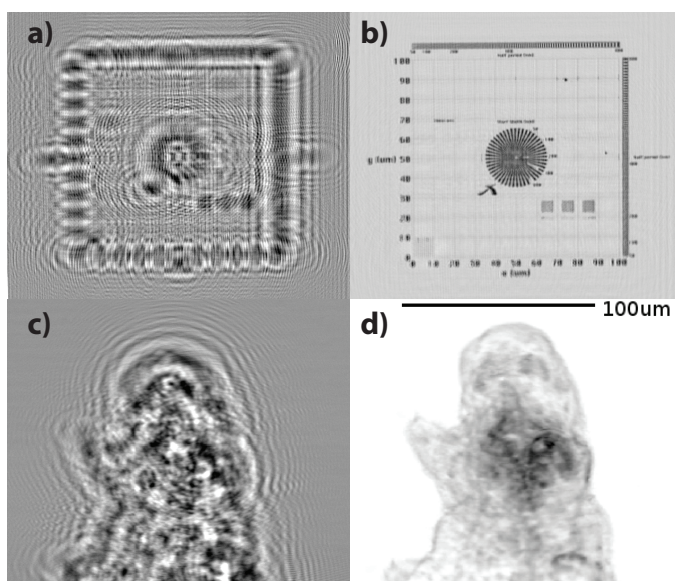
## Towards dose efficient in-vivo microscopy of biological systems at modern sources of synchrotron radiation

P. Vagovič<sup>1,2</sup>, S. Hrivňák<sup>3</sup>, L. Mikeš<sup>4</sup>, M. Franko<sup>3</sup>, J. Uličný<sup>3</sup>, L. Švéda<sup>5</sup>, A. Cecilia<sup>6</sup>, E. Hamann<sup>6</sup>, E. N. Gimenez<sup>7</sup>, Z. Zápražný<sup>8</sup>, D. Korytár<sup>8</sup>, U. Wagner<sup>7</sup>, and T. Baumbach<sup>6</sup>

<sup>1</sup>Center for Free-Electron Laser Science, DESY, Hamburg, Germany, <sup>2</sup>European XFEL, Hamburg, Germany, <sup>3</sup>Department of Biophysics, Faculty of Science, P. J. Šafárik University in Košice, Slovakia, <sup>4</sup>Department of Computer Science, Faculty of Science, P. J. Šafárik University in Košice, Slovakia, <sup>5</sup>FNSPE CTU, Prague, Czech Republic, <sup>6</sup>ANKA Light Source, Karlsruhe Institute of Technology, Karlsruhe, Germany, <sup>7</sup>Diamond Light Source, UK, <sup>8</sup>Institute for Electrical Engineering, Slovak Academy of Sciences, Bratislava, Slovakia

### Abstract

In this work we present the actual status of the development of Bragg magnifier microscope based on in-line Germanium crystals [1,2]. We performed successful testing of this imaging system at Diamond Light Source I13 and B16 and at Spring 8 radiation facilities and applied it for full field holographic imaging of biological samples. This imaging system is using asymmetric Bragg reflections to geometrically magnify X-ray beam up to 250 times and the beam is directly detected by single photon counting detector. Such detection scheme has very high efficiency reaching ca. 70%. The spatial resolution achieved after successful phase reconstruction of recorded holograms (Fig. 1) achieved is 300nm and the acquisition time for one frame at ID13 was 0.3s, which still can be minimized to millisecond region, especially in sources of 4<sup>th</sup> generation. Thanks to high efficiency and high throughput leading to short acquisition time we propose this system for in-vivo 2D/3D quantitative imaging of biological samples such a cells or small animals. We will present the results of improved phase retrieval algorithm [3] and the full 3D reconstruction of selected model organism (Tardigrade) and prospects for future developments towards dose efficient in-vivo biological imaging.



### References:

- [1] Vagovic et al., J. Synchr. Rad. 2013
- [2] Vagovic et al. Opt. Expr. 2014
- [3] S. Hrivnak, to be published

**Figure 1** Measured holograms of X-radia X-50-30-20 test pattern a) and Tardigrade c) and the phase maps b), d) recovered by improved phase retrieval algorithm [3].

Spatial resolution

## A METHOD FOR ESTIMATING SAMPLE IMAGE RESOLUTION

Ryuta Mizutani<sup>1</sup>, Rino Saiga<sup>1</sup>, Susumu Takekoshi<sup>2</sup>, Chie Inomoto<sup>2</sup>, Naoya Nakamura<sup>2</sup>, Makoto Arai<sup>3</sup>, Kenichi Oshima<sup>3</sup>, Masanari Itokawa<sup>3</sup>, Akihisa Takeuchi<sup>4</sup>, Kentaro Uesugi<sup>4</sup>, Yasuko Terada<sup>4</sup>, and Yoshio Suzuki<sup>5</sup>

<sup>1</sup>Department of Applied Biochemistry, Tokai University, Hiratsuka, Kanagawa 259-1292, Japan

<sup>2</sup>Tokai University School of Medicine, Isehara, Kanagawa 259-1193, Japan

<sup>3</sup>Tokyo Metropolitan Institute of Medical Science, Setagaya, Tokyo 156-8506, Japan

<sup>4</sup>Japan Synchrotron Radiation Research Institute (JASRI/SPring-8), Sayo, Hyogo 679-5198, Japan

<sup>5</sup>Graduate School of Frontier Sciences, University of Tokyo, Kashiwa, Chiba 277-8561, Japan

### Abstract

Spatial resolution is a fundamental parameter in structural sciences. Although edge profile are used for estimating the spatial frequency response of optics, the resolution of the sample image depends on a number of experimental factors, including stage drift and sample condition. Therefore, the resolvability of the sample image should be determined from the sample image itself. In this paper, we report a method for estimating the spatial resolution of a sample image without defining a noise level criterion [1].

Test images were generated by convolving a Gaussian point-spread function (PSF) and the original images. The test images were then analyzed by plotting logarithmic intensities of their Fourier transforms. The results indicated that the full width at half maximum (FWHM) of the applied PSF is proportional to the slope of the plots.

Imaging x-ray microtomography using Fresnel zone-plate optics was examined with this method. A cross section of square-wave test patterns [2,3] visualized with imaging microtomography indicated that patterns up to 100-120 nm pitch were resolved (Figure 1). The logarithmic intensity plot was calculated from a tomographic cross section of brain tissue. The FWHM of the point-spread function estimated from the plot was 118 nm (Figure 2), which coincides with the resolution determined from the test patterns.

The resolutions of real images have been estimated from the detection limit of signals against the noise level in the Fourier domain, although there are a number of variations in noise level criteria and hence the resultant resolution. In contrast, the logarithmic intensity plot provided a sound estimate without explicitly defining any criterion. We suggest that the logarithmic intensity plot in the Fourier domain provides a resolvability measure regardless of visualization modality.

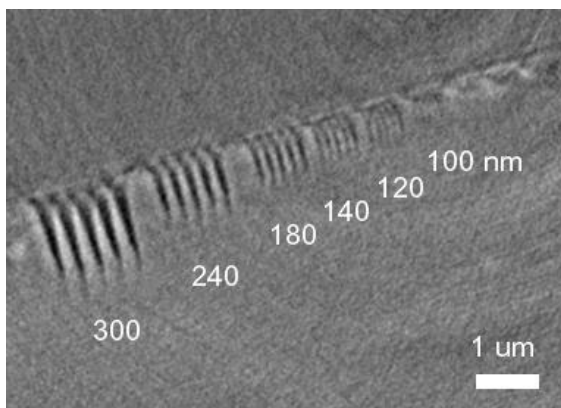


**Figure 1:** X-ray microtomographic cross section of aluminum square-wave patterns with pitches of 300, 240, 180, 140, 120 and 100 nm.

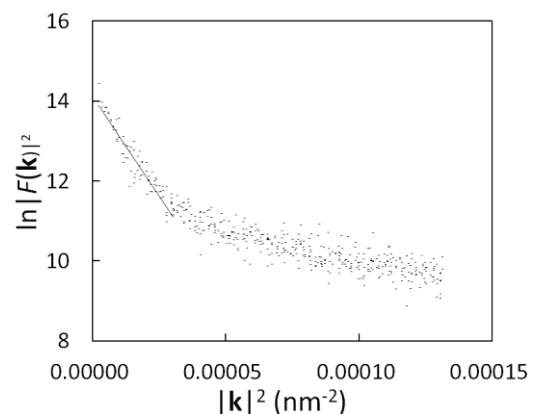


**Figure 2:** Logarithmic intensity plot of brain tissue image. The linear correlation at the left end can be regarded as representing a Gaussian PSF with 118-nm FWHM.

### References

- [1] R. Mizutani et al., J. Microsc. 261, 57-66 (2016).
- [2] R. Mizutani et al., J. Synchrotron Radiat. 15, 648-654 (2008).
- [3] R. Mizutani et al., Nucl. Instrum. Methods Phys. Res. A621, 615-619 (2010).

## TALBOT-BASED THREE-DIMENSIONAL X-RAY PHASE MICROSCOPY FOR BONE SAMPLES

A. Momose<sup>1,2,3</sup>, H. Takano<sup>1,2</sup>, Y. Wu<sup>1,2</sup>, W. Yashiro<sup>1,2</sup>, M. Hoshino<sup>2,3</sup>, N. Nango<sup>4</sup>, S. Kubota<sup>4</sup>, K. Matsuo<sup>5</sup>

<sup>1</sup> IMRAM, Tohoku Univ., 2-1-1 Katahira, Aoba-ku, Sendai 980-8577, Japan

<sup>2</sup> JST-ERATO Momose Proj., 2-1-1 Katahira, Aoba-ku, Sendai 980-8577, Japan

<sup>3</sup> JASRI/SPring-8, 1-1-1 Kouto, Sayo-cho, Hyogo 679-5198, Japan

<sup>4</sup> Ratoc System Engineering, 1-24-8 Sekiguchi, Bunkyo-ku, Tokyo 112-0014, Japan

<sup>5</sup> Keio University School of Medicine, Shinjuku-ku, Tokyo 160-8582, Japan

### Abstract

X-ray Talbot interferometry has been attracting attention for X-ray phase imaging with not only synchrotron radiation but also laboratory X-ray sources. Because of using transmission gratings, flexible optical configurations are allowed. Its combination with an X-ray full-field imaging microscope is one of those configurations and reported here.

Figure 1(a) shows the setup of a phase-sensitive X-ray microscope established by the combination of a Fresnel zone plate (FZP) and a Talbot interferometer consisting of two transmission gratings [1]. Aiming at tomographic observation of bone samples (especially mouse auditory ossicles as they are), X-ray microscopes with a FZP having a 300- $\mu\text{m}$  field of view have been constructed with magnifications of 20 and 100 at SPring-8. By considering the focal point of the FZP as a virtual source, a Talbot interferometer was placed in front of the imaging plane. Bone density deviation can be visualized by phase tomography with this setup. By removing the Talbot interferometer and slightly shifting the FZP, the microscope was switched to a defocus phase-contrast mode (Fig. 1(b)). The system was successfully employed to visualize ossification process in mouse malleus [2] and to discover a new process of demineralization [3]. Figure 2 shows tomograms reconstructed by the two phase-contrast modes shown in Fig. 1 for a mouse tibial sample. By overlaying the two tomograms, significant decrease in mineralization around canaliculi was found, suggesting a new process of demineralization different from the function of osteoclasts [3].

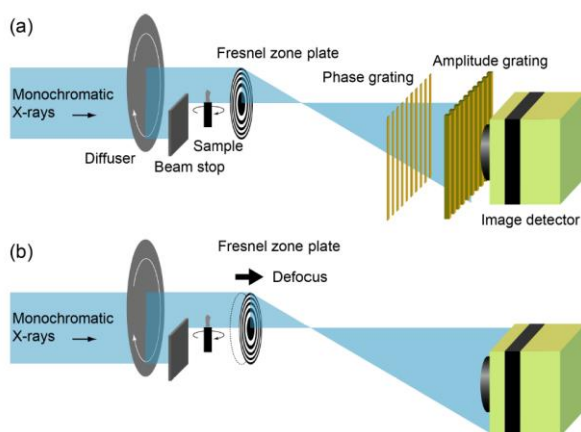


**Figure 1:** Talbot-based X-ray microscope (a) and defocus phase-contrast X-ray microscope (b). They are switchable with each other.

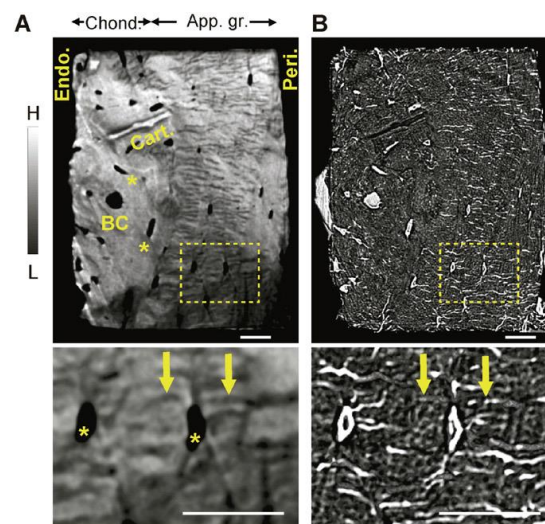


**Figure 2:** Tomograms of tibial diaphyseal cortex in mouse reconstructed by Talbot (A) and defocus (B) configurations.

### References

- [1] N. Nango, S. Kubota, A. Takeuchi, Y. Suzuki, W. Yashiro, A. Momose, K. Matsuo, *Biomed. Opt. Express* 4, 917 (2013).
- [2] K. Matsuo, Y. Kuroda, N. Nango, K. Shimoda, Y. Kubota, M. Ema, L. Bakiri, E. F. Wagner, Y. Takeda, W. Yashiro, A. Momose, *Development* 142, 3912 (2015).
- [3] N. Nango, S. Kubota, T. Hasegawa, W. Yashiro, A. Momose, K. Matsuo, *Bone* 84, 279 (2016).

## IMPROVED STABILITY OF LIQUID-NITROGEN-JET LASER-PLASMA TARGETS FOR COMPACT X-RAY MICROSCOPY

E. Fogelqvist, M. Kördel, M. Selin, H. M. Hertz

*Biomedical and X-Ray Physics, Dept. of Applied Physics, KTH Royal Inst. of Technology/Albanova, 10691 Stockholm, Sweden*

### Abstract

Compact x-ray microscopy (XRM) shows promise to become an attractive alternative to the x-ray microscopes available at the synchrotrons. Present compact water-window XRM [1-3] rely on nitrogen liquid-jet laser-plasma sources. One of the major limitations for high-brightness operation of such sources is the jet stability. When the liquid nitrogen jet is ejected into vacuum, its temperature drops rapidly due to evaporative cooling. Accumulation of frozen nitrogen at the nozzle orifice constitutes a disturbance that destabilizes the frozen nitrogen jet. For high laser power operation it is crucial that the plasma is operated far from the nozzle to avoid inducing spray. Therefore a continuous, stable nitrogen jet is needed.

Two different methods were found to stabilize the liquid nitrogen jet [4]. One method was to increase the ambient pressure to around 100 mbar where evaporation was balanced by recapture, thus counteracting evaporative cooling. This produced a highly stable liquid jet, which showed classical Rayleigh breakup. However, this method was not suitable for our specific application since 500 eV light is absorbed by the ambient gas. The other stabilizing method was to introduce a radiative heating element close to the nozzle orifice. The radiated heat prevents the accumulation of frozen nitrogen, thereby removing the small disturbances that would otherwise form at the nozzle orifice. This resulted in a long, stable frozen nitrogen jet which allowed for long-term stable plasma operation at an increased distance (5 mm) from the nozzle orifice. Figure 1 shows flash-illuminated images of the jet with (b) and without (a) the heating.

In the present contribution we will discuss the radiative heating method in detail as well as the improved emission stability of this high-brightness laboratory water-window source.

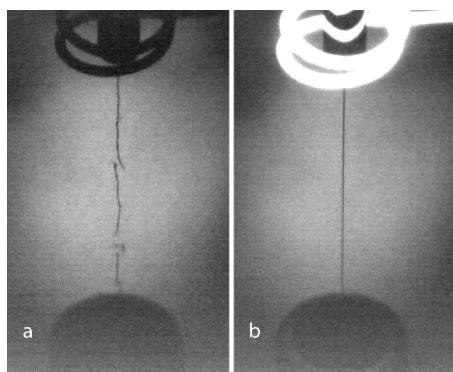


**Figure 1:** This a typical example of nitrogen jet stabilization by using an external heat element that prevents accumulation of frozen nitrogen at the nozzle orifice. A resistive wire is coiled around the nozzle orifice and the radiated heat is controlled by the current through the wire. The non-stabilized jet is shown in a) and the stabilized jet in b).

### References

- [1] P. A. C. Takman, H. Stollberg, G. A. Johansson, A. Holmberg, M. Lindblom and H. M. Hertz, *J. Microsc.* 226 (2), 175 (2007).
- [2] H. Legall, H. Stiel, G. Blobel, C. Seim, J. Baumann, S. Yulin, D. Esser, M. Hofer, U. Wiesemann, M. Wirtz, G. Schneider, S. Rehbein and H. M. Hertz, *J. Phys.: Conf. Ser.* 463 (1), 012013 (2013).
- [3] K. Kyong Woo, K. Youngman, N. Ki-Yong, L. Jong-Hyeok, K. Kyu-Gyum, C. Kwon Su, K. Byoung Hoon, K. Dong Eon, K. JinGon, A. Byoung Nam, S. Hyun Joon, R. Seungyu, K. Ki-Ho, C. Jin Seok, G. Dae Gab, K. Dong Woo, K. Sung Hoon, M. Jin Young, C. Kyu-Sil, Y. Seong Eon, A. K. Eun, N. Yoshiharu and Y. Kwon-Ha, *Phys. Med. Biol.* 51 (6), N99 (2006).
- [4] E. Fogelqvist, M. Kördel, M. Selin, and H. M. Hertz, *J. Appl. Phys.* 118, 174902 (2015).



# IMAGE RESTORATION USING AN ANALYTICAL OPTICAL TRANSFER FUNCTION IN A X-RAY MICROSCOPY

Gang Liu, Fahu Li, Xiaobo Zhang

*National Synchrotron Radiation Laboratory, University of Science and Technology of China,  
NO.42 hezuohua south road, Hefei 230026, China*

## **Abstract**

X-ray microscopy (XRM) is a powerful, noninvasive and three dimensional (3D) imaging tool of nanoscale objects. However, the transmission X-ray microscopy (TXM) is restricted to imaging large size samples due to a limited depth of focus (DOF). When the sample size is larger than the DOF, the defocused blur information and in-focus information will be superimposed in the same projection, which would degrade the quality of the X-ray images. The effects of the defocus blur can be critically analyzed with the optical transfer function (OTF). Here, the OTF of FZP was calculated and applied to restore the images. The OTF was related to the parameters of the imaging system and property of FZP not relied on the experiment data. The OTF of FZP was derived by calculating the function of the FZP, not approximated the FZP as an optical lens. Consequently, the OTF of FZP obtained in this study was different than that of optical lens. The particularity of OTF could interpret why the image contrast reduced in X-ray microscopy employed FZP as key imaging element. In the experiment, the OTF-based method was applied to restore the in-focus and defocus X-ray images. In in-focus restoration process, the contrast of the X-ray image was improved by OTF deconvolution. In defocus restoration process, the corresponding defocus OTF was applied to the defocus images for suppressing the blur, and the in-focus and contrast enhanced image was achieved by OTF-based method. The restoration result proved the OTF-based restoration method could not only suppress the blur also improve the image contrast of X-ray images.



# HIGH-SPATIAL-RESOLUTION NANOPARTICLE X-RAY FLUORESCENCE TOMOGRAPHY

J. C. Larsson, W. Vågberg, C. Vogt, U. Lundström, D. H. Larsson, and H. M. Hertz

*Biomedical and X-Ray Physics, Department of Applied Physics, KTH Royal Institute of  
Technology/Albanova, 10691 Stockholm, Sweden*

## Abstract

X-ray fluorescence tomography (XFCT) has potential for high-resolution 3D molecular x-ray bio-imaging. In this technique the fluorescence signal from targeted nanoparticles (NPs) is measured, providing information about the spatial distribution and concentration of the NPs inside the object. However, present laboratory XFCT systems typically have limited spatial resolution ( $>1$  mm) and suffer from long scan times and high radiation dose even at high NP concentrations, mainly due to low efficiency and poor signal-to-noise ratio.

We have developed a laboratory XFCT system with high spatial resolution (sub-100  $\mu\text{m}$ ), low NP concentration and vastly decreased scan times and dose, opening up the possibilities for in vivo small animal imaging research [1]. The system consists of a high-brightness liquid-metal-jet microfocus x-ray source, x-ray focusing optics and two photon counting detectors. By using the source's characteristic 24 keV line-emission together with carefully matched molybdenum nanoparticles the Compton background is greatly reduced, increasing the SNR. Each measurement provides information about the spatial distribution and concentration of the Mo nanoparticles, as well as the absorption and Compton scattering of the object. An iterative reconstruction method is used to produce the final XFCT image.

Here we present the principles of the method, its experimental verification on phantom studies, and the recent inclusion of Compton and absorption data for improved XFCT reconstruction in object with highly absorbing features.

## References

- [1] H. M. Hertz, J. C. Larsson, U. Lundström, D. H. Larsson, C. Vogt, *Opt. Lett.* 39(9), 2790-2793 (2014)

## PHASE SHIFTING HARD X-RAY MICROSCOPY

Jun Lim and Sangsul Lee

*Pohang Light Source, POSTECH, Pohang, Korea*

### Abstract

Phase-contrast microscopy utilizes the artificial phase delay between the undiffracted reference wave and the diffracted object wave. It is widely employed not only in optical microscopy but also in X-ray microscopy. Optical microscope combined with phase shifting interferometry is a powerful tool for thickness measurement of phase object as well as size. A piezo-driven beam-splitter makes inference and shifts of reference wave's phase. In X-ray field, such optics is not allowed due to high penetration property of X-rays. For that reason limited studies have been done with gratings [1,2]. In this presentation, we proposed a method to get phase information of samples by use of a phase plate with hard X-rays.

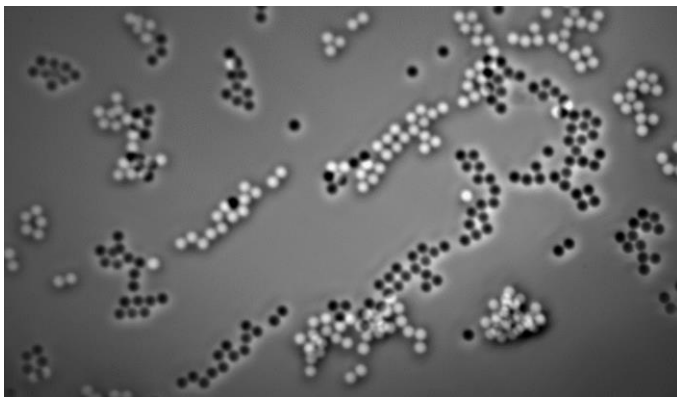


**Figure 1:** Phase difference image of silica spheres.

### References

- [1] W. Yashiro et al., *Phys. Rev. Lett.* **103**, 180801 (2009).
- [2] H. Wen et al., *Nature Comm.* **4**, 2659 (2013).

# CURRENT STATUS OF X-RAY PHASE IMAGING AT SPRING-8: TOWARD 4D X-RAY PHASE TOMOGRAPHY FOR BIOLOGICAL SAMPLES

M. Hoshino<sup>1</sup>, K. Uesugi<sup>1</sup> and N. Yagi<sup>1</sup>

<sup>1</sup> Japan Synchrotron Radiation Research Institute, 1-1-1 Kouto, Sayo, Hyogo 679-5198, Japan

## Abstract

At the bending magnet beamline BL20B2 in SPring-8, X-ray phase tomography using a grating interferometer has been developed to observe biological samples quantitatively [1]. As a monochromatic X-ray beam with a large cross section is available at the end station of the beamline located at more than 200m from the source, it is possible to measure a large-scaled biological sample such as a whole heart of a human infant [2]. On the other hand, the X-ray beam with higher flux density is available for fast imaging at the upstream experimental hutch located at 43m from the source while the vertical field of view is limited by the beam size. In the measurement at the upstream hutch, fast and high-throughput X-ray phase tomography has been developed to apply to quantitative dynamic measurements. Even in a fast measurement, a phase stepping method has been used for the phase retrieval in the grating interferometer. A triangle-shaped analog signal has been used to scan the grating set on a Piezo driven stage to achieve an efficient scan. So far, X-ray phase tomography for fresh biological samples has been conducted in an 8min scan with the voxel size of  $6.5\mu\text{m}$  and the density resolution of  $2.4\text{mg}/\text{cm}^3$ . The scanning technique using sequential triangle waves has been extended to 4D X-ray phase tomography. In this case, a repeatable motion of the sample is combined with an X-ray phase tomographic scan. A photograph of the sample under uniaxial stretching and releasing condition is shown in Fig. 1. A rotational axis in tomography is parallel to the axis of stretching. One of the sectional images of a pig aorta in the 4D measurement is shown in Fig. 2. The sectional images normal to the axis of stretching at beginning and ending in the stretching process and the plots for the cross sectional area size obtained from the 4D measurement are also presented in Fig. 2. By stretching and releasing, the cross sectional area size of the aorta in the sectional plane normal to the stretching axis varies linearly.

Detail of the measurement procedure in 4D X-ray phase tomography and other results including quantitative discussions on the deformation of the sample will be presented. Also, other applications using X-ray phase tomography at BL20B2 in SPring-8 will be presented.

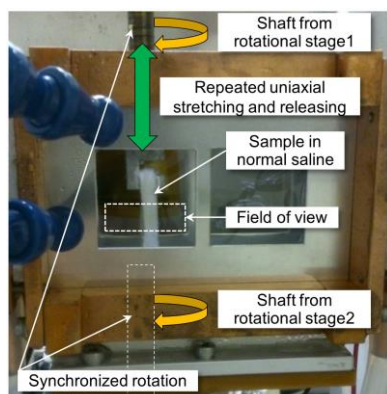


Figure 1: Photograph of a pig aorta under uniaxial stretching and releasing condition. Two rotational stages are operated in synchronization. Repeatable uniaxial stretching and releasing motion is combined with an X-ray phase tomographic measurement.

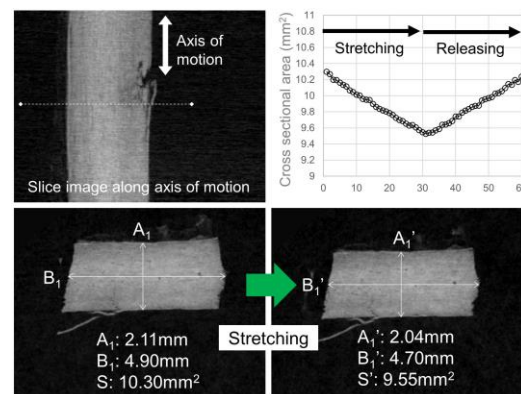


Figure 2: Sectional image of a pig aorta parallel to the rotational axis (upper left). Sectional images normal to the axis of motion at the beginning and ending points in stretching (lower). Plots for the cross sectional area size in stretching and releasing process (upper right).

## References

- [1] M. Hoshino, K. Uesugi, T. Tsukube and N. Yagi, J. Synchrotron Rad. 21, 1347 (2014).
- [2] T. Tsukube, N. Yagi, M. Hoshino, Y. Nakashima, K. Nakagawa and Y. Okita, Gen Thorac Cardiovasc Surg 63, 590 (2015).

# ARRAY SOURCE X-RAY IMAGING: A PRELIMINARY INVESTIGATION INTO MULTI-SOURCE X-RAY VELOCIMETRY TECHNIQUES

G. W. Goonan<sup>1</sup>, S. Dubsy<sup>1</sup>, A. Fouras<sup>1,2</sup>

*1Dept. Mechanical & Aerospace Engineering, Monash University, Clayton, Melbourne Australia  
24Dx Pty Ltd., Notting Hill, Melbourne, Australia*

## Abstract

X-ray velocimetry (XV) has shown promise for investigations into various dynamic biological systems, including the motion of lungs and flow of blood. Previous research in the field of XV has highlighted the need for high spatio-temporal resolution [1] as well as a clear distinction between static and dynamic imaging optimization [2]. In X-ray imaging systems, enhancement of spatial and temporal resolution requires a small focal spot-size and high power output respectively, increasing anode power density requirements. As such, research in X-ray velocimetry has traditionally been limited to expensive and specialized X-ray equipment such as synchrotrons or liquid-metal-jet X-ray sources.

Presented here is the preliminary investigation into multi-source XV imaging. By simultaneously illuminating a sample with multiple sources of small spot size, anode power density is maintained while increasing overall brightness and reducing penumbral blur. Through computational simulations experimentally validated using a liquid metal jet source, we demonstrate this novel technology's capability for increased XV accuracy with reduced incident luminosity. We further demonstrate that these properties can be enhanced by judicious selection of source location and overall system geometry.

Utilisation of the multi-source imaging approach can potentially reduce complexity and cost of XV systems, allowing for widespread adoption of XV for investigations into lung function, and for eventual translation to the clinical setting.

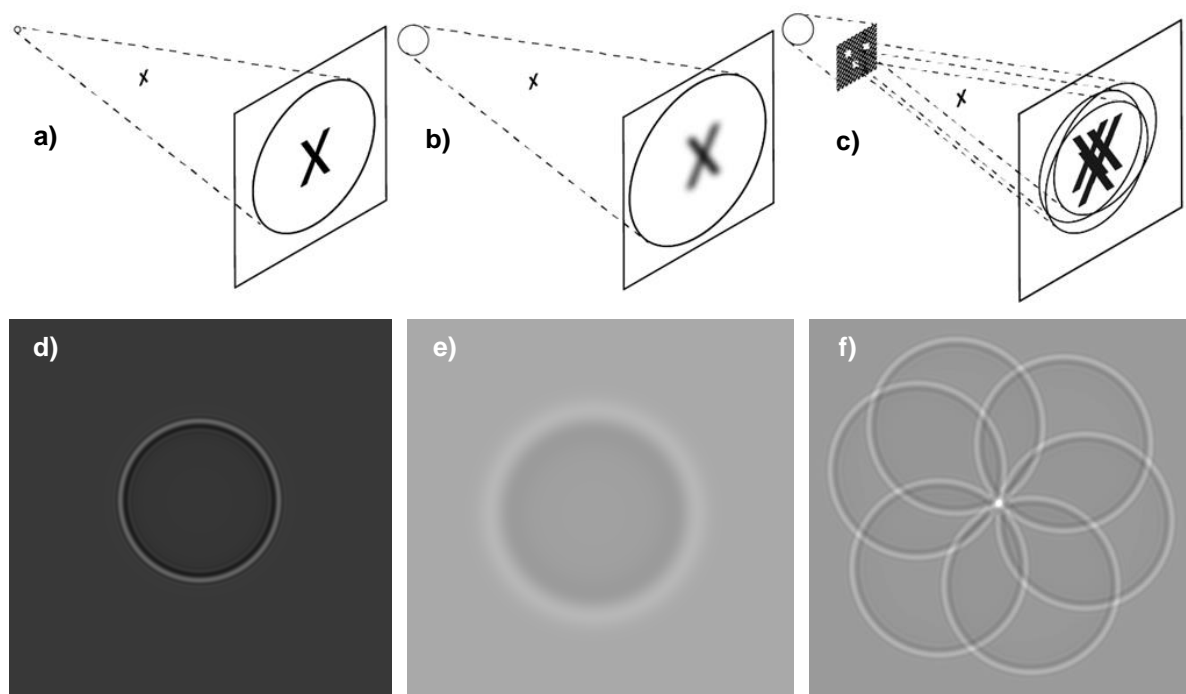


**Figure 1:** A small single-source system (a) is physically limited by material properties such as power density. Increasing the source size (b) increases brilliance, whilst also increasing penumbral blur. By utilising multiple small sources (or an aperture with similar characteristics, as in c) this blur can be mitigated. d-f) High resolution Phase Contrast images showing the effects of a-c respectively.

## References

- [1] S. Dubsy, S. B. Hooper, K. K. W. Siu, and A. Fouras: *J. R. Soc. Interface* 9 (2012) 2213.
- [2] I. Ng, D. M. Paganin and A. Fouras, *J. Appl. Phys.*, vol. 112, no. 074701, pp. 1-11, 2012.

## X-RAY SPECKLE-BASED PHASE-CONTRAST IMAGING

M. Zdora<sup>1,2,3</sup>, P. Thibault<sup>3</sup>, T. Zhou<sup>4</sup>, S. Sala<sup>1,2,3</sup>, F. J. Koch<sup>5</sup>, J. Romell<sup>4</sup>, C. Rau<sup>1</sup>,  
I. Zanette<sup>1</sup>

<sup>1</sup>Diamond Light Source, Harwell Science & Innovation Campus, Didcot, Oxfordshire OX11 0DE, UK  
<sup>2</sup>Department of Physics & Astronomy, University College London, London WC1E 6BT, UK  
<sup>3</sup>Department of Physics & Astronomy, University of Southampton, Southampton SO17 1BJ, UK  
<sup>4</sup>Biomedical and X-ray Physics, KTH Royal Institute of Technology, 10691 Stockholm, Sweden  
<sup>5</sup>Institute of Microstructure Technology, Karlsruhe Institute of Technology, 76344 Eggenstein-Leopoldshafen, Germany

### Abstract

Methods based on X-ray near-field speckle [1,2] have recently attracted increased interest among the different phase-contrast imaging techniques due to their simplicity and robustness. Near-field speckles are generated by the interference of partially coherent X-rays scattered from a random phase modulator (RPM), e.g. a piece of sandpaper. The refraction of X-rays by a sample is translated into a displacement of the speckle pattern directly related to the differential phase signal in the two orthogonal directions. A transmission and dark-field, i.e. small-angle scattering, signal can be extracted from the same data set. Speckle-based techniques do not impose strong requirements on the temporal coherence of the X-rays and have recently been translated to polychromatic laboratory sources [3], also in tomographic mode [4], making them an easily accessible tool for 3D investigation of samples. Beside the single-shot mode, which only achieves a moderate spatial resolution, the RPM can be scanned in small sub-speckle steps to perform a pixel-wise analysis, at the cost of a more elaborate and time-consuming acquisition and analysis process. Recent investigations focus on ways to simplify the stepping process [5].

Here, we present a new approach for image acquisition and data analysis with less stringent conditions on the arrangement, number and spacing of the RPM stepping positions. Images are recorded for different positions of the RPM with step sizes significantly larger than one speckle and a numerical analysis based on least-square minimisation is employed. This allows the use of less precise, less costly scanning motors and shorter scan times while maintaining a high resolution and high contrast of the reconstructed images, see Fig. 1.

The spatial resolution and scan and analysis time can be tuned by the choice of the number of steps and the reconstruction parameters, making it a highly versatile method easily adaptable to different requirements and experimental conditions. Moreover, it can be applied to other reference patterns, e.g. periodic structures. The proposed method has great potential for high-contrast, fast, cost-effective and easily implemented multimodal imaging applications in various fields such as biology and materials science as well as metrology.

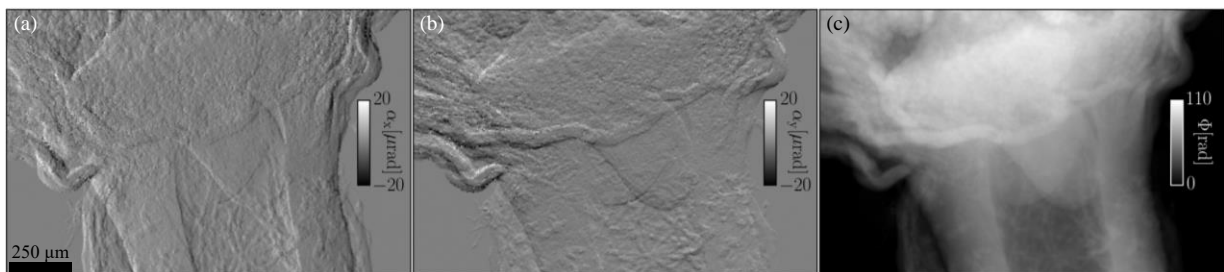


**Figure 1:** Refraction angle in horizontal (a) and in vertical (b) direction and retrieved phase shift (c) of the bottom of a small flower bud obtained with the proposed speckle acquisition and analysis method.

### References

- [1] K. S. Morgan et al., Appl. Phys. Lett. 100, 124102 (2012).
- [2] S. Berujon et al., Phys. Rev. A 86, 063813 (2012).
- [3] I. Zanette et al., Phys. Rev. Lett. 112, 253903 (2014).
- [4] I. Zanette et al., Proc. Natl. Acad. Sci. U.S.A. 112, 12569-12573 (2015).
- [5] S. Berujon and E. Ziegler, Phys. Rev. A 92, 013837 (2015).

# LINKING MATERIAL BEHAVIOUR WITH STRUCTURE USING 4-D LABORATORY X-RAY NANOTOMOGRAPHY WITH *IN-SITU* MECHANICAL TESTING

R. S. Bradley<sup>1</sup>, X. Lu<sup>2</sup>, D. Sykes<sup>1</sup>, R. Hartwell<sup>1</sup>, B. Hornberger<sup>3</sup>, H. Bale<sup>3</sup>, A. Merkle<sup>3</sup>, W. Harris<sup>3</sup>, S. Etchin<sup>3</sup>, M. Leibowitz<sup>3</sup>, W. Qiu<sup>3</sup>, A. Tkachuk<sup>3</sup>, A. Clarke<sup>4</sup>, K. Henderson<sup>4</sup>, N. Cordes<sup>4</sup>, B. M. Patterson<sup>4</sup> and P. J. Withers<sup>1</sup>

<sup>1</sup>Henry Moseley X-ray Imaging Facility, The University of Manchester, Oxford Road, Manchester, UK

<sup>2</sup>UCL, Gower Street, London, UK

<sup>3</sup>Carl Zeiss X-ray Microscopy, Pleasanton, CA, USA

<sup>4</sup>Los Alamos National Laboratory, USA

## Abstract

A more complete understanding of material performance is gained from linking a material's microstructure to observed behaviour under external stimuli. Such information can provide key insights into conditions and mechanisms that limit the lifetime of materials in many industries as well as natural materials. X-ray tomography is well suited to imaging microstructure changes in a time-lapse '4-D' approach, due to its non-destructive nature and high resolution. We report on the application of a novel *in-situ* load stage [1] which allows mechanical tests to be performed while observing microstructural changes by laboratory x-ray nanotomography with resolution down to 50 nm. The load stage operates in several modes including compression, indentation and tension. A number of case studies will be presented to highlight the utility of the load stage, including the study of anisotropic crack growth in dentin by indentation and the tensile testing of beetle cuticle.

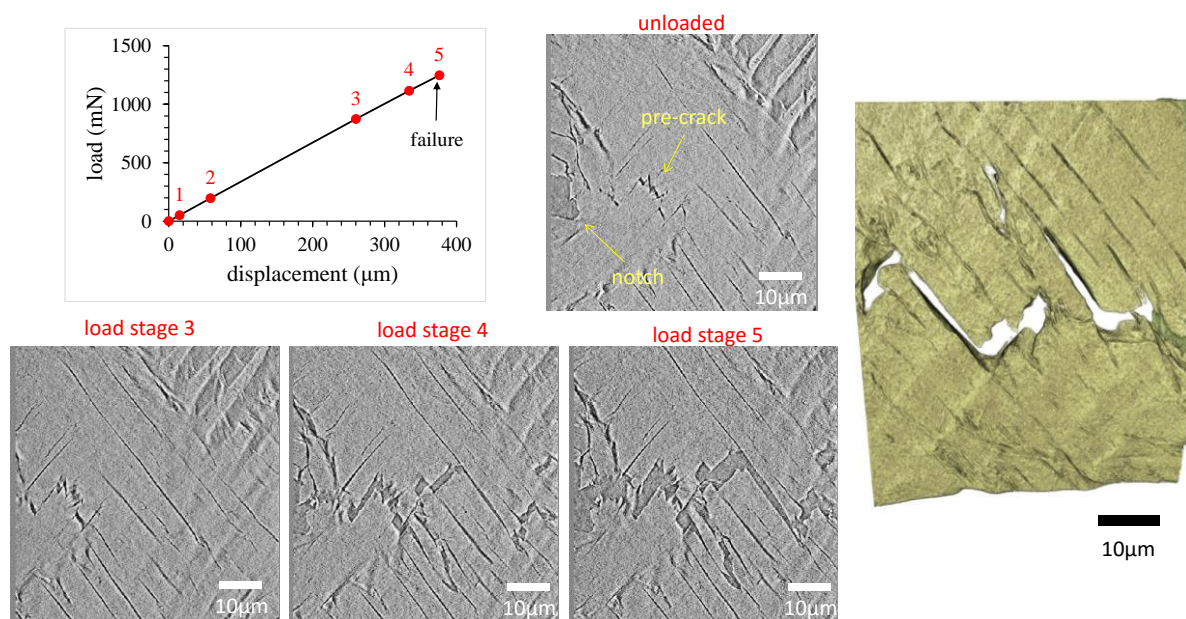


**Figure 1:** Tensile testing of a notched beetle cuticle sample. (Left) Reconstructed slices from 4 stages of loading showing crack propagation. (Right) 3-D rendering of the tortuous crack path in a single cuticle layer.

## References

- [1] B Hornberger *et al.* Proc. SPIE 9592 (2015)



## X-ray Tensor Tomography: Towards Compact Imaging Setups

Y. Sharma<sup>1,2</sup>, M. Wiecek<sup>2</sup>, F. Pfeiffer<sup>1,3</sup>, T. Lasser<sup>2</sup>

<sup>1</sup>Lehrstuhl für Biomedizinische Physik, Physik-Department and Institut für Medizintechnik,

<sup>2</sup>Computer Aided Medical Procedures,

<sup>3</sup>Institut für diagnostische und interventionelle Radiologie, Klinikum rechts der Isar, Technische Universität München

The ultra-small angle scattering of X-rays by sub-micron and micron sized structures is measured as the dark-field signal in a grating interferometry setup. Unlike absorption, the dark-field signal is dependent on the orientation of the scattering structure with respect to the interferometer sensitivity axis [1]. Thus, by varying the relative orientation of a scattering structure with respect to the interferometer, it is possible to deduce information about its orientation from the variations in the dark-field signal. Two-dimensional structure orientations can be recovered from several projections acquired by rotating the sample around the beam propagation direction [2]. Malecki et al. [3] presented an extension of this technique to three dimensions, known as X-ray Tensor Tomography (XTT). This is a promising technique with a number of applications such as visualization of the microstructure of fibrous materials and dentinal tubules of human teeth [4].

In this method, a scattering tensor is reconstructed at every voxel such that its smallest half axis represents the structure orientation. In order to achieve the non-standard acquisition poses required to measure all scattering orientations within the sample, an additional component, known as an Eulerian cradle, is added to the grating interferometer (Figure 1). The Eulerian cradle allows rotation of the sample with three degrees of freedom, and not just around one tomography axis. However, the Eulerian cradle is a bulky component and poses challenges for a compact setup design. Hence, there is a need to design sparse sampling schemes and reduce the number of axes of rotations. In order to do so, it is essential to establish a relationship between the acquisition geometry and the expected result. In this work, we define a metric CM to predict the performance of XTT given an acquisition scheme and a metric PM to evaluate the result obtained using such schemes. We find good correlation between the two measures for different kinds of samples (Figure 2) and conclude that a commercially feasible XTT setup can be achieved by using only two axes of rotations instead of the current three.

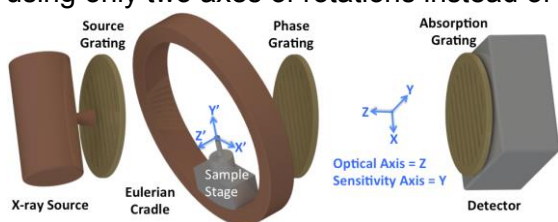


**Figure 1:** Schematic of the XTT acquisition setup showing a non-standard acquisition pose.

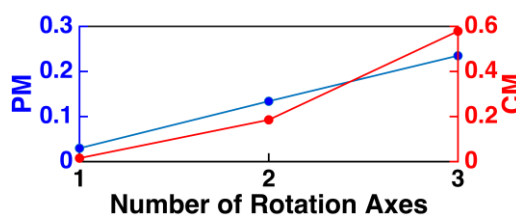


**Figure 2:** Effect of the number of rotation axes on the predicted performance (CM) and the experimental performance (PM) of XTT.

### References

- [1] W. Yashiro et al., *Phys. Rev. B - Condens. Matter Mater. Phys.*, vol. 84, no. 9 (2011).
- [2] F. Schaff et al., *Sci. Rep.*, vol. 4 (2014).
- [3] A. Malecki et al., *EPL (Europhysics Lett.)*, vol. 105, no. 3 (2014).
- [4] J. Vogel et al., *Opt. Express*, vol. 23, no. 12 (2015).

# IMPROVED RESOLUTION IN SOFT X-RAY TOMOGRAPHY USING FOCUS-STACK BACK-PROJECTION

M. Selin<sup>1</sup>, E. Fogelqvist<sup>1</sup>, S. Werner<sup>2</sup> and H. M. Hertz<sup>1</sup>

*1Biomedical and X-Ray Physics, Department of Applied Physics, KTH Royal Institute of Technology/Albanova, 10691 Stockholm, Sweden*

*2Helmholtz-Zentrum Berlin für Materialien und Energie GmbH, Institute for Soft Matter and Functional Materials, Albert-Einstein-Straße 15, 12489 Berlin, Germany*

## Abstract

Combining soft X-ray microscopy with tomographic reconstruction techniques is a powerful tool for obtaining quantitative 3D structural information of biological samples at high resolution. It relies on algorithms that typically assume projection images, i.e., that the imaging system's depth-of-focus (DOF) exceeds the object thickness. However, the DOF of zone-plate-based microscopes is often shorter than the thickness of many relevant biological objects, leading to the imaging scenario depicted in Fig. 1. With higher-resolution zone plates the DOF – object thickness mismatch worsens since the DOF has an inverse-squared relationship with the resolution power.

In order to retain the high resolution, that soft X-ray microscopy offers, the tomographic reconstructions need to take the DOF into account for thick objects. Here we present the novel focus-stack back-projection (FSBP) method [1] to achieve high resolution in the full reconstruction volume when the imaging system's DOF is shorter than object thickness. FSBP utilizes at each tomographic tilt-angle a focus series through the object. We demonstrate the method on theoretical and experimental data. As Fig. 2 clearly indicates, FSBP yield significantly improved reconstructions compared with a conventional projection-based reconstruction algorithm in terms of overall resolution.

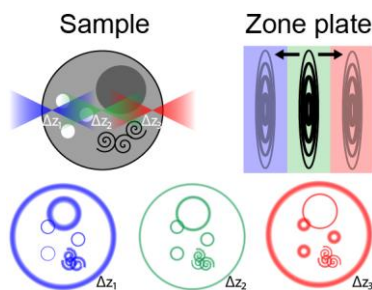


**Figure 1:** Illustration of an imaging case where the object thickness is longer than the microscope's DOF. In neither of the defocus positions  $\Delta z_1$ ,  $\Delta z_2$ , or  $\Delta z_3$  are all features simultaneously sharply imaged.

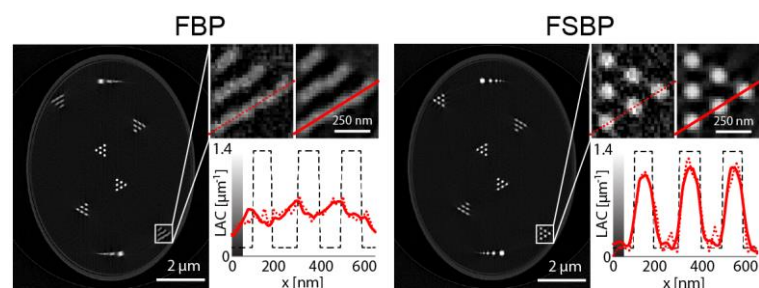


**Figure 2:** Demonstration that the focus-stack back-projection method (FSBP), compared with the conventional projection-based filtered back-projection method (FBP), enhances the resolution and suppresses artifacts in a tomographic reconstruction. The comparison is made for simulated data of a water-and-carbon phantom imaged by a 20 nm zone plate when illuminated by  $\lambda=2.4$  nm X-rays in a  $NA_{eff}=0.02$  cone. The insets show the reconstruction at a total dose of  $7 \times 10^7$  ph/ $\mu\text{m}^2$ /proj. angle (dotted line) and  $7 \times 10^9$  ph/ $\mu\text{m}^2$ /proj. angle (solid line) for both methods.

## References

- [1] M. Selin, E. Fogelqvist, S. Werner, and H. M. Hertz, *Opt. Lett.* **40**, 2201-2204 (2015).

# HIGH-RESOLUTION MICROSCOPY WITH A LABORATORY-SIZED QUASI-MONOCHROMATIC X-RAY SOURCE BASED ON INVERSE COMPTON SCATTERING

B. Günther<sup>1,2,3</sup>, M. Dierolf<sup>1,2</sup>, K. Burger<sup>1,2,4</sup>, R. Gradl<sup>1,2</sup>, L. Hehn<sup>1,2,5</sup>, E. Egl<sup>1,2</sup>,  
K. Achterhold<sup>1,2</sup>, B. Gleich<sup>2</sup>, and F. Pfeiffer<sup>1,2,5</sup>

<sup>1</sup> Department of Physics (E17), Technische Universität München (TUM),  
James-Franck-Str. 1, DE-85748 Garching

<sup>2</sup> Institute for Medical Engineering, TUM, Boltzmannstr. 11, DE-85748 Garching

<sup>3</sup> Max-Planck-Institute for Quantum Optics, Hans-Kopfermann-Str. 1, DE-85748 Garching

<sup>4</sup> Department of Radiation Oncology, Klinikum rechts der Isar, TUM,  
Ismaninger Straße 22, DE-81675 München

<sup>5</sup> Department of Diagnostic and Interventional Radiology, Klinikum rechts der Isar, TUM,  
Ismaninger Straße 22, DE-81675 München

## Abstract

Since the first application of X-rays to radiographic imaging, intensive research dedicated to improving image resolution entailed new imaging techniques like volumetric imaging (CT), efficient detectors and sophisticated X-ray sources like third generation synchrotrons or X-ray micro-focus tubes. Although the latter are compact and inexpensive, their flux is limited and their spectrum is polychromatic. Synchrotrons -on the one hand- deliver a high and monochromatic flux, but require a large facility size and have great operational costs.

The Munich Compact Light Source (MuCLS), developed and constructed by Lyncean Technologies Inc. [1] bridges this performance gap [2] and therefore paves the way to transfer modern synchrotron techniques into industrial applications and biomedical research.

One of these techniques, high-resolution raster-scanning X-ray microscopy, in principle provides valuable insights into the sample's microstructure and composition. However, its applicability to industrial investigations and biomedical research is limited because of the need for large-scale synchrotron facilities.

Meeting this demand for rapid data acquisition on site, a new microscopic method has been developed employing the coherence properties of the MuCLS for a novel multi-beam scanning-microscopy approach. This allows imaging a larger field of view within a significantly reduced acquisition time at sub-micron resolution. Accordingly this technique might become a valuable tool in development and research.

The presentation will introduce the method and discuss first results obtained at the MuCLS.

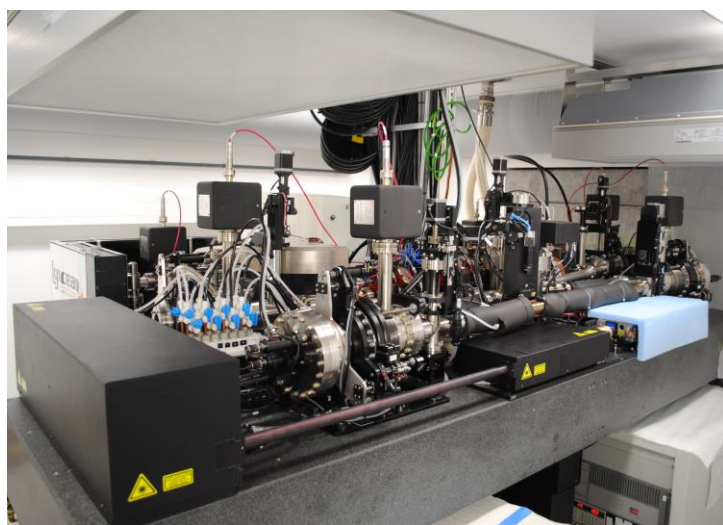


**Figure 1:** Compact size of the MuCLS electron storage ring and the laser system, measuring about 3x2m<sup>2</sup>.

## References

- [1] [www.lynceantech.com](http://www.lynceantech.com)
- [2] E. Egl, M. Dierolf, K. Achterhold, C. Jud, B. Günther, E. Braig, B. Gleich, F. Pfeiffer (submitted 2016)

## A QUANTITATIVE 3-DIMENSIONAL OBSERVATION METHOD FOR SCANNING TRANSMISSION X-RAY MICROSCOPY

T. Ohigashi<sup>1</sup>, Y. Inagaki<sup>1</sup>, A. Ito<sup>2</sup>, K. Shinohara<sup>2</sup> and N. Kosugi<sup>1</sup>

<sup>1</sup>UVSOR Synchrotron, Institute of Molecular Science, Myodaiji, Okazaki-shi, Aichi 444-8585, Japan

<sup>2</sup>School of Engineering, Tokai University, Kitakaname, Hiratsuka-shi, Kanagawa 259-1292, Japan

### Abstract

Combination of X-ray microscopy and computer tomography (CT) is one of the advanced techniques to be realized in forth-coming diffraction limit synchrotron-based light sources, considering the high transmittance of X-rays and the high spatial resolution of the X-ray microscopy. This combination allows us to analyze 3-dimensional structures without any destructive process of samples. Among several CT techniques, the full-field type and projection microscopy are more suitable than the scanning one from the viewpoint of data acquisition time; however, the scanning one has an advantage in energy tunability. The scanning transmission X-ray microscope (STXM) in the soft X-ray region has been established as a powerful tool for the 2-dimensional chemical analysis based on near edge X-ray absorption fine structure (NEXAFS) and also been applied to 3-dimensional chemical state mappings [1,2]. In most cases, tomographic data have been acquired under the condition of restricted angle projection due to the limitations of the measurement time and the shape and mounting of samples. In order to realize more quantitative analysis, full projection ( $180^\circ$  or  $360^\circ$ ) measurement is highly required [3].

We have been developing a full projection CT technique for the STXM beamline in UVSOR Synchrotron (Okazaki, Japan). A sample cell for the CT is designed as shown in Fig. 1. This cell is equipped with a two phase stepper motor (AM-1020, Faulhaber) with a spur gearhead (12/5, Faulhaber) to reduce the step angle. The shape of this cell is compatible with all the ALS-based STXM systems.

As a test measurement, polystyrene spheres with a diameter of  $5\ \mu\text{m}$  were used as a sample. The spheres were set on a tip of a tungsten probe with glue. 50 soft X-ray transmission images were continuously acquired with rotating the sample by  $3.6$  degree each. The X-ray energy was tuned to  $280\ \text{eV}$ , below the C K-edge, and the dwell time per a pixel was  $3\ \text{msec}$  each. It took about  $1.5$  hours to obtain whole data. An STXM image and a reconstructed cross sectional image are shown in Fig. 2(a) and (b), respectively.

In this presentation, the optical configuration of our STXM for quantitative CT studies will be discussed in detail.



**Figure 1:** Photo of a sample cell for computer tomography

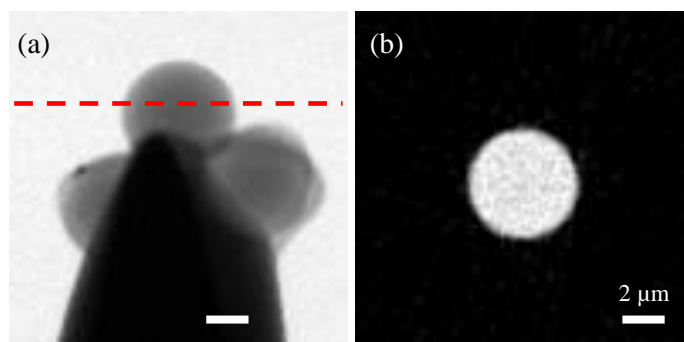


**Figure 2:** (a) STXM image of a latex sphere and (b) cross sectional image along a dashed line shown in (a).

### References

- [1] M. Obst, J. Wang and A. P. Hitchcock, *Geobiol.*, 7, 577-591, (2009).
- [2] V. Berejnov, D. Susac, J. Stumper and A. P. Hitchcock, *ECS Transactions*, 50, 361-368 (2012).
- [3] G. A. Johansson, T. Tyliczszak, G. E. Mitchell, M. H. Keefe and A. P. Hitchcock, *J. Synchrotron Rad.*, 14, 395-402, (2007).

# TIME RESOLVED SYNCHROTRON X-RAY MICRO-TOMOGRAPHY FOR IN-SITU STUDIES OF DYNAMIC MICROSTRUCTURAL PROCESSES

H. S. Barnard<sup>1</sup>, A. A. MacDowell<sup>1</sup>, D. Y. Parkinson<sup>1</sup>, N. M. Larson<sup>2</sup>, F. Zok<sup>2</sup>, F. Parerai<sup>3</sup>, N. Mansour<sup>3</sup>, M. Czabaj<sup>4</sup>, R. O. Ritchie<sup>1</sup>, M. Voltolini<sup>1</sup>, J. Ajo-Franklin<sup>1</sup>, J. I. Pacold<sup>1</sup>, J. Bows<sup>5</sup>, R. Godfroid<sup>5</sup>, D. K. Shuh<sup>1</sup>

*1 Lawrence Berkeley National Laboratory, Advanced Light Source, Berkeley, California USA*

*2 University of California, Santa Barbara, California USA*

*3 NASA Ames Research Center, Moffett Field, California USA*

*4 University of Utah, Salt Lake City, Utah USA*

*5 PepsiCo Inc., Purchase, New York USA*

## **Abstract**

At the Advanced Light Source, beamline 8.3.2 performs micro-tomography analysis under conditions of high temperature, pressure, mechanical loading, and other realistic conditions using environmental test cells. With scan times of 10s -100s of seconds, many in-situ studies have succeeded in capturing the microstructural time-evolution of materials during quasi-static experiments. These in-situ experiments can greatly benefit from improved temporal resolution. We present our recent instrumentation developments that allow increased scan rates approaching 1 Hz, hardware developments enabling continuous tomography with complex environmental cells, and the use of iterative reconstruction techniques to improve 3D image quality. These tomography developments are presented with examples from a) high temperature in-situ mechanical testing, oxidation, and manufacturing processes of ceramic matrix composites, b) simulation of spacecraft thermal protection system components during atmospheric entry, c) microwave heating for food science applications and d) dynamic processes and flows in high-pressure geological systems.



## FAST COMPUTED TOMOGRAPHY USING A LAB-BASED X-RAY PHASE-CONTRAST IMAGING SYSTEM

P. C. Diémoz<sup>1,2</sup>, C. K. Hagen<sup>1</sup>, M. Endrizzi<sup>1</sup>, F. Vittoria<sup>1,2</sup>, U. H. Wagner<sup>3</sup>, C. Rau<sup>3</sup>, I. K. Robinson<sup>2,4</sup>, P. Coan<sup>5</sup>, A. Bravin<sup>6</sup>, A. Olivo<sup>1,2</sup>

<sup>1</sup>Department of Medical Physics and Biomedical Engineering, UCL, WC1E 6BT London, UK

<sup>2</sup>Research Complex at Harwell, Harwell Oxford Campus, OX11 0FA Didcot, UK

<sup>3</sup>Diamond Light Source, Harwell Oxford Campus, OX11 0DE Didcot, UK

<sup>4</sup>London Centre for Nanotechnology, WC1H 0AH London, UK

<sup>5</sup>Faculty of Physics and Institute for Clinical Radiology, LMU, 85748 Garching, Germany

<sup>6</sup>European Synchrotron Radiation Facility, 38043 Grenoble, France

### Abstract

Several X-ray phase-contrast imaging (XPCI) techniques have been developed and are now routinely applied at synchrotron radiation (SR) facilities, enabling the achievement of highly improved contrast. However, the translation of XPCI to laboratory setups remains challenging, due to, among others, strict coherence requirements, complex setups, high radiation doses, long acquisition times, small fields of view. This has so far prevented the widespread implementation of XPCI for laboratory and medical applications.

Edge illumination (EI), an XPCI technique under development at UCL [1], can potentially bridge this gap. EI, in fact, has been shown to be relatively insensitive to beam coherence and is thus applicable to polychromatic sources with focal spots of up to at least 100  $\mu\text{m}$  [1,2]. Moreover, low radiation doses to the sample have been demonstrated [3] and the setup can be adapted to large fields of view, as large masks (up to at least 20x20  $\text{cm}^2$ ) can be manufactured.

The standard procedure for phase retrieval in EI requires the acquisition of one image, then the movement of one of the optical elements (masks) and the acquisition of a second image [2]. However, this is impractical for many real-world applications where short exposure times are needed. Typical examples are *in-vivo* applications, where the subject might move and/or has to be kept under anesthesia, and computed tomography (CT), where the mask movement needs to be combined with the sample rotation [3].

This motivated the development of a new phase retrieval method that requires only the acquisition of a single input image [4]. Following demonstration on synchrotron planar images, this has recently been adapted for implementation with polychromatic beams and in CT mode [5]. Importantly, when applied to CT, this method enables continuous sample rotation, leading to much shorter acquisition times. In this talk, we will first introduce the EI technique, its working principle and the assumptions of the new single-shot method, and then present experimental results obtained both with synchrotron and laboratory setups. We will show how very short exposure times can be achieved in laboratory XPCI CT, down to less than 7 minutes. Finally, we will explain how setup improvements currently underway are expected to lead to even shorter acquisition times and better image quality.



**Figure:** CT of a ground beetle, acquired using a lab-based EI setup with the new single-shot method (acquisition time <7').

### References

- [1] A. Olivo and R. Speller, Appl. Phys. Lett. 91, 074106 (2007).
- [2] P.C. Diémoz et al., Appl. Phys. Lett. 103, 244104 (2013).
- [3] C. K. Hagen et al., Med. Phys. 41, 070701 (2014).
- [4] P.C. Diémoz et al., J. Synchrotron Radiat. 22, 1072-1077 (2015).
- [5] P.C. Diémoz et al., in preparation.

## TABLE-TOP WATER-WINDOW MICROSCOPE USING Z-PINCHING CAPILLARY DISCHARGE SOURCE

T. Parkman<sup>1</sup>, M. F. Nawaz<sup>2</sup>, M. Nevrkla<sup>2</sup>, A. Jancarek<sup>2</sup>, D. Panek<sup>1</sup>, J. Turnova<sup>1</sup>, M. Vrbova<sup>1</sup>

<sup>1</sup>*Czech Technical University in Prague, Faculty of Biomedical Engineering, nam. Sitna 3105,  
272 01 Kladno, Czech Republic*

<sup>2</sup>*Czech Technical University in Prague, Faculty of Nuclear Sciences and Physical Engineering,  
V Holesovickach 2, 180 00 Prague 8, Czech Republic*

### Abstract

We present a design of a compact transmission water-window microscope based on nitrogen plasma induced by the Z-pinching capillary discharge. Nitrogen plasma is ideal for its quasi-monochromatic radiation with wavelength  $\lambda = 2.88$  nm, which corresponds to the quantum transition  $1s^2-1s2p$  of helium-like nitrogen ion [1]. This wavelength falls within the so-called water-window wavelength region ( $\lambda = 2.3 - 4.4$  nm) and thus provides the natural contrast between water and carbon-based substances, e.g. proteins.

We present a characterization of the table-top Z-pinching capillary discharge source. The source was built in-house [2], plasma is generated by a current discharge through a 10 cm long, 3.2 mm inner diameter ceramic capillary filled with nitrogen gas. A ceramic capacitor bank with a maximum capacity of 21 nF is pulse charged by a Marx-Fitch generator up to 100 kV, and switched by self-breakdown spark-gap. The main current has a damped sinus shape, with half-period of 150 ns and maximum amplitude of 30 kA. Average photons flux is  $5.5 \times 10^{13}$  photons/(sr x line x pulse) and plasma spot has a circular shape with diameter 360  $\mu\text{m}$  at full width half maximum.

The spectrum of soft X-ray radiation produced by the source is filtered by titanium filter to achieve monochromatic radiation with wavelength  $\lambda = 2.88$  nm. Filtered radiation is focused by an ellipsoidal nickel coated condenser mirror [3]. We used a Fresnel zone plate to create an image of a sample transmission on a SXR-sensitive CCD camera. To assess the resolution of the microscope, we imaged a standard sample – copper mesh - with magnification 300x and exposure time 1 min. The achieved spatial resolution is 110 nm at half-pitch. The images of Chrysodidymus cells are presented as well as the description of the sample preparation process.

### References

- [1] P. Vrba, M. Vrbova, S. V. Zakharov, V. S. Zakharov, A. Jancarek, M. Nevrkla, J. of El. Spectr. and Rel. Ph. 196, pp. 24-30, (2014).
- [2] M. Nevrkla et al., Source Workshop 2012, Dublin (2012).
- [3] M. F. Nawaz et al., Proc. of SPIE 9510, EUV and X-ray Optics: Synergy between Laboratory and Space IV, 951014-951014-7 (2015).

## ALZHEIMER'S DISEASE UNDER THE (X-RAY) MICROSCOPE

N. D. Telling<sup>1</sup>, J. Everett<sup>1</sup>, V. Tjendana<sup>2</sup>, and J.F. Collingwood<sup>2</sup>

<sup>1</sup>ISTM, Keele University, Stoke-on-Trent, Staffordshire ST4 7QB, UK

<sup>2</sup>School of Engineering, University of Warwick, Coventry, CV4 7AL, UK

### Abstract

Alzheimer's disease is the most common form of dementia, affecting around 30 million people worldwide, but currently without a cure or effective treatment. The major pathological hallmarks of the disease are the aggregation of the amyloid-beta (1-42) peptide fragment into extracellular plaques within the brain (typically 5-100  $\mu\text{m}$  in size), and accumulations of hyperphosphorylated tau protein in neurofibrillary tangles. At present the significance of these structures with regard to the onset and progression of the disease, is not understood. However, decades of research has revealed a strong connection between iron dysregulation and the pathology of the disease (see for e.g.1,2). Thus a complete understanding of how the accumulation, oxidation and magnetic state of iron in the brain is linked to pathology could lead to a much needed step change in understanding the onset and progression of the disease, as well as the development of treatments and early diagnostic tests.

In this talk I will describe our recent work using scanning transmission x-ray microscopy (STXM) to investigate the role of iron and calcium in pathological amyloid-beta structures in *ex vivo* samples. I will show how STXM techniques can be used to obtain speciation specific analysis of protein, peptide, calcium and iron at the nanoscale, even in resin-embedded tissue sections. I will also demonstrate the application of x-magnetic circular dichroism (XMCD) to probe the magnetic state of iron deposits *in situ*. I will present some recent highlights from our work in this area that reveal the existence of potentially neurotoxic redox-active ferrous iron forms in all sample types we have studied to date including transgenic mouse cortical tissue and amyloid plaque cores extracted from human brain tissue. Further, I will discuss how STXM can be used to determine nanoscale correlation of peptide and iron in diffuse amyloid plaques in transgenic mouse cortex as well as showing how the presence of multiple calcium phases can be determined in human Alzheimer's disease plaque cores.

### References

- 1 Collingwood, J. F. *et al.* Three-dimensional tomographic imaging and characterization of iron compounds within alzheimer's plaque core material. *J. Alzh. Dis.* **14**, 235-245 (2008).
- 2 Gallagher, J. J., Finnegan, M. E., Grehana, B. & Dobson, J. Modest amyloid deposition is associated with iron dysregulation, microglial activation, and oxidative stress. *J. Alzh. Dis.* **28**, 147-161 (2012).
- 3 Everett, J. *et al.* Ferrous iron formation following the co-aggregation of ferric iron and the Alzheimer's disease peptide  $\beta$ -amyloid (1-42). *J. R. Soc. Interface* **11**, 20140165 (2014).
- 4 Everett, J. *et al.* Evidence of redox-active iron formation following aggregation of ferrihydrite and the Alzheimer's disease peptide  $\beta$ -amyloid. *Inorg. Chem.* **53**, 2803-2809 (2014).

## 3D PRINTING BIOINSPIRED STRUCTURES FROM X-RAY MICROSCOPY

A. H. Barber<sup>1</sup>, G. Tozzi<sup>1</sup>, M. Pani<sup>1</sup>, M. Curto<sup>1</sup>

<sup>1</sup> School of Engineering, University of Portsmouth, Portsmouth PO1 3DJ, United Kingdom

### Abstract

Biology provides a range of complex structures optimized for particular mechanical functions [1]. The use of optimized mechanical structures is critical for improved engineering application, thus highlighting the importance of bioinspiration. However, many current manufacturing processes are limited in producing suitable bioinspired complex structures. Additive manufacturing provides 3D printed structures that are able to incorporate complexities found in the biological world yet identifying the design features that are translated to 3D printing is challenging. X-ray microscopy approaches, particularly tomographic reconstruction that identifies distribution of mechanical properties in 3-dimensional space, is a powerful method that first provides a dataset describing the design of a biological structure that can then be used to manufacture a bioinspired engineering equivalent using 3D printing.

In this work we examine the mechanical function of a range of biological structures found in marine biology, particularly teeth from limpet teeth that are known to have exceptional mechanical properties [2]. Figure 1 shows an example of these limpet teeth that are robust enough to resist failure when rasping over rock surfaces. Electron microscopy in Figure 1a shows the curved tooth geometry whereas Figure 1b indicates the distribution of hard mineral phase using a scanning proton microprobe [3]. X-ray microscopy shows superiority compared to many other techniques in giving 3D spatial information on the distribution of hard and soft materials within the structures. A workflow approach is then applied to translate the datasets from x-ray microscopy to a 3D printing facility able to produce a composite of hard and soft materials within a single build. This approach is generic and promises a broad range of applications, from new bioinspired tooling based on teeth to designer prosthetics for healthcare.

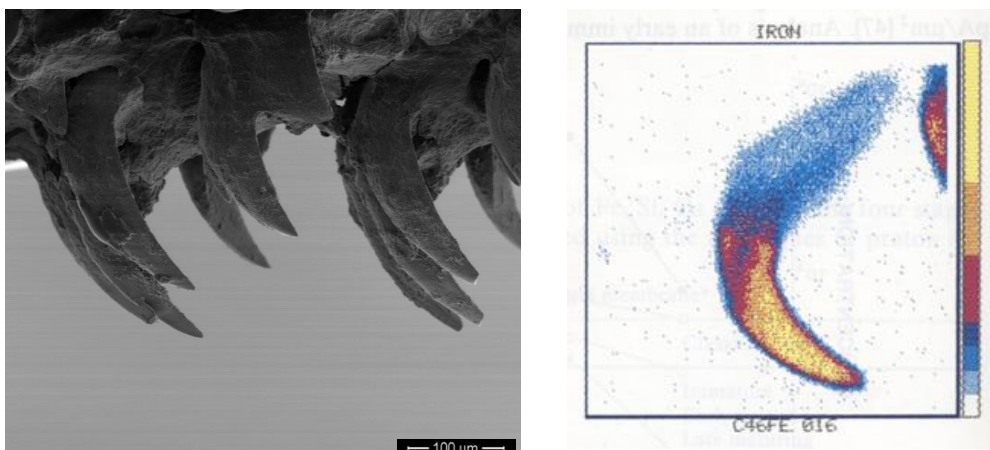


**Figure 1(a)** Scanning electron micrograph of limpet teeth and **(b)** scanning proton microprobe indicating the distribution of the hard (Goethite) phase towards the cusp and cutting edge of the tooth, from [3].

### References

- [1] J. C. W. Dunlop, P. Fratzl, *Annu. Rev. Mater. Res.* 40, 1 (2010).
- [2] A. H. Barber, D. Lu, N. Pugno *J. R. Soc. Interface* 12, 20141326 (2015)
- [3] S. Mann, J. Webb, and R. J. P. Williams, *Biomineralization: Chemical and Biochemical Perspectives* (John Wiley & Sons, 1989).

## TOMOSAIC: Towards Terabyte Tomography

R. F. C. Vescovi<sup>1,2</sup>, D. Gursoy<sup>1</sup>, V. De Andrade<sup>1</sup>, E. Dyer<sup>5</sup>, K. Kording<sup>5</sup>, M. B. Cardoso<sup>2</sup>, F. De Carlo<sup>1</sup>,  
C. Jacobsen<sup>1,4</sup>, N. Kasthuri<sup>3</sup>

*1 Advanced Photon Source, Argonne National Laboratory, 9700 S Cass Ave, Lemont IL 60439 USA*

*2 Brazilian Synchrotron Light Laboratory, Rua Giuseppe Maximo Scolfaro, 10000, Campinas, SP, Brazil*

*3 Center for Nanoscale Materials, Argonne National Laboratory, 9700 S Cass Ave, Lemont IL 60439 USA*

*4 Department of Physics & Astronomy, Northwestern University, 2145 Sheridan Rd, Evanston IL 60208, USA*

*5 Department of Physical Medicine and Rehabilitation, Northwestern University, 345 E Superior St, Chicago IL 60611, USA*

### Abstract

Many applications are revisiting the capabilities of mosaic tomography as science evolves towards highly stable and efficient x-ray microtomography stations. This is especially true for the study of neuroscience samples that need to be imaged at sub-micron resolution with a centimeter field of view and also by other biological and fossil samples with similar volumes. Imaging samples with this resolution and field-of-view produces datasets of multiple terabyte in size, which in turn generates a number of data handling challenges including processing and reconstructing the resulting projection data.

In order to achieve non-limited field of view tomography for imaging large specimens at the required high resolution, we have developed *Tomosaic* a python package to organize and pipeline tomogram registration for mosaic tomography(*Tomosaic*). This package is placed in the framework of the XBrainMap project with the purpose to image a whole mouse brain with sub-micron resolution and is an addition to the already well established tomography packages developed at the APS, *TomoPy*[1], *DXfile* and *DXchange*[2]. It may also be used as a stand alone routine or integrated with other python reconstruction algorithms.

The main kernel underlying *Tomosaic* is a Fourier based method for stitching x-ray tomographic (CT) datasets. The experimental approach relies on taking full tomographic datasets at different positions in a mosaic array and registering the frames using Fourier Phase Correlation. To ensure the accuracy of the registration procedure, we calculate a map from the experimental motor shifts. The masked correlation image is then minimized to obtain the correct shift. The partial datasets are blended in order to create a new complete dataset. As the complete dataset increases in size, it may be unfeasible for single computer workstations handle it. Future work is required to create a metadata structure that allows the reconstruction kernel to access the data without loading the entire dataset into memory. This metadata structure would also allow to realign the data without the need to rewrite it, keeping the raw data safe while saving space. With all this capabilities, *Tomosaic* provide an environment for developing and deploying codes for terabyte tomography.

While this approach is generally applicable, examples will be shown from a challenging project goal: imaging an entire mouse brain at micrometer resolution. We applied *Tomosaic* to reconstruct a 3D image volume from projection data collected in a standard synchrotron tomography beamline. Our results demonstrate that it is possible to stitch and reconstruct terabyte 3D mosaic tomography data from large centimeter-scale volumes.

### References

[1] D. Gursoy, F. De Carlo, X. Xiao, and C. Jacobsen, "TomoPy: a framework for the analysis of synchrotron tomographic data," *Journal of Synchrotron Radiation* 21, 1188-1193 (2014).

[2] F. De Carlo, D. Gursoy, F. Marone, M. Rivers, D.Y. Parkinson, F. Khan, N. Schwarz, D.J. Vine, S. Vogt, S.-C. Gleber, S. Narayanan, M. Newville, T. Lanzirotti, Y. Sun, Y.P. Hong, and C. Jacobsen, "Scientific Data Exchange: a schema for HDF5-based storage of raw and analyzed data," *Journal of Synchrotron Radiation* 21, 1224-1230 (2014).



## ULTRAHIGH BRIGHTNESS X-RAY MICROBEAM DELIVERY SYSTEM WITH MULTIPLE SELECTABLE ENERGIES

Wenbing Yun<sup>1</sup>, Benjamin Stripe<sup>1</sup>, Janos Kirz<sup>1</sup>, Alan Lyon<sup>1</sup>, David Reynolds<sup>1</sup>, Sylvia JY Lewis<sup>1</sup>, Sharon Chen<sup>1</sup>, Vladimir Semenov<sup>1</sup>, Richard Ian Spink<sup>1</sup>, SH Lau<sup>1</sup>.

<sup>1</sup> Sigray, Inc. Concord, CA USA

Both laboratory and synchrotron-based microanalytical techniques have made substantial advances in the past decades, including improved algorithms and faster, higher sensitivity detectors [1-2]. However, laboratory performance has lagged those of the synchrotron in performance (e.g. sensitivity and resolution), primarily due to limited laboratory x-ray source brightness and narrow selection of usable x-ray optics due to the diverging, polychromatic x-ray beam generated by the laboratory source that the optic is coupled to and constraints on system footprint.

Here we present our Sigray XCITE™ system, which produces >50X flux over a conventional x-ray illumination system comprising a microfocus source and polycapillary x-ray optic. The system features a patent-pending microfocus x-ray source design with multiple x-ray targets to provide a varied selection of characteristic x-ray energies coupled to high resolution, high efficiency paraboloidal x-ray mirror lens that can be focusing or collimating in design. The combination of the two enable delivery of flux comparable to the synchrotron, and is designed for new instrumentation development and for upgrading existing laboratory x-ray microanalytical systems.

One key topic that will be explored in-depth is enabling access to new characteristic x-ray energies previously not accessible by laboratory x-ray sources through the incorporation of novel target materials. The XCITE™ provides dual or tri-energy options for rapid software-controlled switching between various target regions (e.g. Pt, Ti, Rh, etc) to enable analysis at two or more energies. A multi-energy approach is essential for optimizing performance and throughput in applications such as protein crystallography/microXRD and microXRF, as will be discussed. Moreover, a multi-energy approach provides a path for refined quantification techniques for a multitude of techniques.

Additionally, we will review key performance considerations for microbeam systems, including: novel strategies to achieve higher source brightness and the significance of often-overlooked optics attributes, such as constant magnification in imaging optics and achromaticity of the focal spot. These design elements contribute significantly to the quantitative capabilities and speed of the system that incorporates the microbeam.

[1] T Skarzynski. *Acta Crystallographica Section D* (2013)

[2] P Lechner, et al. *Nuclear instruments and Methods in Physics Research Section A: Accelerators, Spectrometers, Detectors and Associated Equipment* (2001)

The authors gratefully acknowledge the small business research support that enabled these developments: NSF grant IIP-1448727 and NIH grant 1R43GM11287.